UNIVERSITY OF OKLAHOMA

GRADUATE COLLEGE

AN INVESTIGATION INTO THE INFLUENCE OF SUBSURFACE GEOCHEMISTRY ON MICROBIAL COMMUNITIES IN AN UNCONFINED CONTAMINATED AQUIFER

A DISSERTATION

SUBMITTED TO THE GRADUATE FACULTY

In partial fulfillment of the requirements for the

Degree of

DOCTOR OF PHILOSOPHY

By

DANIEL JOHN CURTIS
Norman, Oklahoma
2018

AN INVESTIGATION INTO THE INFLUENCE OF SUBSURFACE GEOCHEMISTRY ON MICROBIAL COMMUNITIES IN AN UNCONFINED CONTAMINATED AQUIFER

A DISSERTATION APPROVED FOR THE
DEPARTMENT OF MICROBIOLOGY AND PLANT BIOLOGY

BY

Dr. Jizhong Zhou, Chair

Dr. Michael McInerney

Dr. Lee Krumholz

Dr. Tyrrell Conway

Dr. Andrew Elwood Madden

Acknowledgements

To my advisor Dr. Jizhong Zhou, thank you for giving me the opportunity to expand my learning in microbiology at the Institute for Environmental Genomics. I would like to thank each of the members of my committee: Dr. Michael McInerney, Dr. Lee Krumholz, Dr. Tyrrell Conway and Dr. Andrew Elwood Madden, who always made themselves available when sought out and for their guidance during the course of my degree.

I have to acknowledge the support I received from my peers and the senior research staff, especially Dr. Joy Van Nostrand and Dr. Ping Zhang, at the Institute for Environmental Genomics. I am grateful for the time they invested in my training and it was always reassuring to know I only had to ask, and help was at hand.

To the very talented researchers I crossed paths with along the way: Dr. Jelena Bujan, Dr. Arthur Escalas, Dr. Lauren Hale and Dr. Lindsey O'Neal. Each of you made an impact on my personal development.

Last but certainly not least, I have been fortunate to pursue my higher learning overseas and it would not have been possible without the unwavering support from my parents John and Rose, my brother Noel and sister-in-law Sahiba. Thank you.

Table of Contents

List of Tables

List of Figures

Abstract

Microorganisms account for ~ 90 gigatons of carbon in terms of global biomass and are important drivers of elemental cycling especially in oligotrophic subsurface environments. Subsurface ecosystems remain poorly characterized in terms of understanding the roles microorganisms play in biogeochemical processes. While we are handicapped by our ability to cultivate the vast majority of microbial diversity, genomic approaches are rapidly expanding our understanding of the complex microbial communities that are found in these ecosystems. Anthropogenic sources are a major contributor to imbalances in natural systems primarily through the release of environmental contaminants, and changes in environmental geochemistry arising from increased contaminant levels has lasting impacts on microbial function. Contamination at the Oak Ridge Integrated Field Research Center (OR-IFRC) is centered around the waste byproducts of uranium refining operations and the site is defined by a subsurface plume with gradients in pH, uranium (U) and nitrate (NO_3).

In Chapter 2, I investigate the effect of changes in groundwater pH on the subsurface microbial community during a field treatment experiment designed to chemically sequester U(VI) in a highly contaminated zone (Area-3) at the OR-IFRC. A comprehensive microbial functional gene array (GeoChip 4.2) was used to infer changes in microbial community composition and functional potential during KOH amendment. Changes in subsurface geochemistry caused considerable shifts in the overall microbial community structure. Relative to pre-manipulation conditions, functional genes involved in carbon (C), nitrogen (N), sulfur (S), and phosphorus (P) cycling processes increased in relative abundance as pH shifted between 3.5 – 4.5 units before sharply decreasing as the groundwater reached the targeted pH of ~ 5.0 units. Microbial populations promoting metal reducing conditions and known U(VI) reducing species were

studied using nitrate reductase (*nirK/S*), dissimilatory sulfate reductase (*dsrAB*) and *cytochrome c*/*hydrogenase* probes on the array. However, weak responses in relation to pre-manipulation (PM) conditions were observed during KOH amendment. The small increases in gene abundance between pH 3.5 – 4.0 and the subsequent sharp decrease in the abundance of genes across functional categories near pH 5.0 point to the overarching inhibition in functional potential of a low pH adapted community due to changes in subsurface geochemistry. While the concentration of U(VI) was dramatically reduced and thereby rendered the abiotic sequestration successful, a net inhibitory effect of the complex changes in subsurface geochemistry on the microbial community was identified.

Nitrate is primary groundwater contaminant at the OR-IFRC with large gradients observed in the subsurface. In Chapter 3, I examine the composition of subsurface microbial communities at the OR-IFRC along a nitrate gradient. 20 wells were selected from a groundwater survey conducted at the reservation in 2012-2013 and grouped in to three categories spanning low (< 1mgL^{-1} NO_3), moderate (10-100 mgL^{-1} NO_3) and high (> 100 mgL^{-1} NO_3). Groundwater communities were studied using 16S rRNA amplicon sequencing and with the GeoChip 5.0 functional gene microarray. The taxonomic composition of groundwater communities exhibited stronger differences compared to the functional composition between the treatment groups. Overall functional potential for gene spanning C, N, S cycling and electron transfer processes were enriched under NO_3 levels spanning 10-100 mgL^{-1}. Microbial populations important to bioremediation of U(VI) were structured along the gradient based on the analysis of *nirK/S*, *dsrAB* and *cytcochrome c*/*hydrogenase* sequences with increased functional potential evident at moderate NO_3. Apart from NO_3, pH, carbon, anions and redox conditions influenced the taxonomic and functional composition across the treatment groups.

The acidic wastes that characterize the OR-IFRC have generated extremely acidic conditions in the subsurface near the former S-3 waste disposal ponds. However, the underlying geology also induces zones of alkalinity in the unconfined aquifer. Chapter 3 explores the microbial communities identified in 24 wells spanning acidic (pH < 6.0), circumneutral (pH 7.0 – 8.0) and alkaline (pH > 9.0) conditions at the site and the influence of groundwater geochemistry in these wells on microbial function. Groundwater communities were examined using 16S rRNA gene amplicon sequencing and the GeoChip 5.0 functional gene microarray. Differences in taxonomic community composition were not identified between OR_A and OR_{CN} wells while differences in functional composition were evident between all treatments. However, taxonomic differences were stronger compared to those based on functional gene content. The relative gene abundance of genes influencing C, N and S cycling and the transfer of electrons was enriched in OR_{ALK} wells compared to both OR_A and OR_{CN} wells. Populations important to U(VI) remediation efforts at the site were structured along the pH gradient and their functional potential was greatly reduced in OR_A wells, though some sulfate reducing species were enriched under low pH conditions. Al, Ca, SO_4 and DIC (Dissolved Inorganic Carbon) were other components of subsurface geochemistry that influenced both taxonomic and functional gene composition across the treatment groups.

My research highlights how groundwater geochemistry can shape subsurface microbial communities at the OR-IFRC. The response to pH amendment and concomitant changes in geochemistry shed light on the dynamics and reduced functional potential seen in subsurface communities resulting from the first field implementation of this approach to abiotically sequester U(VI). Furthermore, nitrate and pH govern sitewide subsurface community composition and play an important role structuring microbial functional potential at the OR-IFRC.

CHAPTER 1: Introduction

Overview of the Oak Ridge Integrated Field Research Center

The Oak Ridge Integrated Field Research Center (OR-IFRC) is situated on the Y-12 National Security Complex in Bear Creek Valley near Oak Ridge, TN. The site has served as a model location for research examining the fate and transport of subsurface contaminants which are remnants at nuclear legacy sites, established during the period between World War II and the Cold War. Like the Hanford Site in Hanford, WA and the Savannah River Site in Aiken, SC the OR-IFRC is one of many units that were established in the United States as part of the nuclear complex that fueled weapons production. In the nearly three decades that have followed since remediation efforts commenced, these sites are still characterized by high levels of radioactive wastes and other wastes produced from uranium refining processes. At this time, the remaining 16 sites across the United States are currently undergoing clean-up operations managed by the US. DOE to mitigate the environmental legacy. (https://www.energy.gov/em/cleanup-sites).

The OR-IFRC features a 243-acre contaminated area which has and continues to be the focus of both field and laboratory scale experiments furthering remediation efforts, and a 404-acre background area that serves as a location for comparison studies (Watson et al., 2004a). The former unlined Waste Disposal S-3 ponds are the source of the contaminant plume that has spread through the subsurface which has 5 defined contaminant areas and were a defining feature of the site. While the ponds were capped in 1988 and now feature a parking lot, contaminants including nitric acid wastes, uranium, Tc-99, volatile organic solvents and heavy metals have leached through the subsurface. The leaching process was aided by groundwater flow through the unconsolidated sediments and weathered (occurring through fracturing and karstification) rock which define the geology down to about 16m below the surface in the contaminated area (Solomon, 1992). Nitrate (~ 40,000 mgL^{-1}), uranium (~40 mgL^{-1}) and an extremely acidic pH (< 4.0) are the main issues in Area-3 with their levels decreasing with distance from the S-3 ponds.

Area 3 is also characterized by very high levels of Al^{3+} (~700 mgL^{-1}) and high levels of calcium, sodium, magnesium and manganese. The radionuclides and metals are the primary target for research from and various biological and chemical approaches have been evaluated to minimize their escape through the aquifer (Van Nostrand et al., 2011; Zhang et al., 2011).

Radionuclide and Metal Sequestration in the Subsurface

The hydraulic connectivity in the porous layer overlying the bedrock and groundwater flow at the OR-IFRC are the main drivers of contaminant migration through the subsurface (Jardine et al., 1993a; Jardine et al., 1993b; Wilson et al., 1993). Therefore, research has focused on better understanding the conditions that promote radionuclide sequestration. Two avenues for driving uranium sequestration have been evaluated; the first relies on the microbial potential for biological reduction of uranium and the second builds on the chemical sequestration of uranium within the sediment matrix given the unique geochemistry in the subsurface. Microbially driven bio-reduction is possible given the finding that certain metals (Fe(III), Mn(IV), Cr(VI) and U(VI)) can be utilized as terminal electron acceptors (TEAs) to conserve energy and support growth (Lovley, 1993). However, barriers that prevent the flow of electrons to metals in highly contaminated areas at the OR-IFRC are high nitrate concentrations and low pH. Given the availability of organic electron donors, nitrate is a preferentially utilized TEA due to the larger free energy change of the redox couple (Christensen et al., 2000). While the potential for U(VI) reduction has been documented at low pH, constraints stemming from maintaining pH homeostasis and combating acid stress are likely to limit the rates of dissimilatory metal reduction at low pH (Shelobolina et al., 2003). Additionally, apart from the high nitrate and acidic pH, the unconfined aquifer is an oligotrophic environment and microbial populations are therefore known to be carbon limited and restrained in their activity (Istok et al., 2004a). Given

the understanding for the conditions necessary for dissimilatory metal reduction to occur, field treatments driving bio-reduction rely on preconditioning the subsurface to remove inhibitory levels of nitrate and the addition of an electron donor. These manipulations allow terminal electron accepting processes to induce the anaerobic conditions that promote the activity of microbial species which can utilize metals as TEAs (Michalsen et al., 2006; Edwards et al., 2007).

Abiotic sequestration of U(VI) in OR-IFRC sediments is possible through chemical co-precipitation with Al-hydroxides (Luo et al., 2009). This utility of implementing this process in the field builds on research which has highlighted following findings: (1) Analysis of the subsurface geochemistry has revealed a high concentration of Al^{3+} near the contaminant zone, (2) the speciation of UO_2^{2+} is pH dependent, (3) Al begins to precipitate from aqueous phase as pH is raised and (4) the precipitation productions formed as a result can serve as a sink for metals that co-precipitate concomitantly (Watson et al., 2004a; Zhang et al., 2010). The pH range and carbonate concentration over which the co-precipitation occurs is critical as at pH > 5.0 carbonate can influence the formation of uranyl carbonate species which have increased mobility (Gu et al., 2003). While laboratory scale trials have successfully demonstrated the sequestration of U(VI) in result of co-precipitation reactions during titration of acidic sediments (Tang et al., 2013a), this process has been implemented in the field as well (Chapter 2, unpublished data).

Metagenomic Approaches to Investigating Microbial Communities

Since Leeuwenhoek's first foray into the microcosmos of 'animalcules' using a single-lensed microscope in the late 1600's, microbiologists continue to grapple with linking the unseen majority and their roles in the many environments they inhabit (Martiny et al., 2006). Our

capacity to study microorganisms has greatly exceeded Leeuwenhoek's comparatively elementary visual approach, yet we remain largely uninformed on the vast diversity of the microbial world estimated at ~ 90 Gt C (Prosser, 2015; Bar-On et al., 2018). While the application of microscopy in microbiology is certainly not a static technology, microbiologists have expanded their horizons in microbial ecology primarily through the rapid development and implementation of next generation sequencing technology paired with analytical tools (Cole et al., 2008; Caporaso et al., 2010; Mardis, 2013) . Another road-block hindering the characterization of microbes lies in 'The Great Plate Count Anomaly' given our ability to cultivate a tiny fraction of the estimated microbial diversity (Epstein, 2013). In this regard, challenges in obtaining pure cultures are related to replicating the environmental conditions, the importance of synergism for certain microbial species, slow growth and capturing the rare biosphere (Whang and Hattori, 1988; Schink, 2002; Vartoukian et al., 2010; Stewart, 2012).

Given the rapid development of sequencing technologies, computing capacity and analytical software, the study of microbial ecology has moved to capture the information stored in sequence information via culture-independent methods. The greatest challenge in studying the microbiology of an environment presently is not so much addressing "Who is present?" but tackling the "What are they doing?" and the field of metagenomics has ushered a new era in holistically capturing the function of environmental microbes. The main avenues through which metagenomic information can be captured are by focusing on individual genes (gene-centric approaches) and through capturing whole genomes (genome centric) by assembly from sequence data or through single-cell genome sequencing. A metagenomic approach is described as having an open architecture (amplicon sequencing or shotgun sequencing), if *a priori* information about the sequence targets is not required. When the platform can only capture information based on

specified targets (functional gene or phylogenetic microarrays) it is defined by a closed architecture. Though the 16S rRNA gene continues to be the cornerstone of investigations into microbial community composition, other functional markers such as the *amoA*, *nifH*, *nirK/S*, *dsrAB* genes have been routinely employed in discerning the composition and function of the specific populations that encode them (Gubry-Rangin et al., 2011; Bentzon-Tilia et al., 2014; Wilkins et al., 2015; Zhang et al., 2017a). Targeted gene sequencing offers the advantages of detecting novel taxa in a sample and providing phylogenetic information on the taxa present. However, these approaches are limited in their capacity to generate functional diversity of communities, are hindered by biases arising from PCR amplification and sequencing error, tend to be skewed towards the dominant members of the community and can suffer from low reproducibility (Schloss et al., 2011; Lemos et al., 2012; Pinto and Raskin, 2012; Zhou et al., 2013a).

Whole genome shotgun sequencing (WGS) and metatranscriptomics are open architectures that generate large amounts of information describing a broader suite of functions (the metabolic pathways) from the community being examined. The former informs us on the community gene content while the latter sheds light on the contingent of expressed genes within a community. WGS of extracted community DNA does not require amplification prior to sequencing and thus circumvents the biases introduced from a PCR step, however the procedure can be plagued by insufficient sequence depth to cover complex communities. Metatranscriptomics generally involves the sequencing of mRNA from the RNA pool extracted from a sample. Once the sequence information is generated, the relative abundance of gene transcripts is then compared to metagenomic data from the same sample. Therefore, the inherent advantage of implementing the technique is the ability to discern what functions are being expressed and the rates these functions may be occurring in the environment under study. This is a significant advantage over

metagenomic and targeted gene approaches however challenges arise from purification of mRNA targets, preventing their turnover, construction of cDNA libraries and the need for a metagenome 'scaffold' to aid in describing which functions are expressed (Carvalhais et al., 2012; Prosser, 2015). At this juncture, sample processing and data generation are increasingly less of a concern for methodologies leveraging an open architecture. The greater challenge arises from the capacity to extract information from raw data; large computational demands imposed during taxonomic binning, searching/mapping reference databases, annotation and assembly necessitate specialized hardware (Scholz et al., 2012; Thomas et al., 2012).

Closed architecture metagenomic technologies encompass phylogenetic and functional gene microarrays. The former targets rRNA genes while the latter aims to capture functional genes (either from specific populations or entire communities) involved in various biogeochemical cycles (Loy et al., 2002; Franke-Whittle et al., 2009; Abell et al., 2012). The PhyloChip is a comprehensive phylogenetic microarray designed to capture all 9 variable regions of the 16S rRNA gene and version G3 of the array targets more than 50,000 OTUs across the domains *Bacteria* and *Archaea* (Brodie et al., 2006; Hazen et al., 2010). The GeoChip functional gene array targets functional genes using 50mer probes designed to cover important microbially driven (bacteria, archaea, fungi and protists) biogeochemical cycles. The latest version (GeoChip 5.0) targets > 1,500 functional genes spanning 13 functional gene categories from element (C, S, N and P cycling) to antibiotic and metal resistance (He et al., 2007b; Zhou et al., 2015). These microarrays have the distinct advantages of a lower susceptibility to random sampling, limits to detection being less affected by target abundance, higher taxonomic resolution given the greater divergence of functional markers compared to phylogenetic markers and potential for quantification when amplification (either by whole genome amplification or PCR) of template material is not necessary (Tiquia et al., 2004; Wang et al., 2009; Zhou et al., 2010).

The limitations that circumscribe the application of microarrays primarily have to do with the designing specific oligonucleotide probes, variation arising from inconsistencies during the processing of material for hybridization, distinguishing background noise from true probe signals and the predetermined scope of target capture given that a limited number of probes can be accommodated. In addition, functional gene arrays cannot provide information on phylogenetic information (Wu et al., 2001; He et al., 2007b; Zhou et al., 2015).

References

Abell, G.C.J., Robert, S.S., Frampton, D.M.F., Volkman, J.K., Rizwi, F., Csontos, J., and Bodrossy, L. (2012) High-Throughput Analysis of Ammonia Oxidiser Community Composition via a Novel, amoA-Based Functional Gene Array. *PLOS ONE* **7**: e51542.

Bar-On, Y.M., Phillips, R., and Milo, R. (2018) The biomass distribution on Earth. *Proceedings of the National Academy of Sciences*.

Bentzon-Tilia, M., Traving, S.J., Mantikci, M., Knudsen-Leerbeck, H., Hansen, J.L.S., Markager, S., and Riemann, L. (2014) Significant N2 fixation by heterotrophs, photoheterotrophs and heterocystous cyanobacteria in two temperate estuaries. *The Isme Journal* **9**: 273.

Brodie, E.L., DeSantis, T.Z., Joyner, D.C., Baek, S.M., Larsen, J.T., Andersen, G.L. et al. (2006) Application of a High-Density Oligonucleotide Microarray Approach To Study Bacterial Population Dynamics during Uranium Reduction and Reoxidation. *Applied and Environmental Microbiology* **72**: 6288-6298.

Caporaso, J.G., Kuczynski, J., Stombaugh, J., Bittinger, K., Bushman, F.D., Costello, E.K. et al. (2010) QIIME allows analysis of high-throughput community sequencing data. *Nature methods* **7**: 335.

Carvalhais, L.C., Dennis, P.G., Tyson, G.W., and Schenk, P.M. (2012) Application of metatranscriptomics to soil environments. *Journal of Microbiological Methods* **91**: 246-251.

Christensen, T.H., Bjerg, P.L., Banwart, S.A., Jakobsen, R., Heron, G., and Albrechtsen, H.-J. (2000) Characterization of redox conditions in groundwater contaminant plumes. *Journal of Contaminant Hydrology* **45**: 165-241.

Cole, J.R., Wang, Q., Cardenas, E., Fish, J., Chai, B., Farris, R.J. et al. (2008) The Ribosomal Database Project: improved alignments and new tools for rRNA analysis. *Nucleic acids research* **37**: D141-D145.

Edwards, L., Küsel, K., Drake, H., and Kostka, J.E. (2007) Electron flow in acidic subsurface sediments co-contaminated with nitrate and uranium. *Geochimica et Cosmochimica Acta* **71**: 643-654.

Epstein, S.S. (2013) The phenomenon of microbial uncultivability. *Current Opinion in Microbiology* **16**: 636-642.

Franke-Whittle, I.H., Knapp, B.A., Fuchs, J., Kaufmann, R., and Insam, H. (2009) Application of COMPOCHIP Microarray to Investigate the Bacterial Communities of Different Composts. *Microbial Ecology* **57**: 510-521.

Gu, B., Brooks, S.C., Roh, Y., and Jardine, P.M. (2003) Geochemical reactions and dynamics during titration of a contaminated groundwater with high uranium, aluminum, and calcium. *Geochimica et Cosmochimica Acta* **67**: 2749-2761.

Gubry-Rangin, C., Hai, B., Quince, C., Engel, M., Thomson, B.C., James, P. et al. (2011) Niche specialization of terrestrial archaeal ammonia oxidizers. *Proceedings of the National Academy of Sciences* **108**: 21206-21211.

Hazen, T.C., Dubinsky, E.A., DeSantis, T.Z., Andersen, G.L., Piceno, Y.M., Singh, N. et al. (2010) Deep-Sea Oil Plume Enriches Indigenous Oil-Degrading Bacteria. *Science* **330**: 204-208.

He, Z., Gentry, T.J., Schadt, C.W., Wu, L., Liebich, J., Chong, S.C. et al. (2007) GeoChip: a comprehensive microarray for investigating biogeochemical, ecological and environmental processes. *The Isme Journal* **1**: 67.

Istok, J., Senko, J., Krumholz, L.R., Watson, D., Bogle, M.A., Peacock, A. et al. (2004) In situ bioreduction of technetium and uranium in a nitrate-contaminated aquifer. *Environmental Science & Technology* **38**: 468-475.

Jardine, P., Jacobs, G., and O'Dell, J. (1993a) Unsaturated transport processes in undisturbed heterogeneous porous media: II. Co-contaminants. *Soil Science Society of America Journal* **57**: 954-962.

Jardine, P., Jacobs, G., and Wilson, G. (1993b) Unsaturated transport processes in undisturbed heterogeneous porous media: I. Inorganic contaminants. *Soil Science Society of America Journal* **57**: 945-953.

Lemos, L.N., Fulthorpe, R.R., and Roesch, L.F.W. (2012) Low sequencing efforts bias analyses of shared taxa in microbial communities. *Folia Microbiologica* **57**: 409-413.

Lovley, D.R. (1993) Dissimilatory Metal Reduction. *Annual Review of Microbiology* **47**: 263-290.

Loy, A., Lehner, A., Lee, N., Adamczyk, J., Meier, H., Ernst, J. et al. (2002) Oligonucleotide Microarray for 16S rRNA Gene-Based Detection of All Recognized Lineages of Sulfate-Reducing Prokaryotes in the Environment. *Applied and Environmental Microbiology* **68**: 5064-5081.

Luo, W., Kelly, S.D., Kemner, K.M., Watson, D., Zhou, J., Jardine, P.M., and Gu, B. (2009) Sequestering Uranium and Technetium through Co-Precipitation with Aluminum in a Contaminated Acidic Environment. *Environmental Science & Technology* **43**: 7516-7522.

Mardis, E.R. (2013) Next-Generation Sequencing Platforms. *Annual Review of Analytical Chemistry* **6**: 287-303.

Martiny, J.B.H., Bohannan, B.J.M., Brown, J.H., Colwell, R.K., Fuhrman, J.A., Green, J.L. et al. (2006) Microbial biogeography: putting microorganisms on the map. *Nature Reviews Microbiology* **4**: 102.

Michalsen, M.M., Goodman, B.A., Kelly, S.D., Kemner, K.M., McKinley, J.P., Stucki, J.W., and Istok, J.D. (2006) Uranium and Technetium Bio-Immobilization in Intermediate-Scale Physical Models of an In Situ Bio-Barrier. *Environmental Science & Technology* **40**: 7048-7053.

Pinto, A.J., and Raskin, L. (2012) PCR Biases Distort Bacterial and Archaeal Community Structure in Pyrosequencing Datasets. *PLOS ONE* **7**: e43093.

Prosser, J.I. (2015) Dispersing misconceptions and identifying opportunities for the use of 'omics' in soil microbial ecology. *Nature Reviews Microbiology* **13**: 439.

Schink, B. (2002) Synergistic interactions in the microbial world. *Antonie van Leeuwenhoek* **81**: 257-261.

Schloss, P.D., Gevers, D., and Westcott, S.L. (2011) Reducing the Effects of PCR Amplification and Sequencing Artifacts on 16S rRNA-Based Studies. *PLOS ONE* **6**: e27310.

Scholz, M.B., Lo, C.-C., and Chain, P.S.G. (2012) Next generation sequencing and bioinformatic bottlenecks: the current state of metagenomic data analysis. *Current Opinion in Biotechnology* **23**: 9-15.

Shelobolina, E.S., O'Neill, K., Finneran, K.T., Hayes, L.A., and Lovley, D.R. (2003) Potential for In Situ Bioremediation of a Low-pH, High-Nitrate Uranium-Contaminated Groundwater. *Soil and Sediment Contamination: An International Journal* **12**: 865-884.

Stewart, E.J. (2012) Growing unculturable bacteria. *Journal of bacteriology*: JB. 00345-00312.

Tang, G., Luo, W., Watson, D.B., Brooks, S.C., and Gu, B. (2013) Prediction of Aluminum, Uranium, and Co-Contaminants Precipitation and Adsorption during Titration of Acidic Sediments. *Environmental Science & Technology* **47**: 5787-5793.

Thomas, T., Gilbert, J., and Meyer, F. (2012) Metagenomics-a guide from sampling to data analysis. *Microbial informatics and experimentation* **2**: 3.

Tiquia, S.M., Wu, L., Chong, S.C., Passovets, S., Xu, D., Xu, Y., and Zhou, J. (2004) Evaluation of 50-mer oligonucleotide arrays for detecting microbial populations in environmental samples. *Biotechniques* **36**: 664-670, 672, 674-665.

Van Nostrand, J.D., Wu, L., Wu, W.-M., Huang, Z., Gentry, T.J., Deng, Y. et al. (2011) Dynamics of microbial community composition and function during in-situ bioremediation of a uranium-contaminated aquifer. *Applied and environmental microbiology*: AEM. 01981-01910.

Vartoukian, S.R., Palmer, R.M., and Wade, W.G. (2010) Strategies for culture of 'unculturable' bacteria. *FEMS Microbiology Letters* **309**: 1-7.

Wang, F., Zhou, H., Meng, J., Peng, X., Jiang, L., Sun, P. et al. (2009) GeoChip-based analysis of metabolic diversity of microbial communities at the Juan de Fuca Ridge hydrothermal vent. *Proceedings of the National Academy of Sciences* **106**: 4840-4845.

Watson, D., Kostka, J., Fields, M., and Jardine, P. (2004) The Oak Ridge field research center conceptual model. *NABIR Field Research Center, Oak Ridge, TN*.

Whang, K., and Hattori, T. (1988) Oligotrophic bacteria from rendzina forest soil. *Antonie van Leeuwenhoek* **54**: 19-36.

Wilkins, D., Lu, X.-Y., Shen, Z., Chen, J., and Lee, P.K. (2015) Pyrosequencing of mcrA and archaeal 16S rRNA genes reveals diversity and substrate preferences of methanogen communities in anaerobic digesters. *Applied and environmental microbiology* **81**: 604-613.

Wilson, G.V., Jardine, P.M., O'Dell, J.D., and Collineau, M. (1993) Field-scale transport from a buried line source in variably saturated soil. *Journal of Hydrology* **145**: 83-109.

Wu, L., Thompson, D.K., Li, G., Hurt, R.A., Tiedje, J.M., and Zhou, J. (2001) Development and Evaluation of Functional Gene Arrays for Detection of Selected Genes in the Environment. *Applied and Environmental Microbiology* **67**: 5780-5790.

Zhang, F., Parker, J.C., Brooks, S.C., Watson, D.B., Jardine, P.M., and Gu, B. (2010) Prediction of uranium and technetium sorption during titration of contaminated acidic groundwater. *Journal of Hazardous Materials* **178**: 42-48.

Zhang, F., Luo, W., Parker, J.C., Brooks, S.C., Watson, D.B., Jardine, P.M., and Gu, B. (2011) Modeling uranium transport in acidic contaminated groundwater with base addition. *Journal of Hazardous Materials* **190**: 863-868.

Zhang, P., He, Z., Van Nostrand, J.D., Qin, Y., Deng, Y., Wu, L. et al. (2017) Dynamic succession of groundwater sulfate-reducing communities during prolonged reduction of uranium in a contaminated aquifer. *Environmental science & technology* **51**: 3609-3620.

Zhou, J., He, Z., Van Nostrand, J., Wu, L., and Deng, Y. (2010) Applying GeoChip Analysis to Disparate Microbial Communities. *Microbe Magazine* **5**: 60 - 65.

Zhou, J., He, Z., Yang, Y., Deng, Y., Tringe, S.G., and Alvarez-Cohen, L. (2015) High-throughput metagenomic technologies for complex microbial community analysis: open and closed formats. *MBio* **6**: e02288-02214.

Zhou, J., Jiang, Y.-H., Deng, Y., Shi, Z., Zhou, B.Y., Xue, K. et al. (2013) Random Sampling Process Leads to Overestimation of β-Diversity of Microbial Communities. *mBio* **4**.

CHAPTER 2: pH amendment influences aquifer microbial community dynamics during active U(VI) sequestration

Introduction

Managing the off-site transport of radioactive wastes at the Oak Ridge Reservation has posed a challenge owing to the contamination plume emanating from the former unlined surface impoundments known as the S-3 Waste Disposal Ponds. The ponds received mixed wastes produced from processes fueling weapons and energy related research conducted at the industrialized sector of the reservation known as the Y-12 complex. The wastes, characterized by high levels of anionic nitrate and sulfate, cationic aluminum, calcium, magnesium and uranium and very acidic pH, have gradually contaminated the groundwater surrounding the source zone since the unlined disposal ponds were capped in 1983 (Watson et al., 2004). The preservation of natural resources and pressing need to mitigate further damage necessitates the implementation of effective strategies to minimize the environmental impact from uranium refining wastes generated at this U.S DOE weapons complex.

The U.S. EPA has defined MCLs for uranium and nitrate of 0.03 mgL^{-1} and 10 mgL^{-1}, whereas groundwater at Area 3 is characterized by extremely high levels of U(VI) and nitrate contamination (up to 50 mgL^{-1} and 100 mM, respectively) (Wu et al., 2006a; Wu et al., 2006b). Acidic dissolution of carbonate from limestone at the OR-IFRC complexes the uranyl ion (UO_2^{2+}) forming highly mobile U-CO_3 species that are a primary cause for concern and this process is governed by pH and CO_2 partial pressure in the subsurface (Langmuir, 1997). At pH over 6.5 the U-CO_3 complexes have little reactivity with the solid phase and demonstrate enhanced mobility in groundwater (Watson et al., 2004, Gu et al., 2003). The mobility of U-CO_3 complexes at alkaline pH is enhanced by the presence of Ca, furthermore Ca has been found to interfere with bacterial U(VI) reduction (Barnett et al., 2000; Brooks, 2001; Fox et al., 2006).

Reduction of U(VI) to U(IV) prevents these processes and is a strategy for contaminant immobilization (Langmuir, 1997).

Biological remediation offers green, cost-effective options for the restoration of contaminated natural environments. These approaches span both sorption or accumulation of metals via phytoremediation and microbial bio-reduction (Salt et al., 1995; Wall and Krumholz, 2006). Restricting the spread of mobile uranium species through sequestration via microbial bio-reduction and abiotic chemical co-precipitation has proven to be an effective technique (Xu et al., 2010; Van Nostrand et al., 2011; Zhang et al., 2011; Tang et al., 2013a) with the former being successfully implemented in field trials at the OR-IFRC. Microbial bio-reduction involves stimulating members of the native microbial community with electron donors (like lactate or ethanol) under conditions conducive to growth, with nitrate reducing bacteria (NRB) and sulfate reducing bacteria (SRB) generating anaerobic conditions and low redox potentials promoting the activity of dissimilatory metal reducing bacteria (DMRB). Bacterial genera such as *Geobacter*, *Desulfovibrio*, and *Anaeromyxobacter* facilitate electron transfer to U(VI), bringing about its reduction and subsequent immobilization (Wall and Krumholz, 2006; Xu et al., 2010; Van Nostrand et al., 2011).

However prevailing conditions in the Area 3 subsurface are extremely unfavorable for microbial growth primarily due to the high levels of Al^{3+}, NO_3^- and buffered acidic pH (3.5). For sediments with high levels of aluminum, like those at the OR-IFRC, U can be abiotically immobilized via co-precipitation with Al during base addition (Zhang et al., 2011; Tang et al., 2013a). Previous laboratory scale treatment of sediment from Area-3 with base amended groundwater, yielded promising results when quantifying U(VI) sequestration and removal from the re-circulated groundwater (Luo et al., 2009; Tang et al., 2013a). Ground water re-circulation loops have been successfully employed as delivery systems for carbon substrates that stimulate microbial growth

and bio-reduction (Van Nostrand et al., 2011; Zhang et al., 2015). Evaluation of field-scale treatments is through monitoring changes in geochemistry and microbial biomass (using culture based or molecular approaches) in groundwater harvested from borewells. In re-circulation field treatment systems like those driving subsurface microbial bio-reduction, an injection well delivers growth substrates to the subsurface, monitoring wells placed along the flow path of groundwater are used to evaluate the efficacy of treatment and an extraction wells serves to complete the loop by allowing water to be pumped back into the injection well.

Comprehensive functional gene arrays are powerful tools for inferring changes in microbial community functional compositions because they target a wide range of genes involved in the geochemical cycling of C, N, and S, metal resistance and contaminant degradation (Li et al., 2005; Liebich et al., 2006). We applied a microarray, GeoChip 4.2, building on its application in previous studies at the OR-IFRC (Xie et al., 2011; Zhang et al., 2013; Tu et al., 2014) to identify changes in functional microbial communities in response to KOH injection driving abiotic uranium sequestration through co-precipitation with the sediment solid phase. Doing so, we monitor the previously undescribed dynamics of groundwater microbial communities during a field titration experiment driving abiotic U(VI) sequestration and aim to address how changes in subsurface pH and geochemistry during base amendment influence subsurface microbial composition and the functional potential of NRB, SRB and DMRB. This study provides a detailed description of the microbial functional gene responses of populations known to promote bio-reduction and serves as a reference point for future studies that explore biotic and abiotic approaches for long-term sequestration of uranium at the OR-IFRC.

Materials and Methods

Groundwater Recirculation System

A recirculating well system was set-up in Area 3, near the former S-3 ponds at the Oak Ridge Integrated Field Research Center. The system consisted of an injection well FW128 (hereafter referred to as IW), an extraction well FW106 (hereafter referred to as EW) and three multilevel sampling wells FW115, FW129 and FW130 (hereafter referred to as MW_1, MW_2 and MW_3 respectively) located between IW and EW along the groundwater flow path (Figure S12). Hydraulic connectivity between the wells was established by running a Br^- tracer study. Potassium hydroxide (KOH) was used as a titrant for the pH manipulation. Groundwater was first extracted from EW, base added and following removal of precipitates, reinjected into well IW. A computerized system ensured the desired elevation in pH was maintained over the course of the study. Groundwater circulation in the system commenced on October 22, 2010. KOH injection started on November 2, 2010 and ceased November 3, 2011. The system was operated for a total of 366 days.

Groundwater Sampling and Sample Organization

Groundwater was siphoned using peristaltic pumps and microbial biomass was harvested by passing 2 liters of groundwater through 3 μm and 0.2 μm filters that were immediately stored at -80 °C until the time of DNA extraction. Samples were collected from each well in the re-circulation loop prior to base amendment (day 0) and again on days 233, 303 and 352 during the titration experiment. Additionally, samples were collected from a well located outside the recirculation loop (FW126) that was not influenced by the base addition. Various geochemical

parameters were measured over the course of the titration experiment, including cations, anions, pH, inorganic carbon, total organic carbon and acetate as described previously (Wu et al., 2006a, Wu et al., 2006b).

The pH measured in groundwater collected during base recirculation increased gradually due to the high buffering capacity in groundwater in Area 3 (Figure 1, Figure S2) (Watson et al., 2004). To aid in visualizing changes in groundwater geochemistry, Detrended correspondence analysis (DCA) using 17 geochemical variables measured from the monitoring wells was performed (Figure 1D). The samples were grouped to reflect the pH increase observed during the experiment from ~3.5 to 5.0 as follows; PM (pH ~3.5; all samples collected prior to base addition and samples from FW126), pH_a (samples with pH 3.5 - 4.0), pH_b (samples with pH 4.0 - 4.5) and pH_c (samples with pH > 4.5).

DNA Extraction and Sample Processing

Whole community genomic DNA was extracted using a liquid nitrogen freeze-grinding method as detailed in previous work (Zhou et al., 1996). The concentration and quality (assessed by A260/280 and A260/230 ratios) of the extracted DNA were measured using a NanoDrop ND-1000 spectrophotometer (NanoDrop Technologies Inc., Wilmington, DE). Multiple displacement amplification was performed using 1 µl of the eluted DNA from each sample using the TempliPhi kit (GE Healthcare) as described previously (Wu et al., 2006a). Amplified DNA was quantified with PicoGreen using a FLUOstar Optima microplate reader (BMG Labtech, Jena, Germany). 1ug of DNA was labeled with Cy-3 using the Klenow fragment and random primers as described previously (Van Nostrand et al., 2009). Finally, the labeled DNA was purified using the QIAquick purification kit (Qiagen, USA) per the manufacturer's instructions and dried in a SpeedVac (ThermoSavant, USA).

Microarray Hybridization, Scanning and Data Analysis

The functional gene array employed here, GeoChip 4.2, is designed with 50-mer oligonucleotide probes (98,384 probes in all), which target more than 150,000 coding sequences (Tu et al., 2014). The DNA was suspended in 40% formamide hybridization buffer and subsequently hybridized to the functional gene array (overnight; 14 to 16 hours) at 42°C with mixing on a MAUI hybridization station (BioMicro Systems, Salt Lake City, UT, USA). Each array was scanned (NimbleGen MS200, Roche NimbleGen) and pixel density was quantified from scanned images. Raw data was normalized via the data pipeline designed at the Institute for Environmental Genomics, University of Oklahoma (http://ieg.ou.edu/microarray/). Spots with signal-to-noise ratios [(signal mean-background mean)/background standard deviation] lower than 2 were removed prior to statistical analysis. A signal was categorized as positive when a probe was detected in at least 2 samples within a given replicate group. Probe signal intensity was normalized between and within groups using the mean-ratio method (Zhou et al., 2014).

Selection of Environmental Variables

A subset of environmental variables was selected for further analysis using principle component analysis and correlation analyses to help identify and remove strongly co-correlated variables. In conjunction with this, the BioEnv tool was used to identify variables that correlated with the gene abundance data and variance inflation factors (VIF < 20) were taken into consideration so as to identify collinearity between variables.

Statistical Analysis

Probe information for the GeoChip 4.2 microarray used in this study is available at http://www.ou.edu/content/ieg/tools.html. α-diversity was estimated for functional genes based on positive probes numbers utilizing the Shannon-Weiner, Simpson and Peilou's evenness indices (Hill, 1973). Diversity indices and DNA yields for each pair of pH categories were compared using Welsh's t-tests. One-way ANOVAs were utilized to test the difference of means between pH categories for groundwater geochemistry variables, gene abundance data and DNA yields. Post-hoc Tukey's HSD tests were used to test differences between treatments for geochemistry, DNA yields and α diversity estimates. Fisher's LSD tests were used to test differences between treatments for gene abundance data. P values determined from LSD tests for each probe and gene were adjusted using Holm's method (Holm, 1979). Dissimilarity in functional gene content between pH categories was estimated by non-parametric multivariate statistics which included Multi-response Permutation Procedures (Van Sickle, 1997), Analysis of Similarity (ANNOSIM) (Clarke and Warwick, 1994) and Permutational Multivariate Analysis of Variance Using Distance Matrices (Adonis) (Anderson and Walsh, 2013). Pairwise distances among samples were assigned using the Bray-Curtis index. Detrended correspondence analysis was performed on gene abundance data with samples grouped according to pH category to identify clustering resulting from changes in environmental gradients. Canonical correspondence analysis (CCA) was used to identify the environmental variables which had the strongest influence on observed differences in functional gene abundance within each pH category. All statistical calculations were performed using R (v3.3.2; (Team, 2014) www.r-project.org/) using packages VEGAN and AGRICOLAE.

Results

Changes in Groundwater Geochemistry During pH Amendment

The concentrations of NO_3^- and SO_4^{2-} which are important electron acceptors remained stable during base amendment (Figure 1, Figure S1, Figure S2). SO_4^{2-} levels never dropped below 500 mg/L^- in the monitoring wells during the field treatment. There was no preconditioning of the site prior to the injection of KOH and without a barrier towards infiltrating groundwater contaminated by the plume, nitrate concentrations in the monitoring wells were at or above 5000 mg L^{-1} and the redox potential remained high. Owing to the acidic nature of the mixed waste contaminants in the subsurface, prior to base amendment the pH measured in each of the monitoring wells was within a unit of 3.5. A gradual increase in the groundwater pH was evident as base was added to the circulating water. By the end of the experiment the pH in wells MW_1, MW_2 and MW_3 ranged from 3.78 to 4.89. As the pH was raised to ~ 5.0 units, a decrease in the concentration of aqueous phase U mirrored the decrease seen in Al due to co-precipitation in the sediment. DCA ordination using 17 geochemical variables measured from the wells revealed clustering in samples grouped by pH (Figure 2A) indicating clustering of samples based on changes in geochemistry as the pH was raised.

Functional Gene Diversity and Overlap

The average richness of functional genes detected in the subsurface communities at different phases of base addition was 35,877.25 (± 7543) and ranged between ~ 25,000 - 40,000 functional genes depending on the treatment group (Table S1). In relation to functional diversity, following base addition, the Shannon index for category pH_a (pH 3.5-4.0) was close to that of PM (pre-manipulation). Categories pH_b (pH 4.0-4.5) and pH_c (pH > 5.0) had lower diversity

indices in relation to PM but this decrease was not statistically significant ($p > 0.05$). While not statistically significant functional gene richness remained relatively stable between PM through pH_b before decreasing in pH_c. We observed a high overlap in the functional gene composition (54.3-79.6%) between the designated pH categories. Evidence for a response toward the changing pH and subsurface geochemistry was seen in the unique probes detected. Relative to PM, the percentage of unique genes detected increased from 4% up to 10% in pH_b and then decreased sharply in pH_c. Samples with more similar pH values had a higher overlap in functional gene content, suggesting a succession in the functional potential of the communities during the experiment. For example, the community in pH_a had 79.6% similarity in detected gene content relative to PM but only 59.1% similarity when compared to the community composition of pH_c. Though no direct measurement of microbial biomass was made, the mean DNA yield revealed an overall decrease in recovered DNA in samples collected after base addition (Figure S3). The highest DNA yield was seen in category PM whereas the lowest yields were seen in category pH_c however the difference in yields between pH categories was not statistically significant. DCA ordination plots revealed functional gene composition of the microbial communities clustered with respect to pH treatment, reminiscent of microbial community succession (Figure 1B). Dissimilarity tests also indicated significant differences ($p < 0.05$) between groundwater communities in all pairwise comparisons except for the PM – pH_a comparison (Table 1).

Functional Gene Composition During pH Amendment

48,190 microarray probes belonging to 14 gene categories influencing the major geochemical cycles (C cycling, N cycling, S cycling and P cycling), stress responses, organic contaminant degradation, antibiotic resistance and other functional categories were detected across all

samples. A large decrease in gene abundance was consistently observed in those samples grouped in pH_c. Certain specific genes within the functional categories examined, revealed peaks in abundance in those samples representing conditions at pH_b or pH_c.

Changes in C cycling genes

Those genes detected involved in the breakdown of organic C revealed a capability to utilize a diverse range of labile and recalcitrant substrates by the microbial community (Figure S4). Of the 38 bacterial and archaeal C cycling genes detected, 34 showed a significant change ($p < 0.05$) in abundance over the course of the pH amendment with the least gene abundance in pH_c. Nine genes involved in organic C degradation increased in abundance in pH_a and pH_b and suggest the utilization of primarily labile C and C derived from the breakdown of microbial biomass. *cda*, *nplT*, and *endoglucanse* had highest abundance in pH_a, while *endochitinase*, *ara*, and *xylanase* were enriched at pH_b. *cellobiase* was had highest abundance in pH_a and pH_b. *mcrA* genes involved in methanogenesis were seen to have an increased abundance in pH_b while *pmoA* sequences responsible for methane monooxygenases were seen to have a significantly increased abundance at pH_a and pH_b (Figure S5). Forty-five fungal genes driving organic C degradation showed the least abundance in pH_c (Figure S6). Seventeen genes (including *amyA*, *glucoamylase*, *endoglucanase*, *exoglucanase*, *acetylglucosaminidase*, *cutinase* and *phenol oxidase*) had highest abundance in pH_b. These changes point to an increased functional potential for the degradation of both labile and recalcitrant C compounds as the pH in the groundwater increased before the sharp decrease observed at pH_c.

Changes in Genes driving N cycling, S cycling and the Transfer of Electrons

Sixteen N cycling genes showed a significantly reduced abundance in pH_c (Figure S7). This included all the genes governing the denitrification pathway (*narG, norB, nirK, nirS,* and *nosZ*). However, *nirS* sequences representing nitrate reductases were seen to increase in abundance in pH_b. There was an increased abundance of genes driving dissimilatory reduction of nitrate to ammonia, with *napA* enriched at pH_a and pH_b while *nrfA* was increased in pH_b. Genes driving assimilatory nitrate reduction (*nasA,* and *nir*) did not show any significant changes in abundance in these categories. The *amoA* gene driving ammonium oxidation did show enrichment in pH_a and pH_b during the titration in contrast to the *hao* gene, which did not show any changes in abundance in these categories. The *nifH* gene did show maximum abundance during pH_b indicating a potential increase in the fixation of inorganic N. Sequences covering glutamate dehydrogenases (*gdh* genes) driving ammonification, showed a similar pattern of enrichment to the *nifH* gene. Barring 3 genes representing sulfite reductases, most of the genes involved in S cycling processes were seen to have a significant decrease in abundance at pH_c (Figure S8). *sir* sequences encoding the assimilatory sulfite reductase responsible for the production of sulfide from sulfite had the highest abundance at pH_b. Though key genes (*dsrA, dsrB*) encoding subunits for sulfite reductases driving dissimilatory sulfate reduction did show an increase in abundance in pH_b, the contingent of sequences encoding adenyl-sulfate reductases (*aprA*, *aprB*) responsible for the generation of sulfite did not follow this trend. *cytochrome c* sequences represent an important category of enzymes involved in the transfer of electrons during dissimilatory metal reduction. These sequences were enriched in pH_b before decreasing in abundance in pH_c (Figure S9).

Stress and Metal Resistance Genes

Many metal and stress resistance conferring sequences were detected (5206 and 9756 genes, respectively) with sequences conferring resistance towards known metal contaminants at this site (As, Cd, Cr, Co, Ni, Pb, Hg etc.) (Figure S10). 11 genes were seen to have a significantly ($p < 0.05$) increased abundance in pH_a or pH_b as the base amendment increased the pH in the subsurface. Metal resistance conferring transporters encoded by *chrA*, *cadA*, *czcA, copA,* and *TehB* genes were significantly increased in abundance in pH_a. In category pH_b, *czcD*, *corC*, *merG*, *pbrT* and *zntA* encoding transporters showed an enriched abundance. Within the component of stress response genes (Figure S11), significant increases in abundance in pH_a or pH_b were localized to those known to be involved in the stress response towards glucose limitation (*bglP*), nitrogen limitation (*glnA*, *tnrA*), phosphorus limitation (*pstA*, *pstB*, *pstC*, *phoA*), protein turnover (*clpC*, *ctsR*), oxygen stress (*ahpC*) and temperature shock (*desR*, *grpE*). Two transcriptional regulators were increased in pH_b; The "housekeeping" σ70 factor (*sigma_70*) and *fnr*, encoding an Fe-S oxygen sensor. The abundance of *pstA*, *pstB*, *pstC* and *cplC* peaked in pH_a, whereas the remaining genes had maximum abundance in pH_b. *desR* was enriched at both pH_a and pH_b and did not decrease significantly in pH_c.

Changes in Functional Populations Relevant to U(VI) Reduction

Changes in relative gene abundance during base amendment (relative to the PM conditions) revealed subtle changes within functional populations (NRB, SRB and DMRB) known to play an important role in promoting optimal growth conditions for U(VI) bio-reduction in the subsurface, respectively (Table 2). The total number of probes representing nitrate reduction (*nirK/S*), sulfate reduction (*dsrAB*) and electron transfer to metals (*hydrogenase* and *cytochrome c*) increased between pH_a and pH_b and then fell in pH_c. The largest increase in unique probes detected in pH_b

were the *dsrAB, nirK/S* and DMR sequences (15.9%, 12.9% and 11.6%, respectively). The percentages of unique probes in pH_c was very small at less than 1% for *nirK/S* and around 1.5% for both *dsrAB* and DMR sequences. The largest percentage of unique probes detected in PM samples was identified in the PM-pH_c comparison; close to 37% of *nirK/S* and *dsrAB* probes, and 32.7% of DMR probes, indicating a large suppression in these functional populations when pH in the re-circulating groundwater reached the targeted pH 5.0.

Influence of Geochemistry on Community Structure

The following variables were identified as major drivers of changes in the functional structure of the microbial communities: pH (VIF = 9.69), K (VIF = 4.46), Al (VIF = 7.44), SO_4 (VIF = 1.49) and NO_3, VIF = 3.58). In an integrated model (p = 0.048) these five variables explained 29.66% of the variation in gene abundance during base addition with the first CCA axis contributing 11.03% and the second CCA axis, 7.05% of the explained variation (Figure 3A). Though only pH (p = 0.005) was found to significantly impact the model when all the above variables were tested individually using Monte Carlo permutation tests. Potassium and pH both had strong positive correlations with the first CCA axis (the larger size of the vector indicating a stronger influence in the direction on ordination space) while each were negatively correlated with the second axis. Sulfate had the weakest correlation among the variables tested, being positively correlated along the first axis and negatively correlated along the second axis. Al^{3+} and NO_3 were negatively correlated with both the first and second axes, with Al^{3+} showing the stronger correlation of the two. Nitrate had a strong negative influence along the first axis but induced a negligible influence along the second axis. Variance partitioning analysis (VPA) was utilized to identify how CCA variables accounted for variation in microbial community structure both individually and as a result of interactive effects (Figure 3B). Three categories of variables

comprising, base addition (pH and K), Al (many metal ions were strongly co-correlated with the change in Al concentration, likely due to precipitation) and redox conditions (SO_4^{2-}, NO_3^-) explained 13.27%, 3.73% and 8.90% of the total variance, respectively. However, a large portion of the (70.34%) of the changes in community composition could not be explained by the environmental variables selected.

Discussion

Successful attenuation of subsurface contamination at nuclear legacy sites such as the OR-IFRC ultimately relies on employing efficient, cost effective solutions to immobilize or detoxify multiple contaminants. Efforts aimed at harnessing both the microbial component of the subsurface biota and chemical treatment have shown promise in facilitating U(VI) sequestration within the subsurface (Istok et al., 2004; Tang et al., 2013b). The nature of the mixed wastes at the OR-IFRC precludes the use of a single approach and instead necessitates a thorough understanding of the hydrogeology, abiotic factors and subsurface microbial populations that promote and drive U(VI) reduction. The objective of this field study was to track the dynamics and changes in functional potential within the subsurface microbial community during U(VI) co-precipitation facilitated by base amendment. pH exerts a strong effect in controlling microbial community composition and function. This effect has been demonstrated in bacterial communities extracted from soils and those found in freshwater (Fernández-Calviño et al., 2011; Bååth and Kritzberg, 2015). In these studies, the optimal pH for microbial growth closely tracked *in situ* pH, with pH optima for acid adapted communities seen to be slightly higher (< 2 units) than *in situ* pH relative to those communities sampled from neutral or alkaline environments (Fernández-Calviño et al., 2011). This control has been emphasized with small

deviations in pH shown to rapidly constrain bacterial activity up to 50% (Fernandez-Calvinho, 2010).

A characteristic of field treatment experiments involving bio-stimulation to promote subsurface communities driving U(VI) reduction is the observed fluctuations in relative abundance of functional gene categories governing carbon utilization, metal resistance, sulfate metabolism, nitrate metabolism and electron transport stemming from favorable redox conditions and utilization of nutrients (Van Nostrand et al., 2011; Zhang et al., 2015). However, in the current field treatment experiment, large increases in functional gene relative abundance were not observed and instead fell sharply when pH in the subsurface reached 5.0. Such changes were probably not induced in this field experiment as the pH was the only variable directly manipulated and the field site was not pre-conditioned to promote microbial growth with substrate addition under low-redox conditions. Though the communities identified here do not form distinct clusters on ordination plots, there are visible shifts in overall community structure as groundwater pH increased. The percentage of unique sequences detected increased in each pH category prior to decreasing in pH_c and dissimilarity tests revealed significant differences in the overall composition of functional genes detected in each pH category. Without additional carbon input, the subsurface community monitored in this study was likely restricted to the breakdown of simple carbon sources derived from native organic matter permeating through the sediment (cellulose, pectin, lignin and chitin) or hydrocarbons introduced into the subsurface from the contaminant plume. Previous work has indicated subsurface communities affected by mixed waste contamination are metabolically restricted owing to the highly acidic and low nutrient conditions (Akob et al., 2007). Additionally, the repertoire of central carbon pathways identified in metagenomics data generated from highly contaminated FW106 groundwater, revealed a metabolically handicapped community constrained to nitrate respiration or oxidative utilization

of simple carbon substrates (Hemme et al., 2015). We observed few changes in the abundance of genes involved in the degradation of organic contaminants and aromatics in this study. While it is not possible to conclusively state these compounds are not actively catabolized, the results are representative of a reduced capacity for their utilization under prevailing conditions.

NRB and SRB are known to play an important role in inducing conditions that are favorable for the reduction of U(VI) by DMRB such as *Geobacter* spp. and *Desulfovibrio* spp. This role has been demonstrated in microcosm experiments implicating the role of SRB in reducing the concentration of sulfate prior to U(VI) reduction (Tang et al., 2013c) and the role of NRB and SRB in utilizing nitrate and sulfate prior to the onset of U(VI) reduction in field experiments at the OR-IFRC (Van Nostrand et al., 2011; Tang et al., 2013b). It is important to note that during these experiments increased activity of these populations was seen when field conditions were at a circumneutral pH (pH 6.64 for the EVO field test) and when pretreatment of field conditions induced a circumneutral pH and minimized inhibitory levels of nitrate (Wu et al., 2006b, Van Nostrand et al., 2011).

Microbial processes governing the reduction of nitrate are intimately linked to the pH of the environment under consideration, with pH influencing the production of intermediates including nitrite, nitrous oxide and di-nitrogen gas (Stevens et al., 1998; ŠImek and Cooper, 2002; Liu et al., 2010). During pH amendment in this study, functional populations driving the reduction of nitrate (*narG*), nitrite (*nirK*/S), nitric oxide (*norB*) and nitrous oxide (*nosZ)* lacked strong positive increases in abundance as pH increased during the manipulation but were seen to sharply decrease in abundance in pH_c. This potentially indicates a relatively stable potential for these metabolic processes that was inhibited as pH reached 5.0. These findings are supported by evidence that N_2 evolution is preferentially produced at an alkaline pH (ŠImek and Cooper, 2002) and the finding that N_20/N_2 ratios were higher under acidic conditions due to the

sensitivity of N_2O reductases to low pH (Liu et al., 2010). There is evidence for sulfate reduction occurring in highly acidic environments at pH<5 (Sánchez-Andrea et al., 2013; Sánchez-Andrea et al., 2014). However, optimum growth for SRB has been described as between pH 5-9 (Postgate, 1979) with the activity of sulfate reducers at lower pH inhibited by the increased toxicity of H_2S, higher energy requirements to export protons outside the cell and inhibition by dissociation of organic acids inside the cell (Matin, 1990; O'Flaherty et al., 1998). An additional requirement for active sulfate reduction is a negative redox potential, with more complete conversion to sulfide consistently documented to occur at more negative values (Connell and Patrick, 1968). As the pH was maintained below 5.0 and redox potentials remained around 400 mV, it is reasonable to predict SRB activity to be constrained under prevailing conditions with the decrease in abundance of these communities in pH_c likely indicative of a negative response of a population adapted to a lower pH. DMRB capable of U(VI) reduction are naturally occurring in aquifer systems impacted by uranium mining, refining and processing such as those at Rifle, CO and Oak Ridge, TN (Wall and Krumholz, 2006). Through laboratory scale experiments and field trials at these sites, prime conditions for microbial dissimilatory metal reduction have been determined to occur after utilization of terminal electron acceptors with higher redox potential, when ample carbon substrate is available and under strict anaerobic conditions (Watson, 2013). In contrast, *cytochrome c* sequences detected in our study were seen to gradually increase before significantly decreasing in abundance in category pH_c.
In particular, sequences representing *Shewanella* spp. displayed this pattern as the pH increased. It is possible that with increasing pH, growth conditions favored some members within the community, but proliferation was ultimately curtailed by the high concentration of nitrate and the paucity of nutrients. Substrate quality has been identified as a factor in controlling both carbon mineralization and assimilation into biomass (Manzoni et al., 2012). Furthermore, the allotment

of energy towards biosynthesis and the maintenance of non-growth components constraints the proliferation of microbial cultures in oligotrophic environments (Morita, 1988) highlighting the fact that maintenance energy requirements far surpass that which can be supplied from carbon in the soil. When considering the activity of subsurface anoxic communities, DMRB and SRB being at lower trophic levels rely on the fermentative end products generated by species in higher trophic levels which catabolize organic monomers (Miller et al., 2010). Under the prevailing conditions of high redox potential, scarcity of readily available electron donors and low pH, it is reasonable to assume bacterial members at every tier of the energy pyramid associated with bio-reduction were highly constrained, contributing to the small increases in gene abundance during base amendment. While high functional redundancy has been documented in diverse microbial communities, those with less diverse microbial communities are known to be more susceptible to environmental perturbation (Girvan et al., 2005). MPN estimates from groundwater samples collected prior to this experiment estimated bacterial cell density between 10^2-10^3 cells/ml and culture independent molecular surveys at the OR-IFRC aquifer, confirmed that groundwater collected from Area-3 source contamination zone harbored a less diverse community relative to groundwater from background samples (Cardenas et al., 2008; Green et al., 2012). These findings lend some support to the reduced DNA yields from filter samples collected after base amendment representing a reduction in subsurface microbial biomass during the field treatment. The increasing pH and subsequent changes in the subsurface geochemistry occurring during the co-precipitation of U(VI) appeared to be the most important factors influencing the community structure during the operation of the field treatment system. In contrast to the larger portion of variation in functional microbial populations accounted for in the ethanol bio-stimulation experiment at the site (Van Nostrand et al., 2011), close to 30% of variation in functional populations could be accounted for in this study. This is likely due to the pre-conditioning of the

site to induce favorable geochemistry for enhanced microbial activity and the addition of readily metabolizable electron donor in the form of ethanol. However, pH accounted for 14% within this component of explained variance. The complex changes in geochemistry occurring as a result of precipitation reactions involve the removal of trace metals in addition to metal contaminants (Tang et al., 2013a) with the resulting effect on microbial function hard to account for. Moreover, stochastic processes could influence which microbial species were detected on the closed-format microarray during the succession occurring in the subsurface (Stegen et al., 2012; Zhou et al., 2014).

This study aimed to characterize the subsurface microbial communities' response during the titration of acidic sediments promoting U(VI) sequestration. Distinguishable differences in functional potential were evident after analyzing the abundances of over 40,000 probes in groundwater samples collected prior to and during base addition. By the end of base injection, functional genes influencing microbial mediated biogeochemical cycling and those representing functional populations of NRB, SRB and DMRB were greatly reduced, likely indicative of reduced functional potential as environmental conditions changed in the subsurface with the increasing pH. Bio-stimulation field experiments at the OR-IFRC have shown that under favorable conditions, microbes capable of U(VI) sequestration can be stimulated to bolster U(VI) immobilization. At the end of this field trial, bacterial genera driving the active-reduction phases during bio-reduction were still present albeit at a lower abundance. While a convergence in the subsurface community composition was observed following nutrient depletion in a bio-stimulation field experiment (Zhou et al., 2014), such findings could not be confirmed in this study as representative samples were not analyzed and remain to be confirmed. In trying to develop methodologies to effectively sequester U(VI) within highly contaminated areas at the OR-IFRC, utilizing a two-pronged approach of chemical sequestration followed by

preconditioning and bio-stimulation of functional populations to contain residual U(VI) could be one such promising approach.

Acknowledgements

Dr. Ping Zhang provided valuable training for MDA and Dr. Tong Yuang and Dr. Menting Yuan assisted with hybridization of genomic DNA for GeoChip 4.2. Dr. Baohua Gu and Dr. Scott Brooks at Oak Ridge National Lab provided the geochemical data collected during the field experiment. Dr. Joy Van Nostrand helped with sample selection and data analysis. This work was funded by a grant from the U.S Department of Energy, ENIGMA Scientific Focus Area Program.

References

Akob, D.M., Mills, H.J., and Kostka, J.E. (2007) Metabolically active microbial communities in uranium-contaminated subsurface sediments. *FEMS Microbiology Ecology* **59**: 95-107.

Anderson, M.J., and Walsh, D.C. (2013) PERMANOVA, ANOSIM, and the Mantel test in the face of heterogeneous dispersions: what null hypothesis are you testing? *Ecological Monographs* **83**: 557-574.

Bååth, E., and Kritzberg, E. (2015) pH Tolerance in Freshwater Bacterioplankton: Trait Variation of the Community as Measured by Leucine Incorporation. *Applied and Environmental Microbiology* **81**: 7411-7419.

Barnett, M., Jardine, P., Brooks, S., and Selim, H. (2000) Adsorption and transport of uranium (VI) in subsurface media. *Soil Science Society of America Journal* **64**: 908-917.

Brooks, S.C. (2001) Waste Characteristics of the Former S-3 Ponds and Outline of Uranium Chemistry Relevant to NABIR Field Research Center Studies. NABIR Field Research Center, Oak Ridge, Tenn. 2001.

Cardenas, E., Wu, W.M., Leigh, M.B., Carley, J., Carroll, S., Gentry, T. et al. (2008) Microbial communities in contaminated sediments, associated with bioremediation of uranium to submicromolar levels. *Appl Environ Microbiol* **74**: 3718-3729.

Clarke, K., and Warwick, R. (1994) An approach to statistical analysis and interpretation. *Change in marine communities* **2**.

Connell, W.E., and Patrick, W.H. (1968) Sulfate Reduction in Soil: Effects of Redox Potential and pH. *Science* **159**: 86-87.

Fernández-Calviño, D., Rousk, J., Brookes, P.C., and Bååth, E. (2011) Bacterial pH-optima for growth track soil pH, but are higher than expected at low pH. *Soil Biology and Biochemistry* **43**: 1569-1575.

Fox, P.M., Davis, J.A., and Zachara, J.M. (2006) The effect of calcium on aqueous uranium(VI) speciation and adsorption to ferrihydrite and quartz. *Geochimica et Cosmochimica Acta* **70**: 1379-1387.

Girvan, M.S., Campbell, C.D., Killham, K., Prosser, J.I., and Glover, L.A. (2005) Bacterial diversity promotes community stability and functional resilience after perturbation. *Environmental Microbiology* **7**: 301-313.

Green, S.J., Prakash, O., Jasrotia, P., Overholt, W.A., Cardenas, E., Hubbard, D. et al. (2012) Denitrifying Bacteria from the Genus Rhodanobacter Dominate Bacterial Communities in the Highly Contaminated Subsurface of a Nuclear Legacy Waste Site. *Applied and Environmental Microbiology* **78**: 1039-1047.

Hemme, C.L., Tu, Q., Shi, Z., Qin, Y., Gao, W., Deng, Y. et al. (2015) Comparative metagenomics reveals impact of contaminants on groundwater microbiomes. *Frontiers in Microbiology* **6**.

Hill, M.O. (1973) Diversity and evenness: a unifying notation and its consequences. *Ecology* **54**: 427-432.

Istok, J.D., Senko, J.M., Krumholz, L.R., Watson, D., Bogle, M.A., Peacock, A. et al. (2004) In Situ Bioreduction of Technetium and Uranium in a Nitrate-Contaminated Aquifer. *Environmental Science & Technology* **38**: 468-475.

Langmuir, D. (1997) *Aqueous Environmental Geochemistry*. New Jersey: Prentice Hall.

Li, X., He, Z., and Zhou, J. (2005) Selection of optimal oligonucleotide probes for microarrays using multiple criteria, global alignment and parameter estimation. *Nucleic Acids Research* **33**: 6114-6123.

Liebich, J., Schadt, C.W., Chong, S.C., He, Z., Rhee, S.K., and Zhou, J. (2006) Improvement of oligonucleotide probe design criteria for functional gene microarrays in environmental applications. *Appl Environ Microbiol* **72**: 1688-1691.

Liu, B., Mørkved, P.T., Frostegård, Å., and Bakken, L.R. (2010) Denitrification gene pools, transcription and kinetics of NO, N2O and N2 production as affected by soil pH. *FEMS Microbiology Ecology* **72**: 407-417.

Luo, W., Kelly, S.D., Kemner, K.M., Watson, D., Zhou, J., Jardine, P.M., and Gu, B. (2009) Sequestering uranium and technetium through co-precipitation with aluminum in a contaminated acidic environment. *Environ Sci Technol* **43**: 7516-7522.

Manzoni, S., Taylor, P., Richter, A., Porporato, A., and Ågren, G.I. (2012) Environmental and stoichiometric controls on microbial carbon-use efficiency in soils. *New Phytologist* **196**: 79-91.

Matin, A. (1990) Bioenergetics parameters and transport in obligate acidophiles. *Biochimica et Biophysica Acta (BBA)-Bioenergetics* **1018**: 267-270.

Miller, L.D., Mosher, J.J., Venkateswaran, A., Yang, Z.K., Palumbo, A.V., Phelps, T.J. et al. (2010) Establishment and metabolic analysis of a model microbial community for understanding trophic and electron accepting interactions of subsurface anaerobic environments. *BMC Microbiol* **10**: 149.

Morita, R.Y. (1988) Bioavailability of energy and its relationship to growth and starvation survival in nature. *Canadian Journal of Microbiology* **34**: 436-441.

O'Flaherty, V., Mahony, T., O'Kennedy, R., and Colleran, E. (1998) Effect of pH on growth kinetics and sulphide toxicity thresholds of a range of methanogenic, syntrophic and sulphate-reducing bacteria. *Process Biochemistry* **33**: 555-569.

Postgate, J.R. (1979) *The sulphate-reducing bacteria*: CUP Archive.

Salt, D.E., Blaylock, M., Kumar, N.P., Dushenkov, V., Ensley, B.D., Chet, I., and Raskin, I. (1995) Phytoremediation: a novel strategy for the removal of toxic metals from the environment using plants. *Nature biotechnology* **13**: 468-474.

Sánchez-Andrea, I., Sanz, J.L., Bijmans, M.F.M., and Stams, A.J.M. (2014) Sulfate reduction at low pH to remediate acid mine drainage. *Journal of Hazardous Materials* **269**: 98-109.

Sánchez-Andrea, I., Stams, A.J., Amils, R., and Sanz, J.L. (2013) Enrichment and isolation of acidophilic sulfate-reducing bacteria from Tinto River sediments. *Environmental microbiology reports* **5**: 672-678.

ŠImek, M., and Cooper, J.E. (2002) The influence of soil pH on denitrification: progress towards the understanding of this interaction over the last 50 years. *European Journal of Soil Science* **53**: 345-354.

Stegen, J.C., Lin, X., Konopka, A.E., and Fredrickson, J.K. (2012) Stochastic and deterministic assembly processes in subsurface microbial communities. *The ISME journal* **6**: 1653-1664.

Stevens, R.J., Laughlin, R.J., and Malone, J.P. (1998) Soil pH affects the processes reducing nitrate to nitrous oxide and di-nitrogen. *Soil Biology and Biochemistry* **30**: 1119-1126.

Tang, G., Luo, W., Watson, D.B., Brooks, S.C., and Gu, B. (2013a) Prediction of Aluminum, Uranium, and Co-Contaminants Precipitation and Adsorption during Titration of Acidic Sediments. *Environmental Science & Technology* **47**: 5787-5793.

Tang, G., Watson, D.B., Wu, W.-M., Schadt, C.W., Parker, J.C., and Brooks, S.C. (2013b) U(VI) Bioreduction with Emulsified Vegetable Oil as the Electron Donor – Model Application to a Field Test. *Environmental Science & Technology* **47**: 3218-3225.

Tang, G., Wu, W.-M., Watson, D.B., Parker, J.C., Schadt, C.W., Shi, X., and Brooks, S.C. (2013c) U(VI) Bioreduction with Emulsified Vegetable Oil as the Electron Donor – Microcosm Tests and Model Development. *Environmental Science & Technology* **47**: 3209-3217.

Team, R.C. (2014) R: A language and environment for statistical computing. Vienna, Austria: R Foundation for Statistical Computing; 2014. In.

Tu, Q., Yu, H., He, Z., Deng, Y., Wu, L., Van Nostrand, J.D. et al. (2014) GeoChip 4: a functional gene-array-based high-throughput environmental technology for microbial community analysis. *Molecular ecology resources* **14**: 914-928.

Van Nostrand, J.D., Wu, W.-M., Wu, L., Deng, Y., Carley, J., Carroll, S. et al. (2009) GeoChip-based analysis of functional microbial communities during the reoxidation of a bioreduced uranium-contaminated aquifer. *Environmental Microbiology* **11**: 2611-2626.

Van Nostrand, J.D., Wu, L., Wu, W.-M., Huang, Z., Gentry, T.J., Deng, Y. et al. (2011) Dynamics of Microbial Community Composition and Function during In Situ Bioremediation of a Uranium-Contaminated Aquifer. *Applied and Environmental Microbiology* **77**: 3860-3869.

Van Sickle, J. (1997) Using mean similarity dendrograms to evaluate classifications. *Journal of Agricultural, Biological, and Environmental Statistics*: 370-388.

Wall, J.D., and Krumholz, L.R. (2006) Uranium Reduction. *Annual Review of Microbiology* **60**: 149-166.

Watson, D., Kostka, J., Fields, M., and Jardine, P. (2004) The Oak Ridge field research center conceptual model. *NABIR Field Research Center, Oak Ridge, TN*.

Wu, L., Liu, X., Schadt, C.W., and Zhou, J. (2006a) Microarray-based analysis of subnanogram quantities of microbial community DNAs by using whole-community genome amplification. *Appl Environ Microbiol* **72**: 4931-4941.

Wu, W.M., Carley, J., Fienen, M., Mehlhorn, T., Lowe, K., Nyman, J. et al. (2006b) Pilot-scale in situ bioremediation of uranium in a highly contaminated aquifer. 1. Conditioning of a treatment zone. *Environmental Science & Technology* **40**: 3978-3985.

Xie, J., He, Z., Liu, X., Liu, X., Van Nostrand, J.D., Deng, Y. et al. (2011) GeoChip-Based Analysis of the Functional Gene Diversity and Metabolic Potential of Microbial Communities in Acid Mine Drainage. *Applied and Environmental Microbiology* **77**: 991-999.

Xu, M., Wu, W.M., Wu, L., He, Z., Van Nostrand, J.D., Deng, Y. et al. (2010) Responses of microbial community functional structures to pilot-scale uranium in situ bioremediation. *Isme j* **4**: 1060-1070.

Zhang, F., Luo, W., Parker, J.C., Brooks, S.C., Watson, D.B., Jardine, P.M., and Gu, B. (2011) Modeling uranium transport in acidic contaminated groundwater with base addition. *J Hazard Mater* **190**: 863-868.

Zhang, P., Van Nostrand, J.D., He, Z., Chakraborty, R., Deng, Y., Curtis, D. et al. (2015) A Slow-Release Substrate Stimulates Groundwater Microbial Communities for Long-Term in Situ Cr(VI) Reduction. *Environmental Science & Technology* **49**: 12922-12931.

Zhang, Y., Lu, Z., Liu, S., Yang, Y., He, Z., Ren, Z. et al. (2013) Geochip-based analysis of microbial communities in alpine meadow soils in the Qinghai-Tibetan plateau. *BMC Microbiol* **13**: 72.

Zhou, J., Bruns, M.A., and Tiedje, J.M. (1996) DNA recovery from soils of diverse composition. *Appl Environ Microbiol* **62**: 316-322.

Zhou, J., Deng, Y., Zhang, P., Xue, K., Liang, Y., Van Nostrand, J.D. et al. (2014) Stochasticity, succession, and environmental perturbations in a fluidic ecosystem. *Proceedings of the National Academy of Sciences*.

Chapter 2 – Figure legends

Figure 1. Geochemical measurements from well FW129 during base amendment. Groundwater concentrations of A) nitrate and sulfate B) redox potential and C) pH and uranium are shown. Subsurface biomass was harvested at T_0 (prior to base addition) and 233, 303 and 352 days after amendment.

Figure 2. Detrended correspondence analysis using A) 17 geochemical variables measured and B) functional genes detected prior to (PM) and during base amendment (pH_a, pH_b and pH_c).

Figure 3. A) Canonical correspondence analysis (CCA) for samples (symbols) grouped by pH measured in the groundwater during base amendment and B) variance partitioning analysis (VPA) for the subset of environmental variables selected for CCA. The VPA diagram represents the relative effect of the groups of variables upon the functional microbial community. All functional genes detected on the array were used for each procedure.

Figure 1.

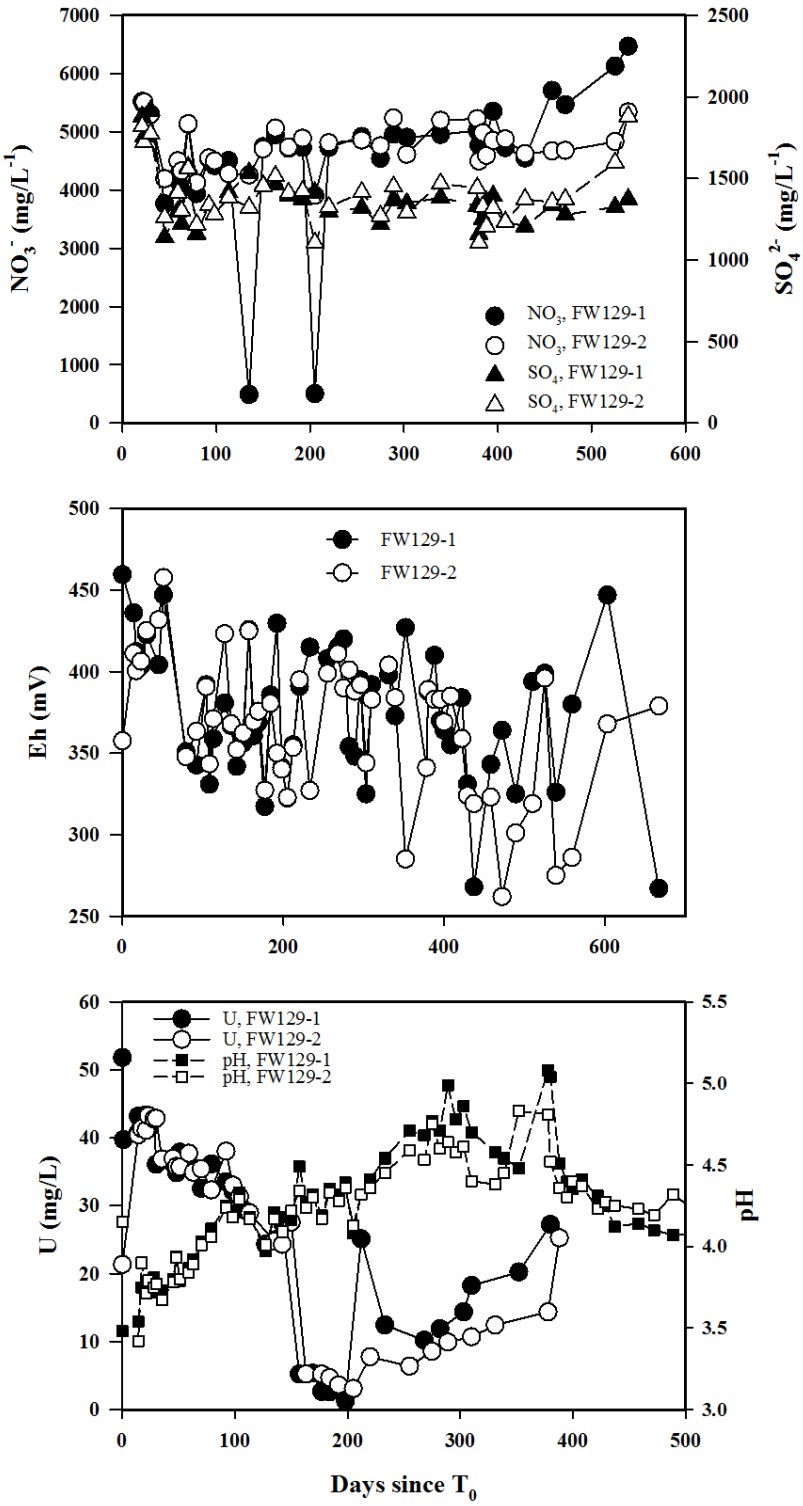
NO3, FW129-1
NO3, FW129-2
SO4, FW129-1
SO4, FW129-2
NO3- (mg/L-1)
SO4 2- (mg/L-1)
FW129-1
FW129-2
Eh (mV)
U, FW129-1
U, FW129-2
pH, FW129-1
pH, FW129-2
U (mg/L)
pH
Days since T0

Figure 2A.

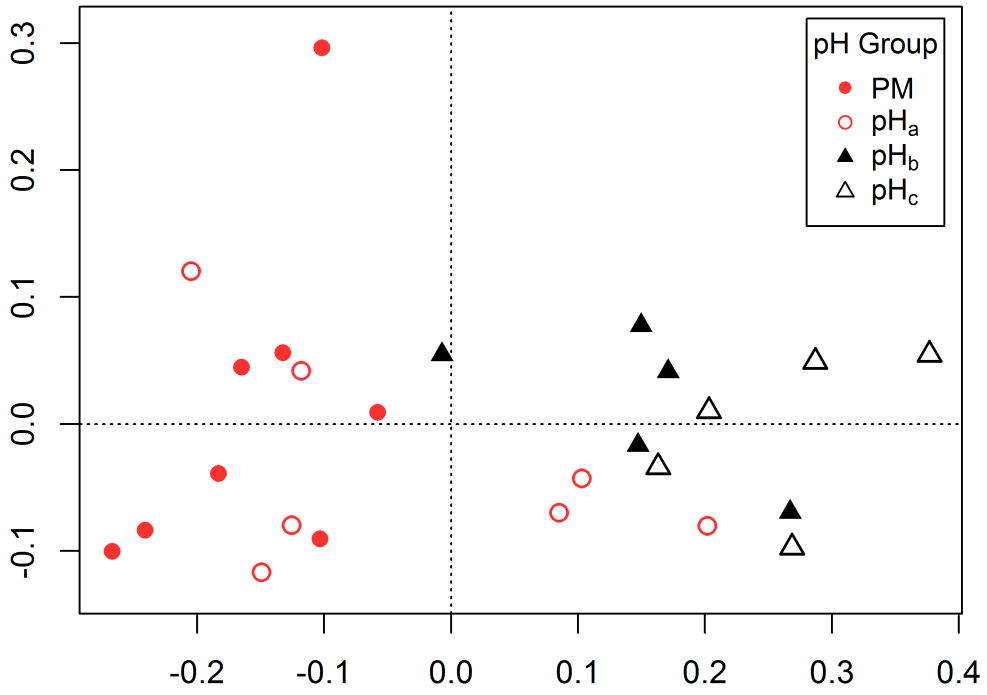

Figure 2B.

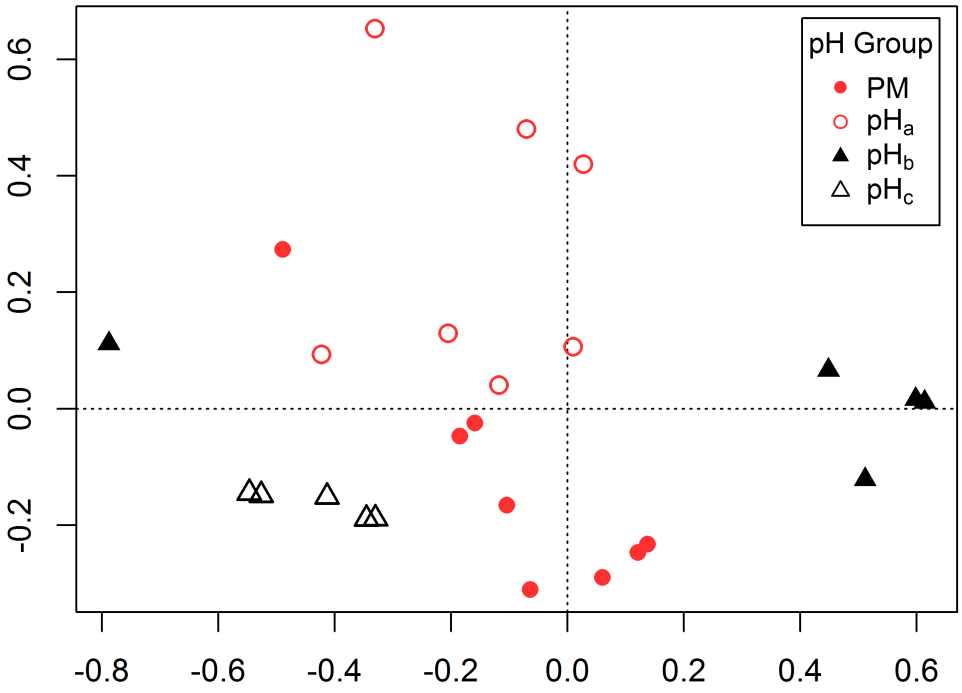

Figure 3A.

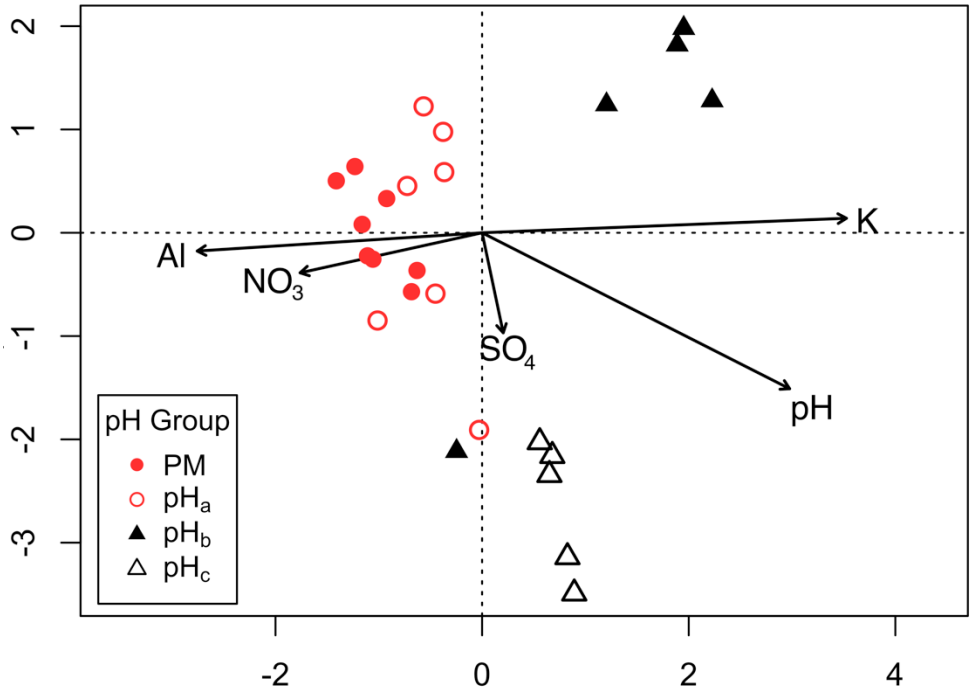

Figure 3B.

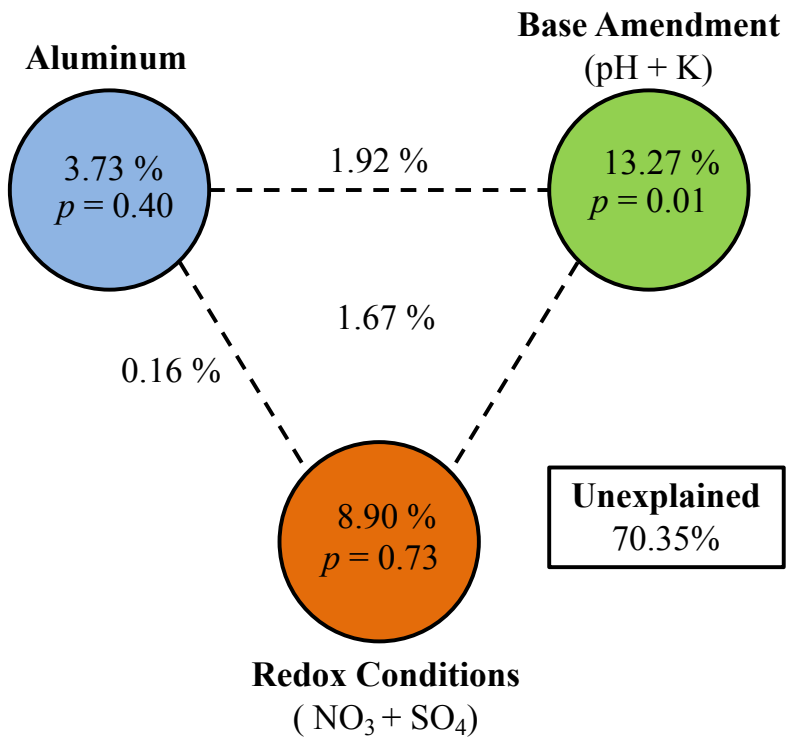
Aluminum
3.73 %
p = 0.40
Base Amendment
(pH + K)
13.27 %
p = 0.01
1.92 %
1.67 %
0.16 %
8.90 %
p = 0.73
Unexplained
70.35%
Redox Conditions
(NO3 + SO4)

Chapter 2

Table 1.

Significance of changes in overall microbial community composition after base amendment revealed by nonparametric multivariate analyses based on Bray-Curtis dissimilarity. MRPP, multiple response permutation procedure; ANOSIM, analysis of similarity and Adonis, permutational multivariate analysis of variance (MANOVA) using distance matrices. All functional genes detected on the array were utilized for each test. Differences between pH categories are considered significant when at least two tests yield a p value < 0.05 (bold).

Comparison	Sample set	MRPP		ANOISM		Adonis	
		δ	p	R	p	F	p
Among pH groups	All 25 samples	0.298	**0.001**	0.39	**0.001**	2.483	**0.001**
PM vs pH_a	15 samples	0.279	0.065	0.164	**0.03**	1.444	0.113
PM vs pH_b	13 samples	0.359	**0.015**	0.368	**0.014**	1.623	0.138
PM vs pH_c	13 samples	0.26	**0.002**	0.58	**0.002**	4.443	**0.001**
pHa vs pH_b	12 samples	0.339	**0.007**	0.322	**0.018**	1.965	**0.021**
pHa vs pH_c	12 samples	0.232	**0.004**	0.488	**0.01**	5.166	**0.008**
pHb vs pH_c	10 samples	0.326	**0.009**	0.592	**0.006**	2.756	**0.028**

Table 2.

Response of functional populations important to microbially driven U(VI) sequestration through bio-reduction; Nitrate reducing bacteria (NRB), Dissimilatory metal reducing bacteria (DMRB) and Sulfate reducing bacteria (SRB). Numbers in bold represent probes that were significantly increased or decreased in abundance during base amendment.

Functional population		Comparison		
		(PM-pH_a)	**(PM-pH_b)**	**(PM-pH_c)**
NRB (*nirK/S* sequences)	Total probes detected	656	656	656
	Unique probes in control group	84	86	242
	Unique probes in treatment group	49	85	4
	Total up	238	208	139
	Total down	218	246	159
	90% CI up	**11**	**0**	**6**
	90% CI down	**0**	**0**	**3**
DMRB (*cytrochrome c* & *hydrogenase sequences*)	Total probes detected	431	431	431
	Unique probes in control group	37	35	141
	Unique probes in treatment group	32	50	6
	Total up	184	135	113
	Total down	144	195	112
	90% CI up	**3**	**1**	**5**
	90% CI down	**2**	**0**	**1**
SRB (*dsrAB* sequences)	Total probes detected	1152	1152	1152
	Unique probes in control group	138	132	435
	Unique probes in treatment group	119	184	20
	Total up	421	353	221
	Total down	347	421	250
	90% CI up	**13**	**0**	**3**
	90% CI down	**4**	**0**	**6**

Supplemental material

Table S1.

Unique and overlapping genes identified during base amendment. [a] Values in bold and italic are unique genes identified in each group. [b] Values not in bold or italic are genes overlapping between two pH categories. [c] Values in bold are the total number of genes detected in each pH category.

Group	No. (%) of overlapping genes			
	PM **(39,244)**	pH_a **(39,441)** [c]	pH_b **(40,244)**	pH_c **(24,580)**
PM	***1,637(4.17%)*** [a]	34,894(79.68%) [b]	33,696(73.58%)	23,721(59.15%)
pH_a		***2,160(5.48%)***	33,228(71.52%)	24,147(60.56%)
pH_b			***4,250(10.56%)***	22,838(54.39%)
pH_c				***54(0.22%)***
Shannon	10.176	10.251	9.863	9.901
I Simpson	28009.42	28731.81	28736.85	20160.85
Simpson E	0.994	0.993	0.994	0.992

Chapter 2 – Supplementary figure legends

Figure S1. Geochemical measurements from well FW130 during base amendment. Groundwater concentrations of A) nitrate and sulfate B) redox potential and C) pH and uranium are shown.

Figure S2. Geochemical measurements from well FW115 during base amendment. Groundwater concentrations of A) nitrate and sulfate B) redox potential and C) pH and uranium are shown.

Figure S3. Mean DNA yield from samples grouped in each respective pH category. PM, samples collected prior to base addition (pH ~3.5); pH_a, samples with groundwater pH 3.5 – 4.0; pH_b, samples with groundwater pH 4.0 – 4.5; pH_c, samples with groundwater pH > 4.5.

Figure S4. Normalized relative abundance of detected archaeal and bacterial C cycling genes. Significant differences ($p < 0.05$) between group means are indicated by different letters. C cycling categories: A, Starch; B, Cellulose; C, Hemicellulose; D, Chitin; E, Lignin; F, Pectin; G, Vanillin; H, Others.

Figure S5. Normalized relative abundance of genes involved in A, methane cycling (*mcrA*, *mmoX* and *pmoA*); B, acetogenesis (*fthfs*) and C, carbon fixation (*aclB*, *codh*, *rubisco* and *pcc*). Significant differences ($p < 0.05$) between group means are indicated by different letters.

Figure S6. Normalized signal intensity of fungal C cycling genes detected in each treatment group. C cycling categories: A, starch; B, cellulose; C, hemicellulose; D, Chitin; E, cutin; F, pectin; G, lignin; H, aromatic carboxylic acid. Significant differences ($p < 0.05$) between means are indicated by different letters.

Figure S7. Normalized signal intensity of N cycling genes detected in each treatment group. N cycling categories: A, ammonification; B, anammox; C, assimilatory N reduction; D, denitrification; E, nitrification; F, dissimilatory N reduction; G, nitrogen fixation. Significant differences ($p < 0.05$) between means are indicated by different letters.

Figure S8. Normalized signal intensity of S cycling genes detected in each treatment group. S cycling categories: A, adenylylsulfate reductase; B, sulfite reductase; C, sulfur oxidation; D, sulfide oxidation. Significant differences ($p < 0.05$) between means are indicated by different letters.

Figure S9. Normalized signal intensity of genes involved in transfer of electrons. Significant differences ($p < 0.05$) between means are indicated by different letters.

Figure S10. Normalized signal intensity of metal resistance genes detected in each treatment group. Significant differences ($p < 0.05$) between means are indicated by different letters.

Figure S11. Normalized signal intensity of stress response genes detected in each treatment group. Stress categories: A, heat shock; B, nitrogen limitation; C, oxygen stress; D, phosphate limitation; E, protein stress; F, sigma factor; G, cold shock; H, glucose limitation. Significant differences ($p < 0.05$) between means are indicated by different letters.

Figure S12. Groundwater re-circulation loop employed in the Area 3 field treatment system at the OR-IFRC.

Figure S1.

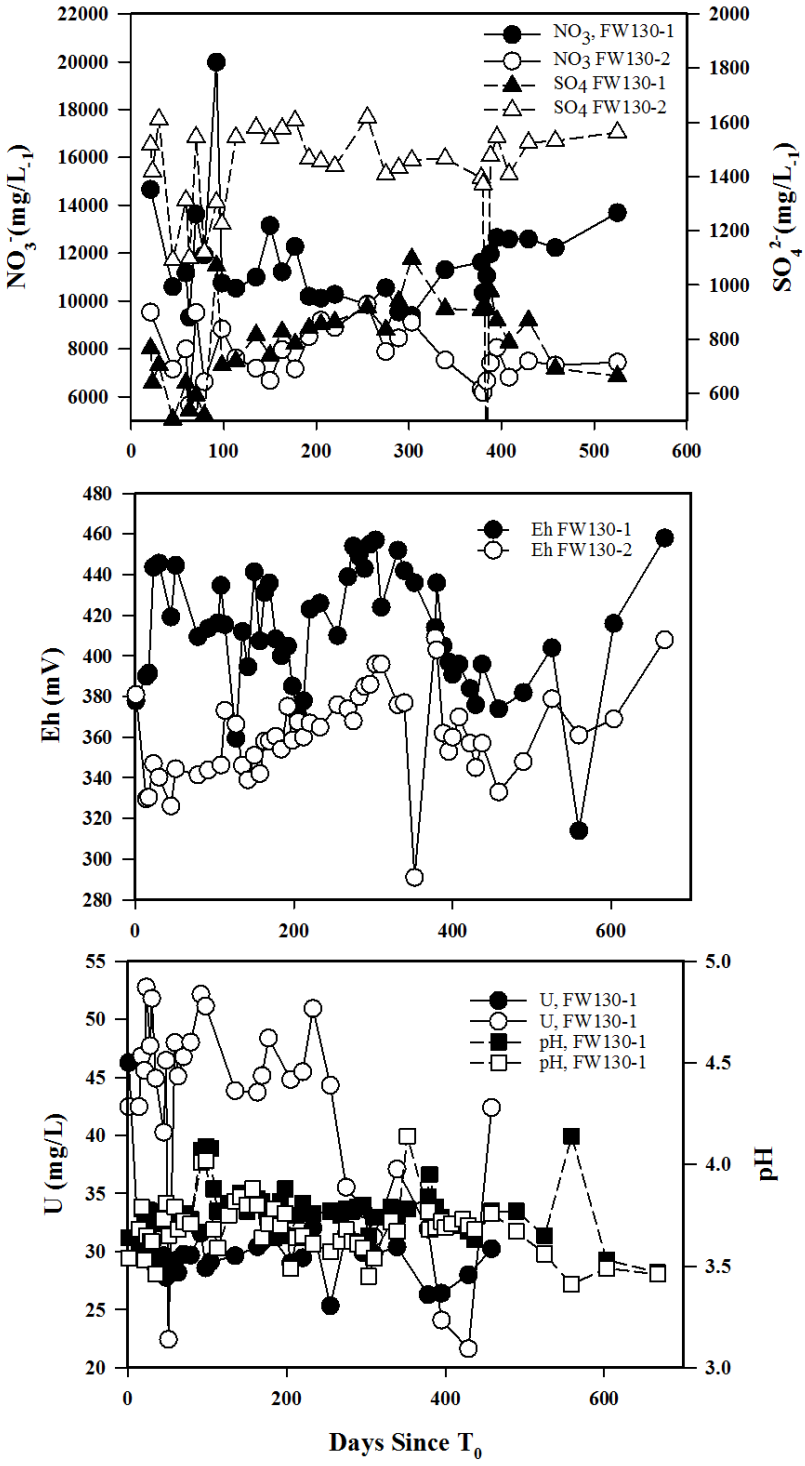
NO3, FW130-1
NO3 FW130-2
SO4 FW130-1
SO4 FW130-2
NO3- (mg/L-1)
SO4 2- (mg/L-1)
Eh FW130-1
Eh FW130-2
Eh (mV)
U, FW130-1
U, FW130-1
pH, FW130-1
pH, FW130-1
U (mg/L)
pH
Days Since T0

Figure S2.

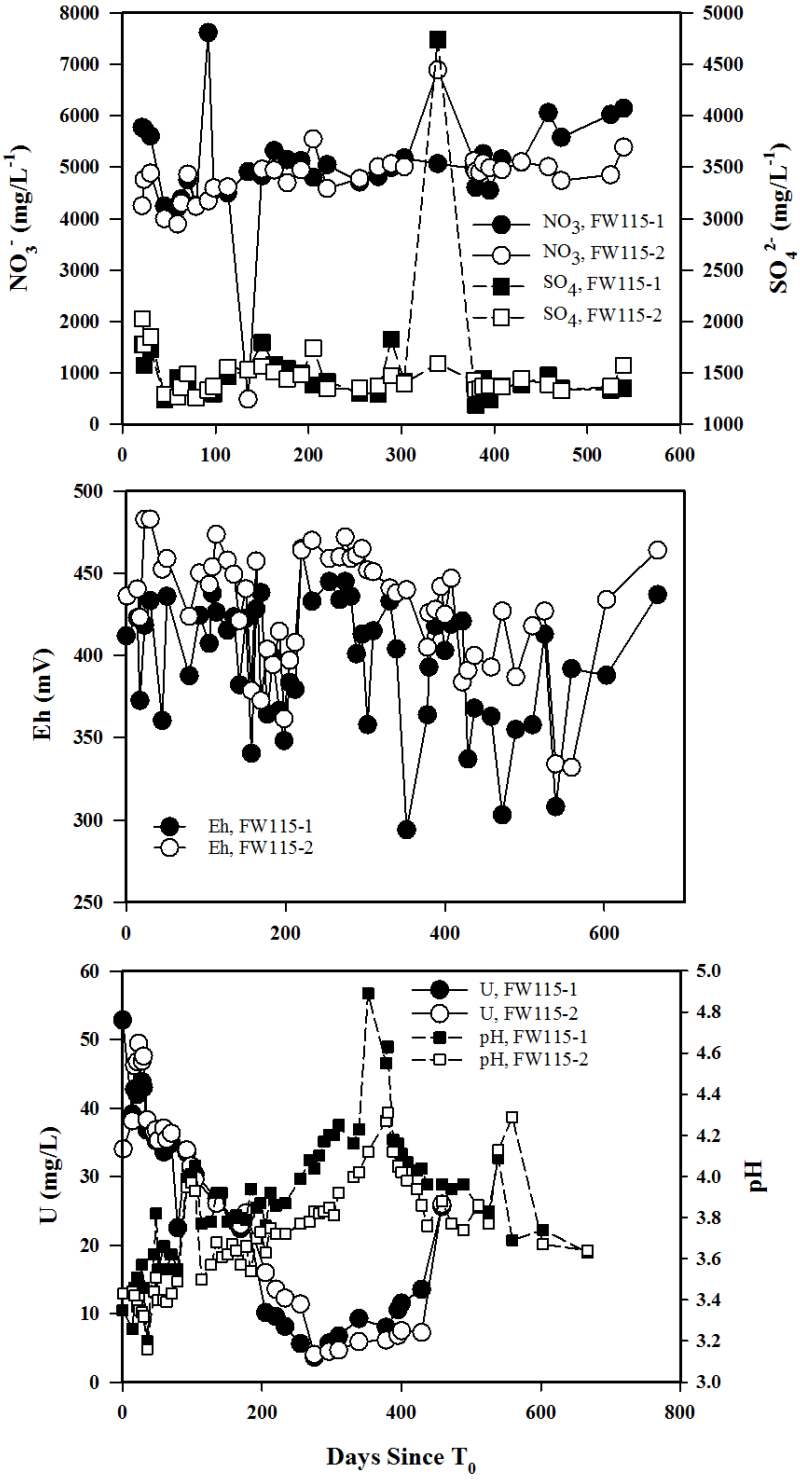
NO3, FW115-1
NO3, FW115-2
SO4, FW115-1
SO4, FW115-2
NO3- (mg/L-1)
SO4 2- (mg/L-1)
Eh, FW115-1
Eh, FW115-2
Eh (mV)
U, FW115-1
U, FW115-2
pH, FW115-1
pH, FW115-2
U (mg/L)
pH
Days Since T0

Figure S3.

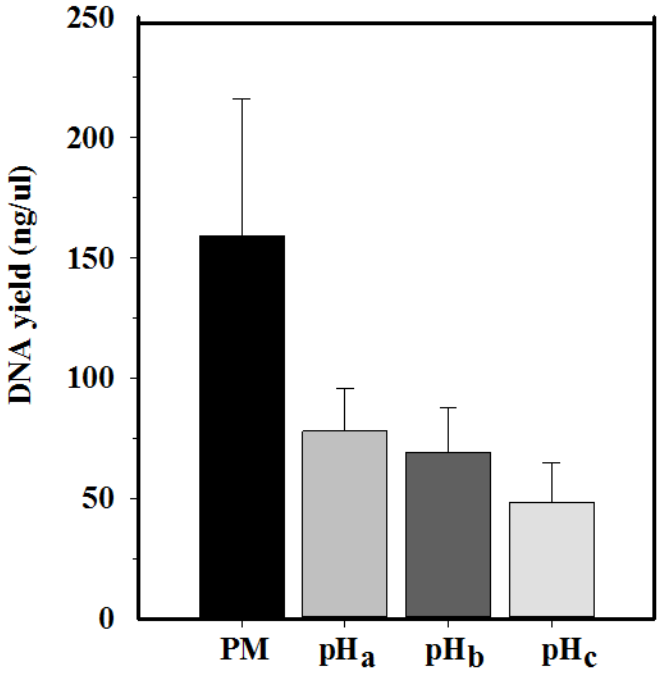

Figure S4.

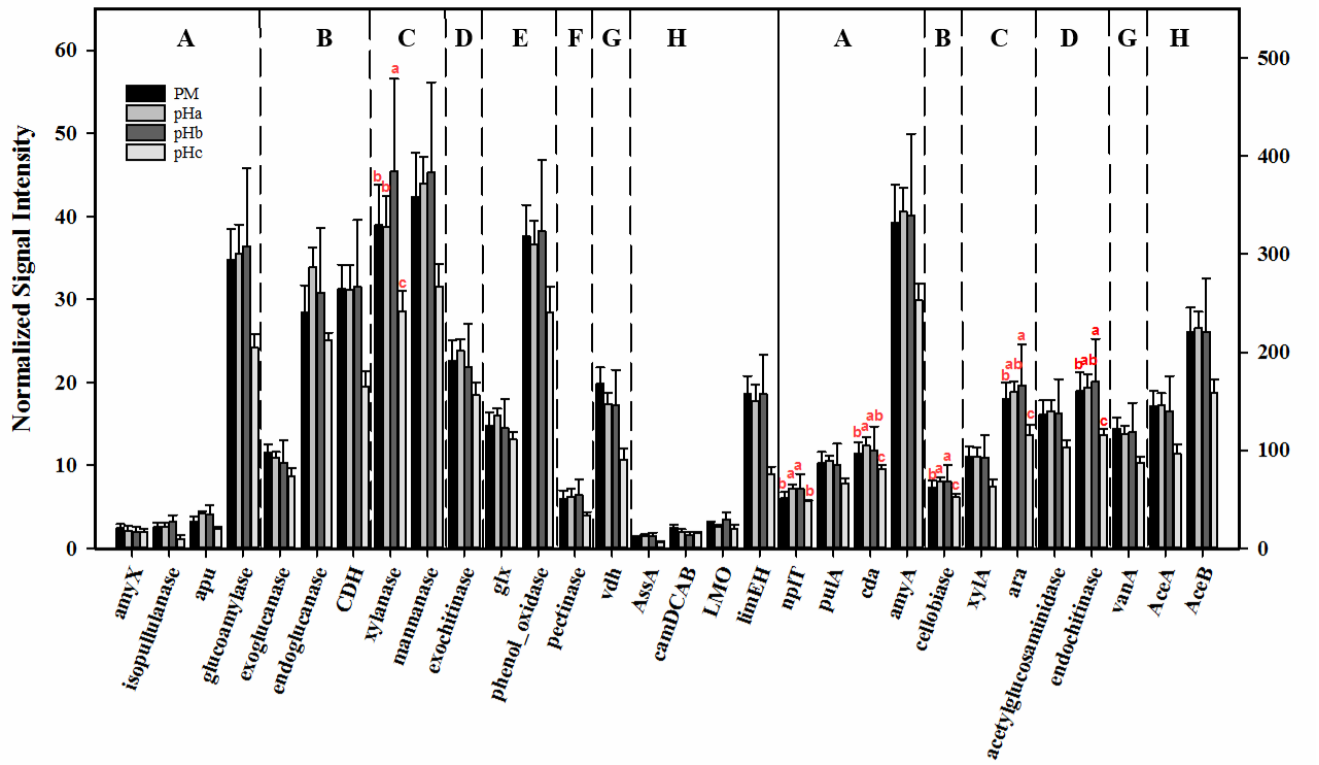
Normalized Signal Intensity
PM
pHa
pHb
pHc
A
B
C
D
E
F
G
H
amyX
isopullulanase
apu
glucoamylase
exoglucanase
endoglucanase
CDH
xylanase
mannanase
exochitinase
glx
phenol_oxidase
pectinase
vdh
AssA
camDCAB
LMO
limEH
nplT
pulA
cda
amyA
cellobiase
xylA
ara
acetylglucosaminidase
endochitinase
vanA
AceA
AceB

Figure S5.

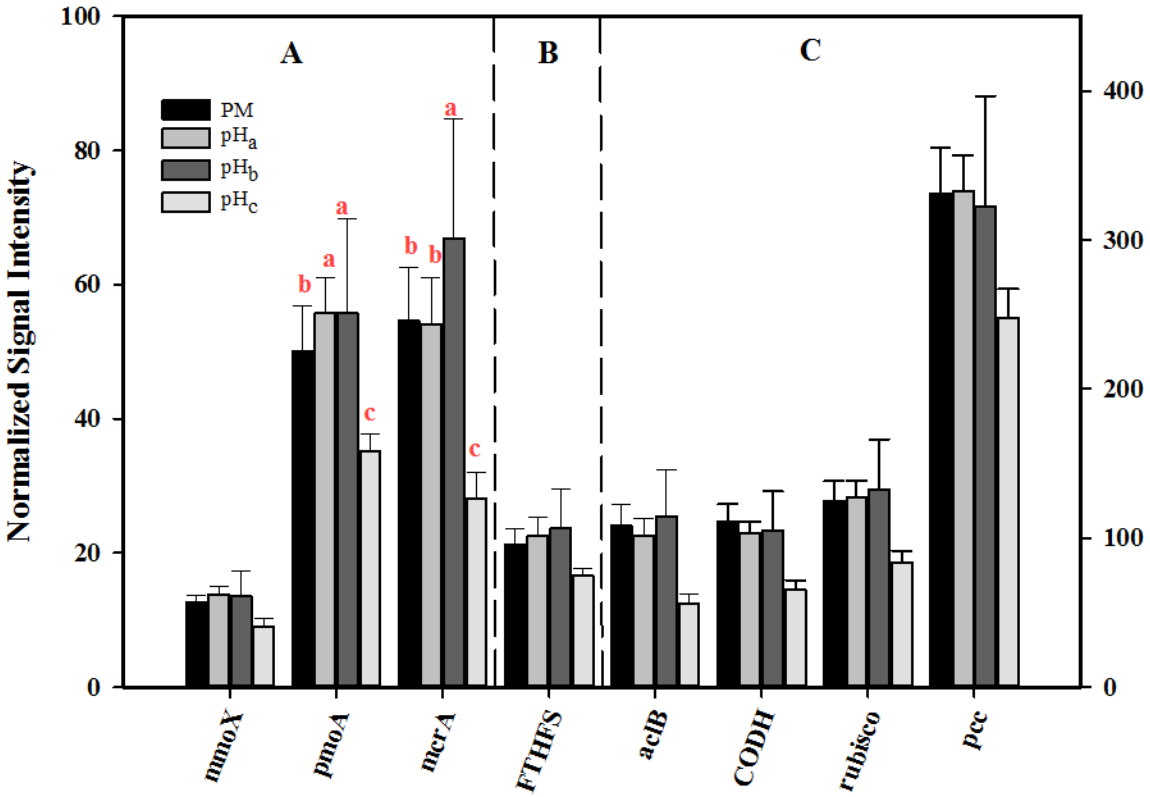
A
B
C
PM
pHa
pHb
pHc
Normalized Signal Intensity
100
80
60
40
20
0
400
300
200
100
0
a
b
c
mmoX
pmoA
mcrA
FTHFS
aclB
CODH
rubisco
pcc

Figure S6A.

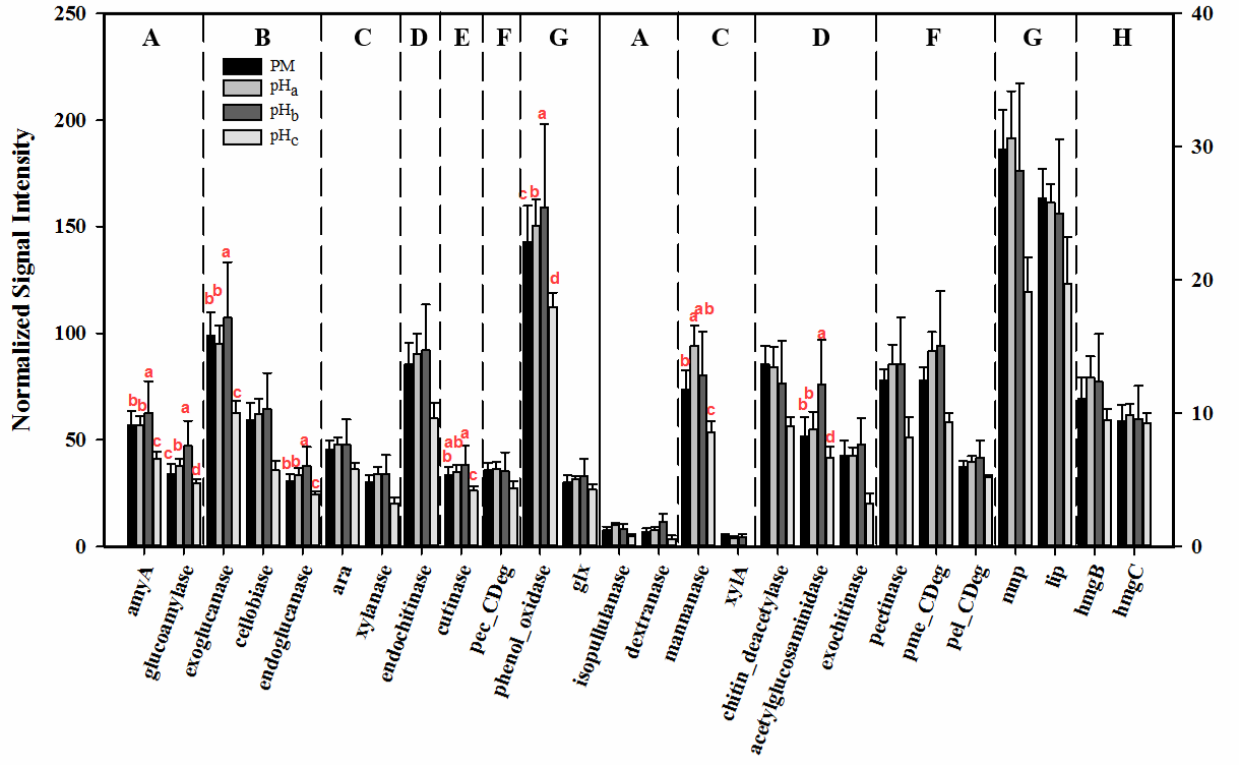
Normalized Signal Intensity
PM
pHa
pHb
pHc
A
B
C
D
E
F
G
A
C
D
F
G
H
amyA
glucoamylase
exoglucanase
cellobiase
endoglucanase
ara
xylanase
endochitinase
cutinase
pec_CDeg
phenol_oxidase
glx
isopullulanase
dextranase
mannanase
xylA
chitin_deacetylase
acetylglucosaminidase
exochitinase
pectinase
pme_CDeg
pel_CDeg
mnp
lip
hmgB
hmgC

Figure S6B.

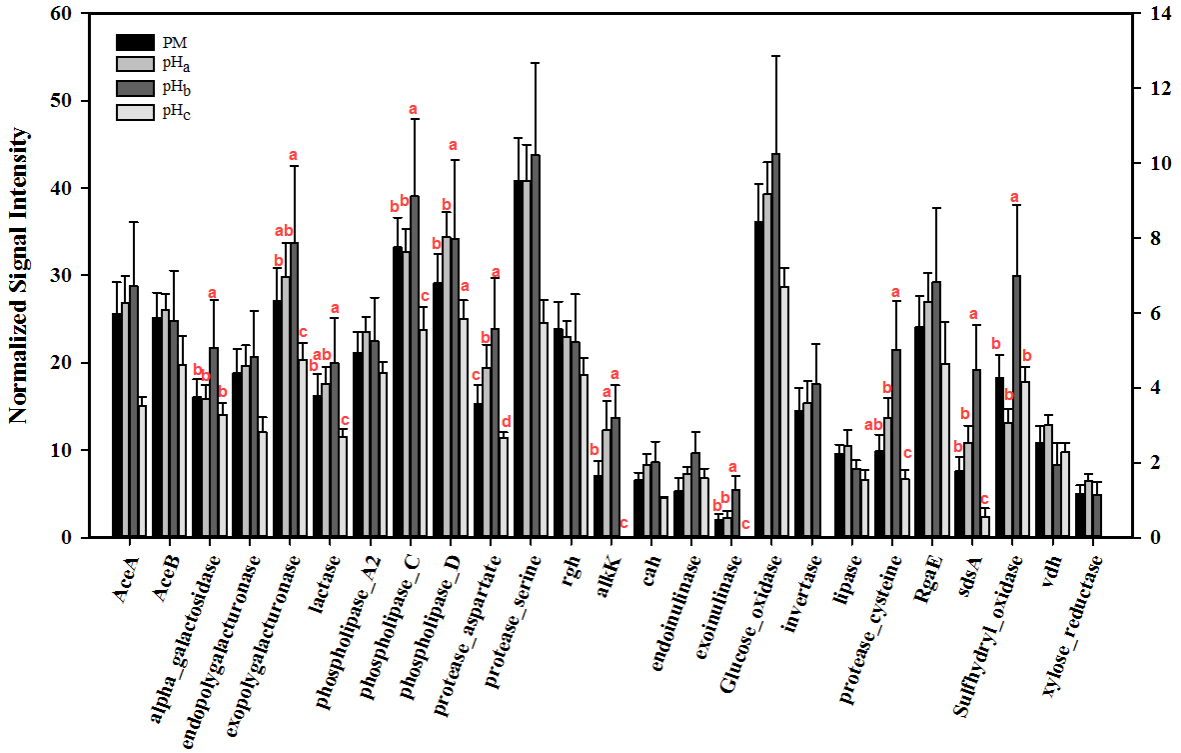
Normalized Signal Intensity
PM
pH$_a$
pH$_b$
pH$_c$
AceA
AceB
alpha_galactosidase
endopolygalacturonase
exopolygalacturonase
lactase
phospholipase_A2
phospholipase_C
phospholipase_D
protease_aspartate
protease_serine
rgh
alkK
cah
endoinulinase
exoinulinase
Glucose_oxidase
invertase
lipase
protease_cysteine
RgaE
sdsA
Sulfhydryl_oxidase
vdh
xylose_reductase

Figure S7.

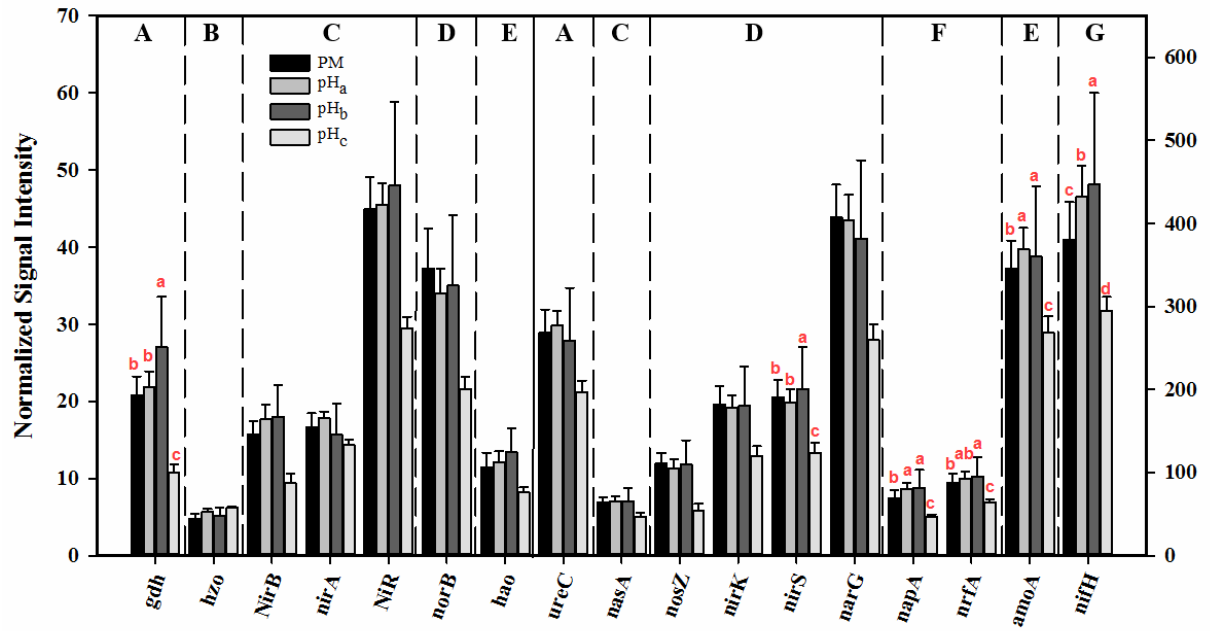
Normalized Signal Intensity
PM
pHa
pHb
pHc
A
B
C
D
E
A
C
D
F
E
G
gdh
hzo
NirB
nirA
NiR
norB
hao
ureC
nasA
nosZ
nirK
nirS
narG
napA
nrfA
amoA
nifH

Figure S8.

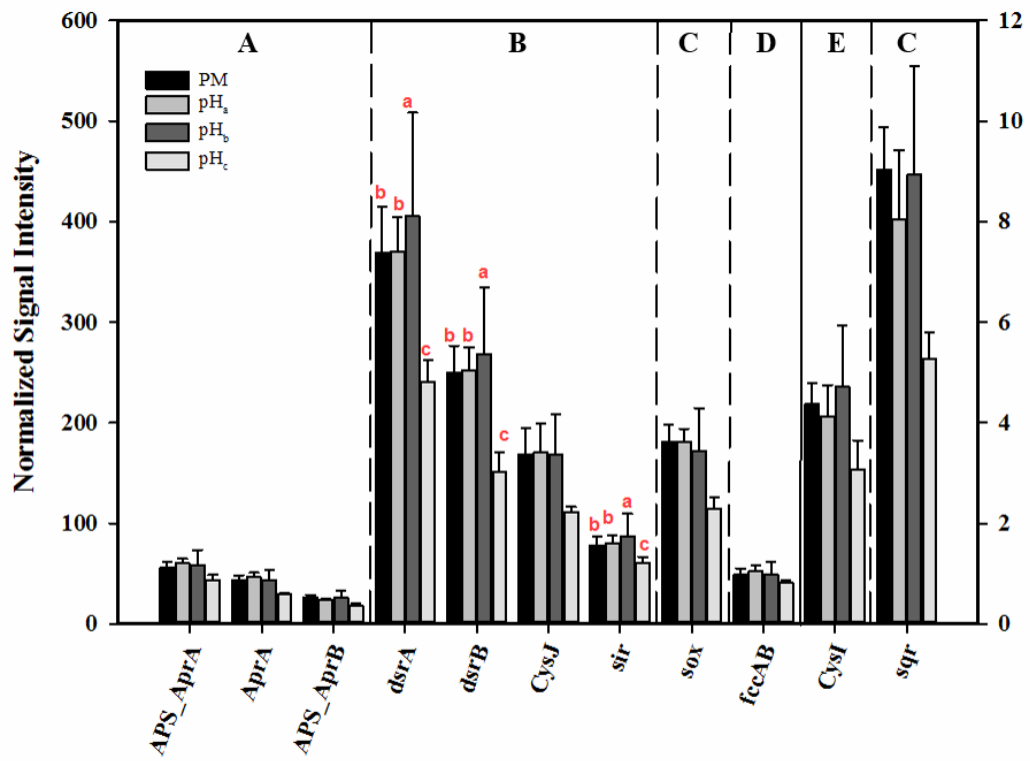
Normalized Signal Intensity
600
500
400
300
200
100
0
12
10
8
6
4
2
0
A
B
C
D
E
C
PM
pH$_a$
pH$_b$
pH$_c$
a
b
b
c
b
b
a
c
b
b
a
c
APS_AprA
AprA
APS_AprB
dsrA
dsrB
CysJ
sir
sox
fccAB
CysI
sqr

Figure S9.

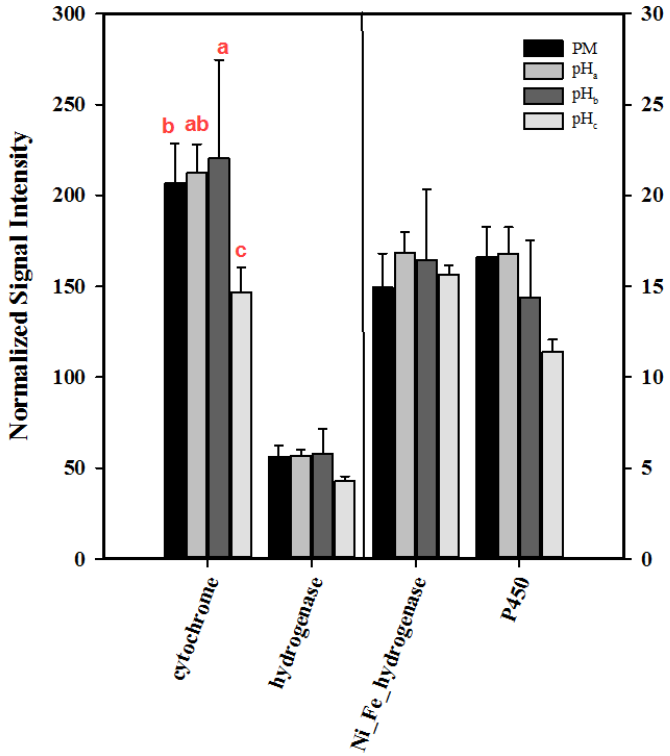
Normalized Signal Intensity
300
250
200
150
100
50
0
30
25
20
15
10
5
0
PM
pH$_a$
pH$_b$
pH$_c$
a
b
ab
c
cytochrome
hydrogenase
Ni_Fe_hydrogenase
P450

Figure S10.

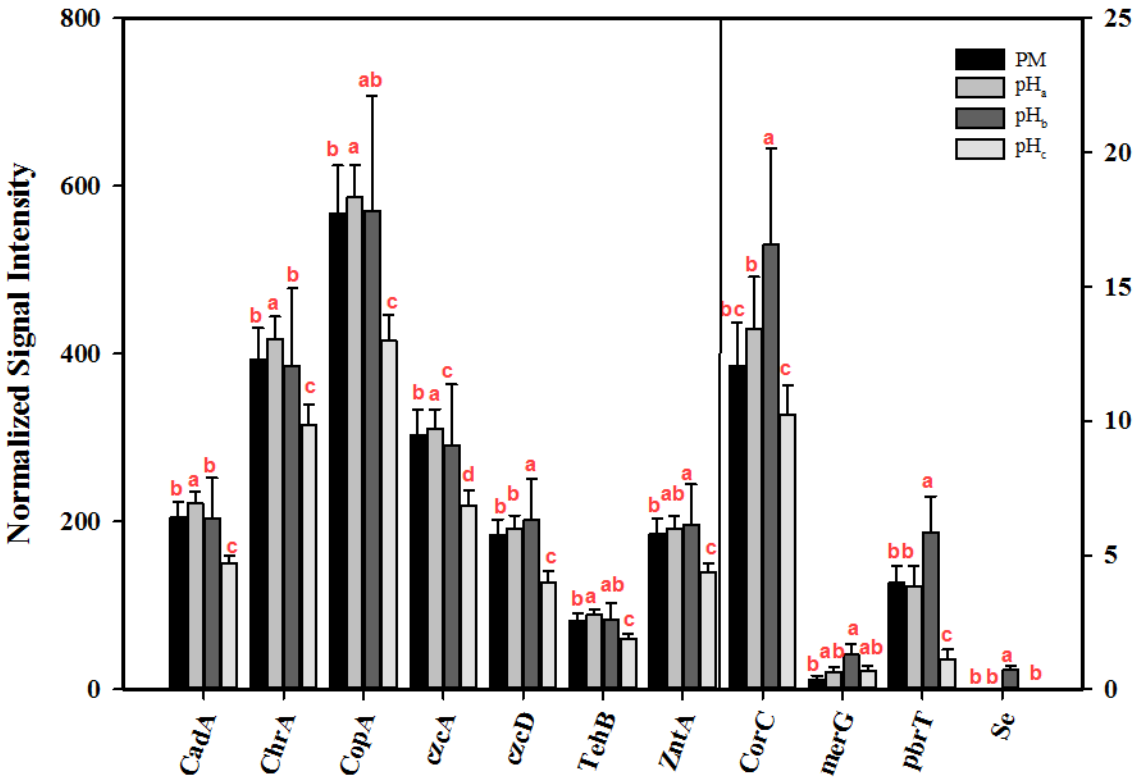
Normalized Signal Intensity
800
600
400
200
0
25
20
15
10
5
0
PM
pH$_a$
pH$_b$
pH$_c$
CadA
ChrA
CopA
czcA
czcD
TchB
ZntA
CorC
merG
pbrT
Se

Figure S11.

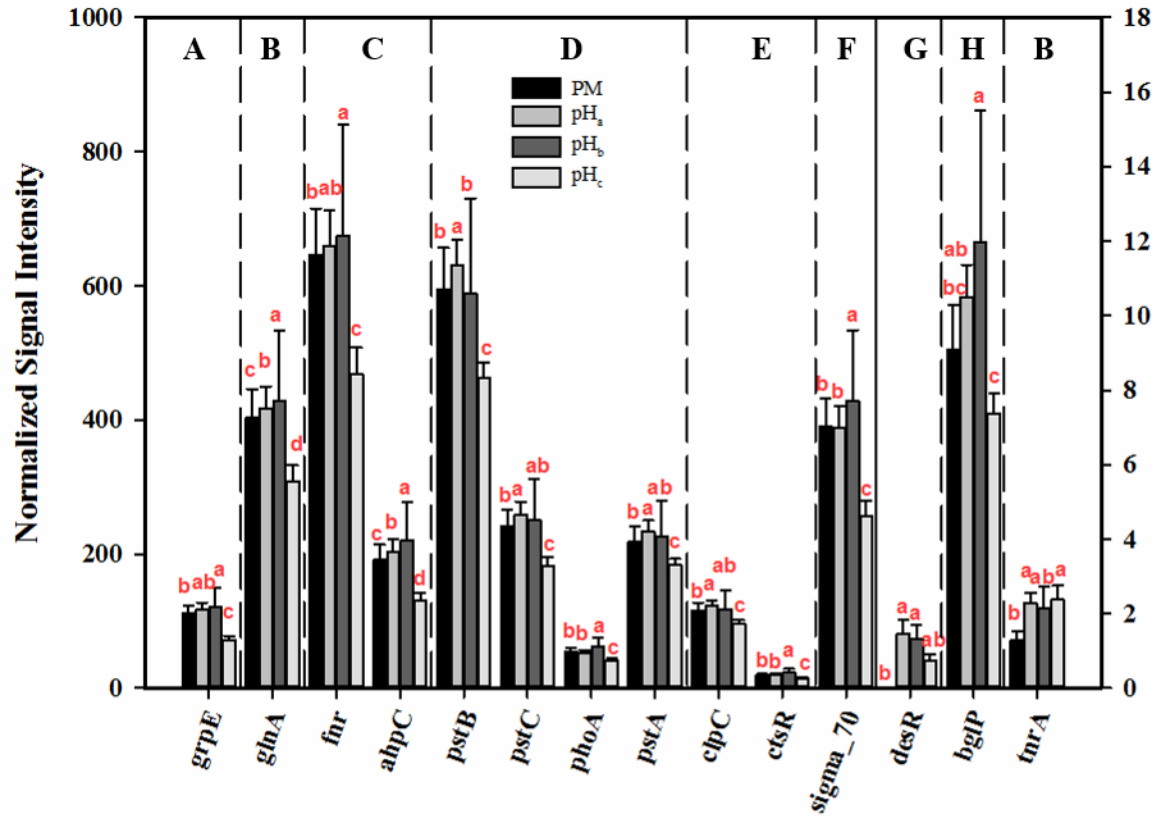
Normalized Signal Intensity
1000
800
600
400
200
0
18
16
14
12
10
8
6
4
2
0
A
B
C
D
E
F
G
H
B
PM
pH$_a$
pH$_b$
pH$_c$
grpE
glnA
fnr
ahpC
pstB
pstC
phoA
pstA
clpC
ctsR
sigma_70
desR
bglP
tnrA

Figure S12.

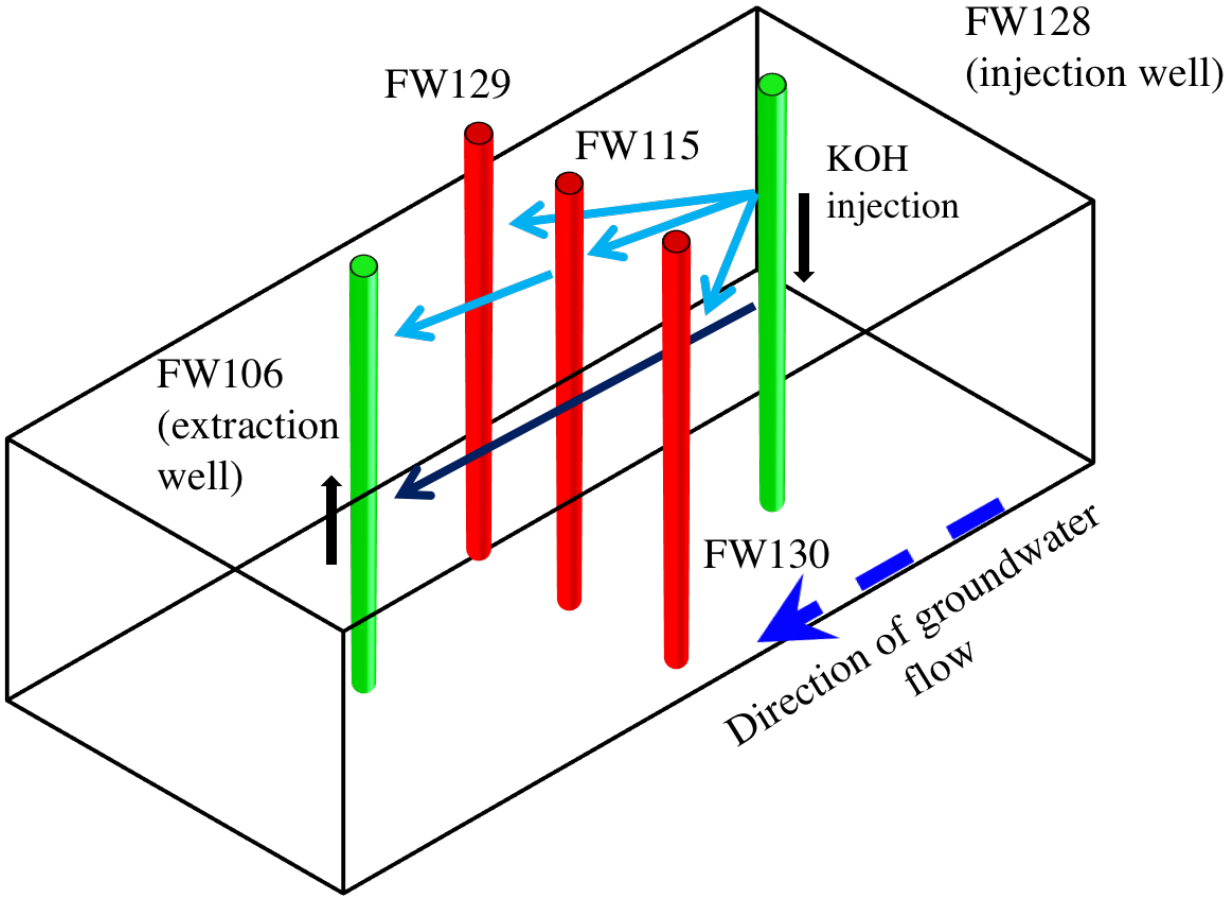
FW128
(injection well)
FW129
FW115
KOH
injection
FW106
(extraction
well)
FW130
Direction of groundwater
flow

CHAPTER 3: Influence of NO_3 on groundwater microbial communities at the OR-IFRC: a unimodal functional response along a NO_3 gradient.

Introduction

Nitrate is contaminant of primary concern in many natural systems due to the imbalance in N cycling stemming from increased anthropogenic activity. From a human health perspective, exposure to excessive nitrate is linked with methemoglobinemia and increased risk of various cancers though the action of genotoxic *N*-nitroso compounds (Ward, 2005). While fertilizer runoff is the primary contributor to the migration of nitrate into water resources worldwide, other sources encompass landfill leachate, discharge of animal and human wastes and the combustion of fossil fuels (e.g. for utilities and energy generation) (Kendall et al., 2007; Burow et al., 2010; Sebilo et al., 2013). While much more localized in terms of their environmental impact, the operation of nuclear facilities such as the Y-12 complex Oak Ridge Reservation has contributed to considerable environmental damage given the nature of wastes generated from refining and processing operations.

At peak operation during the latter part of the 1940s, uranium refining facilitating weapons production at the Y-12 Plant resulted in the disposal of large amounts of mixed wastes in the S-3 Waste Disposal Ponds (Watson et al., 2004b). The unlined surface impoundments continued to receive wastes till they were closed and capped in 1983 and 1988 respectively. Overtime, a large contaminant plume has spread through the aquifer, driven by the natural groundwater flow and higher porosity of the saprolite layer above the bedrock (Cook et al., 1996; Ward, 2005). Nitrate is a main constituent of the plume, with levels of up to ~50,000 mg/L-1 measured in the subsurface adjoining the former S-3 ponds (Gasperikova et al., 2012).

Microbially driven nitrate removal is an important pathway in the N cycle which contributes to the removal of excess nitrate from the environment (Burgin and Hamilton, 2007; Lind et al., 2013). The biological processes driving the cycling of nitrate include dissimilatory nitrate reduction, assimilatory and dissimilatory reduction of nitrate to ammonia (ANRA and DNRA),

chemoautotrophic denitrification and anaerobic ammonia oxidation (annamox). While there is considerable capacity for biological nitrate removal in natural systems, the activity of microbial populations driving the reduction of nitrate is tightly governed by environmental factors spanning pH, oxygen concentration and the availability of suitable electron donors (Kraft et al., 2014). Another constraint on microbial growth stemming from the process of nitrate reduction to dinitrogen gas is the through the action of intermediates from the denitrification process. In this regard, inhibition occurs through the buildup of nitrite and nitric oxide. Nitric oxide is a reactive nitrogen species and exerts cytotoxicity through the disruption of iron centers in proteins, the production of strongly oxidizing species and via mutagenesis resulting from nucleotide transitions in DNA (Zumft, 1997; Lilja and Johnson, 2017). Meanwhile the buildup of NO_2^- has also been attributed to drive bacterial inhibition though mechanisms involving the generation of nitrous acid (Glass et al., 1997).

The study of microbial communities important to denitrification has been a focus at the OR-IFRC given the unique conditions characterized by the extremely high levels of nitrate in areas adjacent to the S-3 ponds. Molecular characterization of *nirK/S* sequences targeting denitrifying communities has revealed them to be structured depending on geochemical conditions (i.e.- pH, nitrate level) along the flow path and in the background area (Yan et al., 2003; Spain et al., 2007). In addition, a comparison of groundwater metagenomes constructed from contaminated and background wells revealed the metabolic capability of the denitrifying genus *Rhodanobacter* was predominantly responsible for metabolic processes under extreme levels of nitrate (Hemme et al., 2015).

Given the potential for microbially induced U(VI) sequestration in contaminated sediments at sites like the OR-IFRC, establishing parameters promoting the activity of subsurface microbial communities during in situ bio-reduction has been the focus of laboratory and field scale

experimentation (Wu et al., 2006b; Van Nostrand et al., 2009a; Tang et al., 2013b). Findings from these studies highlight that nitrate is an important factor contributing to the suppression of the succession of terminal electron acceptor processes (TEAPs), which need to proceed to reach anaerobic conditions favoring metal reduction in the subsurface (Wu et al., 2006b). Such field treatments driving U(VI) sequestration in the sediment proceed to metal reducing conditions when competition from nitrate as a terminal electron acceptor is removed and electron donors are supplied. Furthermore, microcosms evaluating the potential for denitrification revealed that while the process occurred at a slower rate, high nitrate was not a potent barrier to denitrification. (Edwards et al., 2007).

Subsurface communities at the Oak Ridge Integrated Field Research Center have been studied by molecular surveys targeting the 16S rRNA gene and functional genes (*dsrAB*, *nirK/S*) (Spain and Krumholz, 2011; Zhang et al., 2017b) and metagenomic approaches leveraging the GeoChip functional gene array have primarily been employed to trace microbial functional potential primarily during field experiments evaluating how subsurface respond during and after treatment (Van Nostrand et al., 2009b; Van Nostrand et al., 2011). Here we used a tandem approach pairing 16S rRNA gene sequencing with metagenomic analysis using the comprehensive functional gene array (GeoChip 5.0) to address i) How groundwater NO_3 levels spanning a gradient of < 1mgL^{-1} to > 100 mgL^{-1} influence community functional gene composition and abundance at circumneutral pH? ii) What is the taxonomic composition of these communities? and iii) What other environmental factors contribute to influencing both the taxonomic and functional gene profiles across the wells sampled in this study?

Materials and Methods

Site Description and Subsurface Geochemistry

The Oak Ridge Integrated Field Research Center (OR-IFRC) is situated on the Y-12 complex in Oak Ridge, TN. Currently under United States Department of Energy management, the Y-12 complex served as a site for uranium processing that fed nuclear weapons production during the cold war and consists of a 243-acre contaminated site and a 402-acre background uncontaminated site. The disposal of mixed wastes generated from processing ore, has led to subsurface contamination that has come to define this site and the unlined former S-3 ponds which were capped in 1988, have contributed to a contaminant plume that has characterized by uranium, nitrate and pH gradients (Watson et al., 2004b). Detailed information on site can be found at http://www.esd.ornl.gov.orifrc/. Between 2012 and 2013, extensive sampling was undertaken from 100 borewells across the OR-IFRC in support of a groundwater microbial survey so as to better understand the geochemical variables that contributed to shaping microbial community structure. An array of geochemical parameters spanning 38 variables including dissolved gasses, cations and anions were measured from the groundwater collected from each of the wells surveyed. A detailed description of the procedures employed to obtain these parameters can be found here (Smith et al., 2015b).

DNA Extraction and Sample Processing

DNA was extracted using a modified Miller method as described (Miller et al., 1999). Briefly the process involved bead beating with a mixture of phosphate-Tris buffer and phenol-chloroform-isoamyl alcohol. Following this the samples were processed using the MoBio Power Soil Kit

(MoBio Laboratories Inc., Carlsbad, CA) as per the manufacturer's instructions. 100µl of solution S5 was used as the eluent for all samples. Once extracted, DNA was stored at -80°C till the samples were processed for microarray hybridization and 16S rRNA gene sequencing. Multiple displacement amplification (MDA) was performed using 10 ng of the eluted DNA from each sample using the TempliPhi kit (GE Healthcare) as described previously (Wu et al., 2006a). 0.1 mM spermidine and 267 ng ml^{-1} single stranded binding protein was incorporated into the standard buffer to increase the efficiency of amplification. Samples were amplified for 6 h. Samples for which DNA amplification proved troublesome, were concentrated to a volume of 10 µL before using 2-5 µL of the sample for amplification. Amplified DNA was quantified with Quant-iT PicoGreen (Molecular Probes, Eugene, OR) using a FLUOstar Optima microplate reader (BMG Labtech, Jena, Germany) and labeled with Cy-3 using the Klenow fragment and random primers. Finally, the labeled DNA was purified using the QIAquick purification kit (Qiagen, USA) per the manufacturer's instructions and dried in a SpeedVac (ThermoSavant, USA). The DNA was suspended in a cocktail containing hybridization HI-RPM hybridization buffer, Acgh blocking agent, Cot-1 DNA, universal standard DNA and formamide (10%) and subsequently hybridized to a functional gene array, GeoChip 5.0, over 24hrs at 67°C on a MAUI hybridization station (BioMicro Systems, Salt Lake City, UT, USA). The GeoChip is a high-density functional gene array and version 5.0 used in this study, has 4 arrays containing 50-mer oligonucleotide probes (1670.44 probes in all). Detailed information on the probes used on the array is available at www.ou.edu/ieg/tools.html/.

Microarray Scanning and 16S rRNA amplicon processing

Arrays were scanned on an Agilent SureScan microarray scanner (Agilent Technologies, Santa Clara, CA) and pixel density quantified from scanned images and spots with signal-to-noise

ratios lower that 2 were removed prior to statistical analysis. Positive signals were classified based on a signal-to-nose criterion ≥2 ({signal mean-background mean}/background standard deviation). A positive signal in a minimum of 2 probes was the threshold for a signal to be categorized a positive. Signal intensity of each spot was normalized by the mean-ratio method (He et al., 2007a). Data normalization was performed on raw microarray data generated from custom scripts incorporated on a pipeline designed at the IEG. Sequence data from the V4 hypervariable region of the 16S rRNA gene was trimmed using BTRIM (Kong, 2011)with a quality score threshold of 25 over a 5bp sliding window size. Minimum length for trimmed sequences was 100bp. FLASH (Magoč and Salzberg, 2011) was used to join forward and reverse reads with a minimum 50bp overlap and 25% mismatch threshold. Sequences with joined length between 245-260bp were subjected to chimera removal using UCHIME (Edgar et al., 2011) and the SILVA 132 Ref NR database (Quast et al., 2013) after removal of ambiguous bases (i.e. Ns). OTU clustering was performed at the 97% similarity level using UPARSE (Edgar, 2013) and singletons were removed resulting in a final dataset with 8854 OTUs. Each sample was randomly resampled to 21,800 sequences to account for differences in sequencing depth between each sample. The above steps pertaining to 16S rRNA sequence processing were performed on the Galaxy Amplicon Sequence Pipeline (https://zhoulab5.rccc.ou.edu/) Taxonomic assignment of representative sequences was performed using the RDP Classifier (Wang et al., 2007) available at https://rdp.cme.msu.edu/classifier/classifier.jsp with a confidence threshold of 0.5. Sequences assigned taxonomic ranks with bootstrap values below 50% were assigned an 'Unclassified' rank. To examine correlations between detected OTUs and environmental variables only those OTUs that were present in more than 50% of all samples were used.

Statistical Analysis

All statistical tests and ordination analysis were performed using R (v3.4.0; www.r-project.org/). Unique and overlapping probes detected on the microarray and OTUs detected by 16S rRNA gene amplicon sequencing were determined using custom R scripts. Comparisons estimating the difference in means for geochemical variables and α diversity indices were estimated using one-way ANOVAs. Post-hoc Tukey's honest significant difference (HSD) tests were implemented to test differences between treatments for geochemical variables and α diversity estimates. Post-hoc Fisher's least significant difference (LSD) tests were paired with ANOVAs fort the analysis of functional gene abundance data and p values were adjusted using Holm's method. Non-parametric multivariate analysis based on dissimilarities between samples in different groups estimated using Bray-Curtis distances were used to determine the dissimilarity of microbial taxonomic composition and functional gene profiles. This was performed using Multiresponse Permutation Procedures (MRPP) (Van Sickle, 1997), Analysis of Similarity (ANOISM) (Clarke, 1993) and Permutational Multivariate Analysis of Variance using Distance Matrices (Adonis) (Anderson, 2001). Canonical correspondence analyses (CCA) (Ter Braak, 1986) was performed to identify the correlations between groundwater geochemistry and microbial community composition. BIOENV (Clarke and Ainsworth, 1993) and forward selection were used to identify the subset of variables used for CCA analysis. R packages used for statistical analysis included VEGAN (Oksanen et al., 2013) and AGRICOLAE (De Mendiburu, 2014). Plots were prepared in R or SigmaPlot 13.0 (Systat Software, Inc., San Jose, CA).

Sample Selection

Since DNA yields from many of the samples were very low, a subset of 69 wells which covered the broad geochemical gradients observed in the wells sampled during the survey could be used

to generate metagenomic information using the functional gene array (He et al., 2018). 16S rRNA gene sequence data generated from 0.2um filters was available for all 100 wells sampled during the comprehensive survey (Smith et al., 2015a). For this study, wells were selected which covered a gradient in nitrate and for which data was available from both the GeoChip 5.0 functional gene array and from 16S rRNA gene sequencing datasets. These wells were selected such that each had a circumneutral pH (pH 6.0 – 8.0) at the time of sampling and were organized into three groups- OR_{LN} (< 1mgL^{-1} NO_3^-, 6 wells), OR_{MN} (10 – 100 mgL^{-1} NO_3^-, 8 wells) and OR_{HN} (> 100 mgL^{-1} NO_3^-, 6 wells) (Table S3, Figure S1). These groups were established according to Maximum Contaminant Levels (MCL) established by the United States Environmental Protection Agency (https://www.epa.gov/ground-water-and-drinking-water/table-regulated-drinking-water-contaminants#two). For nitrate, the MCL is 10 mgL^-.

Results

Groundwater Microbial Composition and Structure

Acridine orange direct counts (AODC) measurements revealed lower average cell counts in the OR_{MN} and OR_{HN} treatments, however the differences in counts between treatments was not significant (Figure S2). There were no significant differences identified either in the number of OTUs or probes detected in wells across the three treatments (Table S1). Furthermore, α diversity estimates based on analysis of the 16S rRNA genes and detected functional genes revealed insignificant differences between treatments. While a clear grouping of samples by treatment was absent in DCA ordination plots when analyzing the 16S rRNA gene, stronger clustering of samples was evident in ordination plots using functional gene data (Figure S3). DCA plots representing functional populations important to remediation efforts (NRB, SRB and

DMRB), revealed each of these populations forming distinct clusters in OR_{LN}, OR_{MN} and OR_{HN} wells (Figure S4). Dissimilatory tests (MRPP, Adonis and ANOSIM) revealed differences in composition based on taxonomy to be significant ($p < 0.05$) between OR_{LN} and OR_{HN} wells and OR_{MN} and OR_{HN} wells respectively. Additionally, differences in functional gene composition based on all genes detected were significant for comparisons between all three treatments (Table 1). The highest percentage of unique OTUs were identified in the OR_{HN} wells (38%) while the OR_{LN} and OR_{MN} wells had similar numbers of unique OTUs present. 25 – 39% of the ~ 4000 OTUs detected across treatments were shared between groups (Table S2). Over 80% of the functional genes detected were shared between treatment groups with the highest number of genes detected in the OR_{MN} wells. The OR_{MN} wells also had a higher percentage of unique functional genes (7.13%) when compared to the OR_{LN} and OR_{HN} wells. Between 22 – 43% of OTUs could not be assigned accurately to a class across the treatment groups (Figure S11). Nine taxonomic classes were found to differ significantly ($p < 0.05$) in relative abundance between at least two treatment groups. From those taxonomic classes that were present >1% in each treatment, OTUs assigned to *Sphingobacteria*, *Chlamydiia* and *Nitrospira* were most abundant in OR_{LN} wells and those assigned to *Alphaproteobacteria* were found at highest abundance in OR_{MN} wells. Those taxonomic classes (*Anaerolineae*, *Ignavibacteria*, *Acidobacteria_Gp15*, *Acidobacteria_Gp17*) with significantly higher abundance in the OR_{HN} wells were found to be present at <1% RA of those detected. At the OTU level (Figure S10), 12 OTUs of which 5 could be assigned to the genera *Nitrosopumilus* (9.6%), *Pseudomonas* (3.4%), *Sediminibacterium* (2.4%), *Brevundimonas* (1%) and *Sideroxydans* (1%) were at >1% of the total OTUs in OR_{LN} wells. 15 OTUs were found to be >1% RA in OR_{MN} wells, 9 of these could be assigned to the genera *Brevundimonas* (7.5%), *Rhodopseudomonas* (3.6%), *Massilia* (2.6%), *Arthrobacter* (1.9%), *Cupriavidus* (1.9%), *Roseateles* (1.8%), *Malikia* (1.3%) and *Afipia* (1.2%). The OR_{HN}

wells contained the highest number (11) of OTUs at >1% RA for which a taxonomic rank at the genus level could not be assigned. *Sideroxydans* (8.9%), *Pseudonomas*(2.6%), *Acidobacteria_Gp6* (1.18%) and two members identified as *Nitrospira* (*2%* and *1%*) made up the remainder of these OTUs.

Changes in Functional Genes Involved in Important Microbial Processes

C Cycling Genes

A total of 7201 bacterial and archaeal probes, representing 34 genes associated with the metabolism of labile and recalcitrant C compounds were detected across the treatment groups (Figure S5). Twenty-three of these genes had the highest abundance in the OR_{MN} wells and were significantly different ($p < 0.05$) between at least two of the treatment groups. From those genes that differed between all three treatment groups, *lmo* involved in the breakdown of terpenes was found to have the lowest relative abundance in the OR_{HN} wells. *aceB, amyA, pulA, cellobiase, ara, xylA, acetylglucosaminidase, chitinase* and *vdh* had the lowest relative abundance in the OR_{LN} wells. Methane cycling was evaluated using 84 probes covering genes involved in methanogenesis and 70 probes representing methane oxidation genes detected in all treatment groups. *mcrA*, had peak relative abundance in OR_{MN} wells and was significantly different between all groups of wells. *pmoA* was the only gene involved in methane oxidation that significantly deferred between two treatments with highest abundance in OR_{MN} wells.

N Cycling Genes

Nitrate is a major contaminant and serves as an electron acceptor in the groundwater. Eighteen of the 25 genes involved in N cycling were found to be significantly different ($p < 0.05$) across the three treatment groups with the highest relative gene abundance detected in the OR_{MN} group

(Figure 1). Eight of the genes were found to have lowest relative abundance in the OR_{LN} group. *ureC* and *gdh* encoding urease and glutamate dehydrogenase respectively are involved in the generation of ammonia for biosynthesis. Denitrification genes that followed this trend included *narG* encoding nitrate reductase, *nirK/S* encoding nitrite reductases and *nosZ* encoding nitrous oxide reductase. Finally, *nrfA* and *nifH* encode a nitrate reductase involved in dissimilatory nitrate reduction and dinitrogen reductase respectively. Nitrate reductase enzymes encoded by *nasA, narB, nirA, nirB* and *NiR* involved in assimilatory nitrate reduction and *napA* encoding a dissimilatory nitrate reductase had highest relative abundance in OR_{MN} wells. *norB* encoding nitric oxide reductase involved in denitrification and *amoA* and *hao* genes involved in nitrification also followed this trend. Overall, functional potential for assimilatory processes and N mineralization were relatively equal in OR_{LN} and OR_{HN} wells. The functional potential for genes responsible for N ammonification, denitrification and N fixation were lowest in the OR_{LN} group. Significant ($p < 0.05$) correlations between key genes involved in denitrification revealed 25 *nirK/S* sequences to be positively correlated with nitrate while 52 *nirK/S* sequences to be negatively influenced by the nitrate gradient.

S Cycling Genes

Four genes involved in S cycling that significantly ($p < 0.05$) differed in abundance were detected at highest relative abundance in the OR_{MN} wells and relatively equal abundance in both OR_{LN} and OR_{HN} wells (Figure 2). *dmdA* encoding a transferase involved in DMSP degradation, *cysI/J* encoding sulfite reductase subunits, a sulfide dehydrogenase (*fccAB*) and *sox* encoding a sulfide oxidase enzyme for H_2S reoxidation. *5f1_DMSP_lyase* encoding a DMSP lyase gene, *sir* encoding a sulfite reductase and *sqr* encoding a sulfide reductase were at highest relative abundance in OR_{MN} wells. Sequences representing dissimilatory adenosine-5'-phospho-sulfate

reductase (*aprAB*) and sulfite reductase (*dsrAB*), which are key genes in dissimilatory sulfate reduction were detected at highest relative abundance in OR_{MN} wells and lowest relative abundance in OR_{LN} wells. Further analysis of *dsrAB* sequences (Figure S6) revealed *Desulfatibacillum*, *Desulfobacterium*, *Desulfobulbus, Thioalkalivibrio* like sequences were found at highest relative abundance in OR_{LN} wells. *Desulfohalobium, Desulfomicrobium, Desulfosporosinus,* and *Pleodictyon* had highest functional potential in OR_{MN} wells. *Ammonifex*, *Chlorobium*, and *Methanosarcina* like species were detected at highest relative abundance in OR_{HN} wells. *Pyrobaculum* like sequences were enriched in OR_{LN} and OR_{HN} wells while sequences from *Desulfovibrio* species were enriched in wells with higher nitrate levels. *Desulfotomaculum* like sequences were enriched in each of the treatment groups. 34 *dsrAB* sequences were found to be significantly ($p < 0.05$) positively correlated with the gradient in nitrate across the wells. Sequences from identified genera among those positively correlated belonged to *Chlorobium*, *Desulfotomaculum*, *Methanohalophilius*, *Methanosarcina* and *Pyrobaculum*. 100 *dsrAB* sequences were negatively correlated with the nitrate gradient. These included sequences belonging to 15 genera which included *Acetobacterium*, *Chlorobium* , *Clostridium*, *Desulfacinum*, *Desulfoglaeba*, *Desulfohalobium*, *Desulfotomaculum*, *Desulfovibrio*, *Geobacter*, *Methanohalophilus*, *Methanoregula*, *Pyrobaculum Syntrophobacter*, *Thermodesulfobacterium* and *Thermoproteus*.

Genes Involved in Metal Reduction

Cytochrome c and some *hydrogenase* genes are known to be involved in electron transfer driving dissimilatory metal reduction. 212 *cytochrome c* and 66 *hydrogenase* probes were detected across the three treatments (Figure S7, Figure S8). c*ytochrome c* sequences from *Pseudomonas*, were seen to be enriched in either OR_{LN} or both OR_{MN} and OR_{HN} wells. Those from *Geobacter*

were enriched in OR_{LN} wells while those from *Shewanella* species were found to be enriched in either OR_{MN} or OR_{HN} wells. *hydrogenase* sequences from *Geobacter* and *Desulfovibrio* were found to be enriched in wells with higher nitrate concentrations while *Shewanella* like *hydrogenase* sequences were enriched in OR_{LN} wells. 6 *cytochrome c* sequences were significantly ($p < 0.05$) positively correlated while 28 *cytochrome c* sequences showed the opposite trend in relation to the nitrate gradient. None of the *hydrogenase* sequences were positively correlated with the nitrate gradient.

Influence of Groundwater Geochemistry on Microbial Community Structure

CCA analysis using OTUs detected revealed pH (VIF = 2.15), NO_3^- (VIF = 2.32), Ca (VIF = 2.39), Eh (VIF = 1.72), S^{2-} (VIF = 1.82), DOC (VIF = 1.46) and Mn (VIF = 1.67) to best explain the variation in taxonomic composition (Figure 4A) however, the model was only marginally significant ($p < 0.1$). Higher pH, Mn and Eh exerted the strongest influence on composition in most of the wells across the treatment groups. These 7 variables accounted for 39.99% of the taxonomic variation. The first axis accounted for 7.42% and the second 6.67% respectively. DO (VIF = 1.32), Eh (VIF = 1.40), DIC (VIF = 1.79), NO_3^- (VIF = 2.32), SO_4 (VIF = 1.77), Na (VIF = 2.33) and pH (VIF = 1.53) were identified to play an important role in influencing the groundwater microbial community structure based on functional gene composition (Figure 4A). The CCA model incorporating these 7 environmental variables was able to explain (42.16%) of the total variation in gene abundance across the three treatments. The first CCA axis contributed 11.66% and the second axis contributed 9.78% of the explained variation. Eh, DO and pH were seen to exert the strongest influence for samples in the OR_{LN} and OR_{MN} wells. Na, K and NO_3^- had the strongest influence on the microbial composition in the OR_{HN} wells. Variance

partitioning analysis (VPA) indicated NO_3 explained a greater percentage of the variation seen in functional gene composition compared to taxonomy in the wells (Figure S9A, Figure S9B).

Discussion

Microbial communities play a key role in supporting ecosystem function and it is important to understand the effects anthropogenic disturbances have on them. In this study we examine the effects of contaminants along a nitrate gradient on subsurface microbial community composition at the OR-IFRC. Additionally, we describe the effects this gradient has on the functional potential of groundwater microbial communities driving C, N and S cycling and those populations playing an important role in remediation efforts at the site (i.e. NRB, SRB and DMRB). The results indicate that community function is structured along the nitrate gradient whereas taxonomic composition is less clearly defined by this gradient. Furthermore, at extremely high nitrate levels overall functional potential was reduced and similar to that seen in wells with low nitrate.

Studies exploring the influence of mixed contamination on microbial function and diversity, consistently report a negative correlation in relation to increased contamination in a given environment (Kandeler et al., 1996; Pérez-Leblic et al., 2012; Thavamani et al., 2012). This is also evident at the OR-IFRC site where a previous 16S rRNA gene clone library survey identified a limited consortium in contaminated sediments to be defined by the high levels of nitrate, toxic metals (e.g., U, Cr and Ni) and highly acidic pH (Fields et al., 2005). Furthermore, an analysis of the diversity of sediment associated SS rRNA gene clones similarly revealed the negative correlation between bacterial diversity and co-contaminants (low pH and high nitrate) in sediments from the site (Akob et al., 2007). Our findings did not identify any significant differences for either taxonomic or functional α diversity between wells while stronger

differences in taxonomic composition were evident in wells with higher nitrate when compared to the functional composition in these wells. The greater evenness in function and overlapped genes compared to taxonomic profiles points to function being conserved across the nitrate gradient. This could indicate that different species contribute to the same functions which take advantage of changing conditions along the nitrate gradient in the subsurface. The similar number of unique OTUs and functional genes detected in each of the groups of wells also lends support to this explanation, but further tests are required to conclusively prove this.

For those genera that were present at > 1% relative abundance (RA) in OR_{LN} wells, members belonging to the genus *Nitrosopumilus* are known to play important roles in nitrogen and carbon cycling. They have also been described to grow chemoautotrophically by aerobically oxidizing ammonia to nitrite (Mosier et al., 2012). Members belonging to the genus *Pseudomonas* are frequently encountered in sediment and groundwater at the OR-IFRC and along with those belonging to *Brevundimonas* have been described to be important in nitrate cycling at the site (Spain and Krumholz, 2011; Techtmann and Hazen, 2016). Most of the genera present at > 1% RA in the OR_{MN} wells belong to the order *Burkholderiales* which are common soil bacteria, frequently encountered at the site (Hemme et al., 2015; Wu et al., 2018) and are capable of denitrification. Of those OTUs from the OR_{HN} wells that could be assigned taxonomy to the genus level, *Sideroxydans* sp. are iron oxidizing bacteria, *Pseudomonas* sp. are capable of denitrification. The coupling of Fe(II) oxidation to nitrate reduction has been described for a close relative of *Sideroxydans lithotrophicus* (Blöthe and Roden, 2009). While there is no clear role for subdivision 6 *Acidobacteria* members in key N cycling processes, they have been described in a variety of ecosystems (Kielak et al., 2016). An OTU assigned to genus *Sideroxydans* was also abundant in OR_{LN} wells and this could possibly be linked to the higher concentration of Fe(II) that was present in OR_{LN} and OR_{HN} wells.

Without the addition of exogenous carbon, groundwater microbial communities at the OR-IFRC are known to be electron donor limited due to the oligotrophic nature of the aquifer (Istok et al., 2004b). Electron donors available in aquifers predominantly constitute organic carbon from decaying microbial biomass and organic matter available from plant material (Christensen et al., 2000; McMahon et al., 2011). The highest functional potential for C utilization occurs in wells with moderate nitrate levels and is spread across genes involved in the breakdown of labile and recalcitrant forms of available C. Since the AODC measurements from the wells utilized here were similar, the higher functional potential observed under moderate levels of nitrate points to an enhanced ability to use these substrates given the availability of suitable TEAs. Based on free energy released, electron acceptors in groundwater systems are sequentially utilized in the order O_2, NO_3, Mn, Fe, SO_4 and finally CO_2 (Christensen et al., 2000; McMahon and Chapelle, 2008). The utilization of nitrate, Fe and SO_4 has been experimentally verified during bio-stimulation experiments conducted at the OR-IFRC and contaminated aquifers in Rifle, CO and Hanford, WA (Van Nostrand et al., 2011; Liang et al., 2012; Tang et al., 2013b; Zhang et al., 2015a). As both NO_3 and SO_4 levels were higher and comparable in the OR_{MN} wells (Table S3), the higher functional potential in this group of wells could be attributed to the greater availability of TEAs known to be utilized by groundwater communities at this site.

Nitrite and nitric oxide are two intermediates of the denitrification process that are known to inhibit bacterial activity (Glass et al., 1997; Glass and Silverstein, 1998; Choi et al., 2006) and the mechanism of action has been proposed to occur though the disruption of the proton gradient and electron transport chain by the buildup of nitrous acid (Rowe et al., 1979; Yarbrough et al., 1980; Almeida et al., 1995). Inhibition due to nitrite accumulation has been demonstrated to disrupt denitrification at high levels of nitrate in in pure cultures and activated sludge processes at circumneutral pH (Baumann et al., 1997; Krishna Mohan et al., 2016). Inhibition stemming

from a buildup of nitrite could be a reason behind the decreased functional potential in wells with extremely high levels of nitrate in relation to those with moderate nitrate. Another factor that could be contributing to the buildup of nitrite is the documented finding that nitrate can outcompete nitrite for the active site of nitrite reductase as described in studies examining nitrate reduction in *Azospirillum brasilense* SP7 (Chauret and Knowles, 1991). Nitrate inhibition of nitrite reduction has also been described in *Pseudomonas stutzeri,* where the addition of excess nitrate was determined to repress the nitrite reducing activity of the cells (Kodama et al., 1969). In addition to the above, metal co-factors are important for the activity of enzymes involved in the denitrification pathway with Cu, Fe and Mo all being identified as key to their activity (Tavares et al., 2006). A recent study relating the effect of groundwater Mo on denitrification activity under high nitrate at OR-IFRC brought to light the finding that minimal Mo concentrations in wells with highest NO_3 levels was responsible for restricting the use of nitrate as a TEA (Thorgersen et al., 2015). The reduction in functional potential for denitrification enzymes in wells with high nitrate is in line with this finding.

Sulfate reducing bacteria are known to be inhibited by the nitrite produced from nitrate reduction (Greene et al., 2003) and this nitrite inhibition of SRBs has been demonstrated to successfully limit the evolution of sulfide in the environment (Davidova et al., 2001). Furthermore, oxidative stress responses are known to be triggered by reactive nitrogen species (Mukhopadhyay et al., 2004). Along these lines, transcriptomic analysis has previously identified the upregulation of oxidative stress response genes to be triggered in response to nitrite stress in *D. vulgaris* and that genes involved in the generation of ATP were downregulated while under nitrite stress (He et al., 2006). Inhibition of the DsrAB complex in *D. vulgaris* by nitrite, which is slowly reduced to ammonia and the loss of periplasmic protons has also been attributed to the reduction in utilization of sulfite and ultimate growth inhibition under nitrate stress (Haveman et al., 2004).

These findings lend support to the decreased functional potential for sulfate reduction at extreme levels of nitrate observed here. The reduced functional potential for *cytochrome c* genes in wells with high nitrate, is supported by dissimilatory metal reducing conditions at the OR-IFRC being contingent on electron donor amendment and nitrate removal (Istok et al., 2004b; Edwards et al., 2007; Akob et al., 2008). Nitrate utilization is more energetically favorable than redox active metals (e.g. Fe(III), Mn(IV) and U(VI)) and this can inhibit the progression towards deriving energy from metal reduction (DiChristina, 1992). Progressive metal reduction was observed in sediment microcosms with 100mM nitrate only after buffering to circumneutral pH and delayed until substantial nitrate removal occurred (Thorpe et al., 2012). Furthermore, metal reduction occurring at this stage did so at alkaline pH.

In summation, the combination of nitrite toxicity under high nitrate levels in an electron donor limited environment is likely to inhibit the activity of dissimilatory metal reducing species. DO, Eh and SO_4^{2-} were seen to be the most important geochemical variables influencing groundwater community structure in the OR_{LN} and OR_{MN} wells whereas higher levels of NO_3^- and Na governed community structure in the OR_{HN} wells. Given the availability of electron donors and conditions favoring growth, TEAs (e.g. SO_4, NO_3), groundwater Eh and the presence of metals in high concentrations (e.g. U(VI), Fe(III), Cr(VI)) have been identified to influence subsurface microbial composition (Van Nostrand et al., 2009a; Van Nostrand et al., 2011; Liang et al., 2012; Zhang et al., 2015a). That these observations came to light during field experiments exploring microbial community changes during bio-reduction and reoxidation of aquifer environments across sites in Hanford, WA; Rifle, CO and the OR-IFRC support the important role of these variables in determining groundwater microbial composition. Since over 50% of the variation in community structure was unaccounted for, the unexplained variation in this study is higher than the range (~30-50%) reported in these studies. Aquifer systems are known to be oligotrophic

(Jones et al., 2018) and in conjunction with high nitrate levels one can expect microbial dormancy to facilitate persistence under prevailing conditions. This unexplained variation could arise from measured environmental variables representing conditions at the time of sampling and therefore not able to capture conditions shaping the sites over time. In addition, stochastic processes are known to influence community succession and could contribute to opportunistic species which were detected across the treatment wells (Zhou et al., 2013b; Zhou et al., 2014). Interactions between geochemical variables that cannot be accounted for could also contribute to the higher percentage of unexplained variation in community structure.

By analyzing relative abundances of ~ 76,000 functional genes and ~ 8,800 OTUs from groundwater samples at the OR-IFRC across a nitrate gradient, we identified distinct differences in the functional potential and taxonomic composition in the three treatment groups. The highest functional potential for genes driving C, N, S cycling and electron transfer processes was detected in OR_{MN} wells, while functional potentials were similar in wells with < 1mgL^{1-} NO_3 and > 100 mgL^{-1} NO_3. Taxonomic profiles of the most abundant members identified distinct species to be present, with little overlap between treatments. Apart from nitrate, heterogeneity in groundwater geochemistry across the wells was important in influencing community composition with anions (SO_4, S^{2-}), cations (Na, Ca, Mn), carbon and pH governing composition across the wells. However, whether these communities represent a steady state or change over time needs to be tested. Further studies on process rates across spatial and temporal scales are needed to better characterize the complex response of the subsurface microbial community to geochemical gradients at the OR-IFRC.

Acknowledgements

Dr. Ping Zhang completed the MDA and processing of genomic DNA for GeoChip 5.0 hybridization and 16S rRNA gene amplicon sequencing via the Illumina MiSeq platform. This work was funded by a grant from the U.S Department of Energy, ENIGMA Scientific Focus Area Program.

References

Akob, D.M., Mills, H.J., and Kostka, J.E. (2007) Metabolically active microbial communities in uranium-contaminated subsurface sediments. *FEMS Microbiology Ecology* **59**: 95-107.

Akob, D.M., Mills, H.J., Gihring, T.M., Kerkhof, L., Stucki, J.W., Anastácio, A.S. et al. (2008) Functional Diversity and Electron Donor Dependence of Microbial Populations Capable of U(VI) Reduction in Radionuclide-Contaminated Subsurface Sediments. *Applied and Environmental Microbiology* **74**: 3159-3170.

Almeida, J.S., Julio, S.M., Reis, M.A., and Carrondo, M.J. (1995) Nitrite inhibition of denitrification by Pseudomonas fluorescens. *Biotechnol Bioeng* **46**: 194-201.

Anderson, M.J. (2001) A new method for non-parametric multivariate analysis of variance. *Austral ecology* **26**: 32-46.

Baumann, B., van der Meer, J.R., Snozzi, M., and Zehnder, A.J.B. (1997) Inhibition of denitrification activity but not of mRNA induction in Paracoccus denitrificans by nitrite at a suboptimal pH. *Antonie van Leeuwenhoek* **72**: 183-189.

Burgin, A.J., and Hamilton, S.K. (2007) Have we overemphasized the role of denitrification in aquatic ecosystems? A review of nitrate removal pathways. *Frontiers in Ecology and the Environment* **5**: 89-96.

Burow, K.R., Nolan, B.T., Rupert, M.G., and Dubrovsky, N.M. (2010) Nitrate in groundwater of the United States, 1991− 2003. *Environmental Science & Technology* **44**: 4988-4997.

Chauret, C., and Knowles, R. (1991) Effect of tungsten on nitrate and nitrite reductases in Azospirillum brasilense Sp7. *Canadian journal of microbiology* **37**: 744-750.

Choi, P.S., Naal, Z., Moore, C., Casado-Rivera, E., Abruña, H.D., Helmann, J.D., and Shapleigh, J.P. (2006) Assessing the Impact of Denitrifier-Produced Nitric Oxide on Other Bacteria. *Applied and Environmental Microbiology* **72**: 2200-2205.

Christensen, T.H., Bjerg, P.L., Banwart, S.A., Jakobsen, R., Heron, G., and Albrechtsen, H.-J. (2000) Characterization of redox conditions in groundwater contaminant plumes. *Journal of Contaminant Hydrology* **45**: 165-241.

Clarke, K., and Ainsworth, M. (1993) A method of linking multivariate community structure to environmental variables. *Marine Ecology-Progress Series* **92**: 205-205.

Clarke, K.R. (1993) Non-parametric multivariate analyses of changes in community structure. *Australian journal of ecology* **18**: 117-143.

Cook, P., Solomon, D., Sanford, W., Busenberg, E., Plummer, L., and Poreda, R. (1996) Inferring shallow groundwater flow in saprolite and fractured rock using environmental tracers. *Water Resources Research* **32**: 1501-1509.

Davidova, I., Hicks, M., Fedorak, P., and Suflita, J. (2001) The influence of nitrate on microbial processes in oil industry production waters. *Journal of Industrial Microbiology and Biotechnology* **27**: 80-86.

De Mendiburu, F. (2014) Agricolae: statistical procedures for agricultural research. *R package version* **1**.

DiChristina, T.J. (1992) Effects of nitrate and nitrite on dissimilatory iron reduction by Shewanella putrefaciens 200. *Journal of Bacteriology* **174**: 1891-1896.

Edgar, R.C. (2013) UPARSE: highly accurate OTU sequences from microbial amplicon reads. *Nature methods* **10**: 996.

Edgar, R.C., Haas, B.J., Clemente, J.C., Quince, C., and Knight, R. (2011) UCHIME improves sensitivity and speed of chimera detection. *Bioinformatics* **27**: 2194-2200.

Edwards, L., Küsel, K., Drake, H., and Kostka, J.E. (2007) Electron flow in acidic subsurface sediments co-contaminated with nitrate and uranium. *Geochimica et Cosmochimica Acta* **71**: 643-654.

Fields, M.W., Yan, T., Rhee, S.-K., Carroll, S.L., Jardine, P.M., Watson, D.B. et al. (2005) Impacts on microbial communities and cultivable isolates from groundwater contaminated with high levels of nitric acid–uranium waste. *FEMS Microbiology Ecology* **53**: 417-428.

Gasperikova, E., Hubbard, S.S., Watson, D.B., Baker, G.S., Peterson, J.E., Kowalsky, M.B. et al. (2012) Long-term electrical resistivity monitoring of recharge-induced contaminant plume behavior. *Journal of Contaminant Hydrology* **142-143**: 33-49.

Glass, C., and Silverstein, J. (1998) Denitrification kinetics of high nitrate concentration water: pH effect on inhibition and nitrite accumulation. *Water Research* **32**: 831-839.

Glass, C., Silverstein, J., and Oh, J. (1997) Inhibition of Denitrification in Activated Sludge by Nitrite. *Water Environment Research* **69**: 1086-1093.

Greene, E., Hubert, C., Nemati, M., Jenneman, G., and Voordouw, G. (2003) Nitrite reductase activity of sulphate-reducing bacteria prevents their inhibition by nitrate-reducing, sulphide-oxidizing bacteria. *Environmental Microbiology* **5**: 607-617.

Haveman, S.A., Greene, E.A., Stilwell, C.P., Voordouw, J.K., and Voordouw, G. (2004) Physiological and Gene Expression Analysis of Inhibition of Desulfovibrio vulgaris Hildenborough by Nitrite. *Journal of Bacteriology* **186**: 7944-7950.

He, Q., Huang, K.H., He, Z., Alm, E.J., Fields, M.W., Hazen, T.C. et al. (2006) Energetic Consequences of Nitrite Stress in Desulfovibrio vulgaris Hildenborough, Inferred from Global Transcriptional Analysis. *Applied and Environmental Microbiology* **72**: 4370-4381.

He, Z., Gentry, T.J., Schadt, C.W., Wu, L., Liebich, J., Chong, S.C. et al. (2007) GeoChip: a comprehensive microarray for investigating biogeochemical, ecological and environmental processes. *The ISME journal* **1**: 67.

He, Z., Zhang, P., Wu, L., Rocha, A.M., Tu, Q., Shi, Z. et al. (2018) Microbial Functional Gene Diversity Predicts Groundwater Contamination and Ecosystem Functioning. *mBio* **9**.

Hemme, C.L., Tu, Q., Shi, Z., Qin, Y., Gao, W., Deng, Y. et al. (2015) Comparative metagenomics reveals impact of contaminants on groundwater microbiomes. *Frontiers in Microbiology* **6**.

Istok, J.D., Senko, J.M., Krumholz, L.R., Watson, D., Bogle, M.A., Peacock, A. et al. (2004) In Situ Bioreduction of Technetium and Uranium in a Nitrate-Contaminated Aquifer. *Environmental Science & Technology* **38**: 468-475.

Jones, R.M., Goordial, J.M., and Orcutt, B.N. (2018) Low Energy Subsurface Environments as Extraterrestrial Analogs. *Frontiers in Microbiology* **9**.

Kandeler, F., Kampichler, C., and Horak, O. (1996) Influence of heavy metals on the functional diversity of soil microbial communities. *Biology and Fertility of Soils* **23**: 299-306.

Kendall, C., Elliott, E.M., and Wankel, S.D. (2007) Tracing anthropogenic inputs of nitrogen to ecosystems. *Stable isotopes in ecology and environmental science*: 375-449.

Kodama, T., Shimada, K., and Mori, T. (1969) Studies on anaerobic biphasic growth of a denitrifying bacterium, Pseudomonas stutzeri. *Plant and Cell Physiology* **10**: 855-865.

Kong, Y. (2011) Btrim: A fast, lightweight adapter and quality trimming program for next-generation sequencing technologies. *Genomics* **98**: 152-153.

Kraft, B., Tegetmeyer, H.E., Sharma, R., Klotz, M.G., Ferdelman, T.G., Hettich, R.L. et al. (2014) The environmental controls that govern the end product of bacterial nitrate respiration. *Science* **345**: 676-679.

Krishna Mohan, T.V., Renu, K., Nancharaiah, Y.V., Satya Sai, P.M., and Venugopalan, V.P. (2016) Nitrate removal from high strength nitrate-bearing wastes in granular sludge sequencing batch reactors. *Journal of Bioscience and Bioengineering* **121**: 191-195.

Liang, Y., Van Nostrand, J.D., N′Guessan, L.A., Peacock, A.D., Deng, Y., Long, P.E. et al. (2012) Microbial Functional Gene Diversity with a Shift of Subsurface Redox Conditions during In Situ Uranium Reduction. *Applied and Environmental Microbiology* **78**: 2966-2972.

Lilja, E.E., and Johnson, D.R. (2017) Metabolite toxicity determines the pace of molecular evolution within microbial populations. *BMC Evolutionary Biology* **17**: 52.

Lind, L.P., Audet, J., Tonderski, K., and Hoffmann, C.C. (2013) Nitrate removal capacity and nitrous oxide production in soil profiles of nitrogen loaded riparian wetlands inferred by laboratory microcosms. *Soil Biology and Biochemistry* **60**: 156-164.

Magoč, T., and Salzberg, S.L. (2011) FLASH: fast length adjustment of short reads to improve genome assemblies. *Bioinformatics* **27**: 2957-2963.

McMahon, P.B., and Chapelle, F.H. (2008) Redox Processes and Water Quality of Selected Principal Aquifer Systems. *Groundwater* **46**: 259-271.

McMahon, P.B., Chapelle, F.H., and Bradley, P.M. (2011) Evolution of Redox Processes in Groundwater. In *Aquatic Redox Chemistry*: American Chemical Society, pp. 581-597.

Miller, D., Bryant, J., Madsen, E., and Ghiorse, W. (1999) Evaluation and optimization of DNA extraction and purification procedures for soil and sediment samples. *Applied and environmental microbiology* **65**: 4715-4724.

Mukhopadhyay, P., Zheng, M., Bedzyk, L.A., LaRossa, R.A., and Storz, G. (2004) Prominent roles of the NorR and Fur regulators in the Escherichia coli transcriptional response to reactive nitrogen species. *Proceedings of the National Academy of Sciences* **101**: 745-750.

Oksanen, J., Blanchet, F.G., Kindt, R., Legendre, P., Minchin, P.R., O'hara, R. et al. (2013) Package 'vegan'. *Community ecology package, version* **2**.

Pérez-Leblic, M.I., Turmero, A., Hernández, M., Hernández, A.J., Pastor, J., Ball, A.S. et al. (2012) Influence of xenobiotic contaminants on landfill soil microbial activity and diversity. *Journal of Environmental Management* **95**: S285-S290.

Quast, C., Pruesse, E., Yilmaz, P., Gerken, J., Schweer, T., Yarza, P. et al. (2013) The SILVA ribosomal RNA gene database project: improved data processing and web-based tools. *Nucleic Acids Research* **41**: D590-D596.

Rowe, J., Yarbrough, J., Rake, J., and Eagon, R. (1979) Nitrite inhibition of aerobic bacteria. *Current Microbiology* **2**: 51-54.

Sebilo, M., Mayer, B., Nicolardot, B., Pinay, G., and Mariotti, A. (2013) Long-term fate of nitrate fertilizer in agricultural soils. *Proceedings of the National Academy of Sciences* **110**: 18185-18189.

Smith, M.B., Rocha, A.M., Smillie, C.S., Olesen, S.W., Paradis, C., Wu, L. et al. (2015a) Natural bacterial communities serve as quantitative geochemical biosensors. *MBio* **6**: e00326-00315.

Smith, M.B., Rocha, A.M., Smillie, C.S., Olesen, S.W., Paradis, C., Wu, L. et al. (2015b) Natural Bacterial Communities Serve as Quantitative Geochemical Biosensors. *mBio* **6**.

Spain, A.M., and Krumholz, L.R. (2011) Nitrate-reducing bacteria at the nitrate and radionuclide contaminated Oak Ridge Integrated Field Research Challenge site: a review. *Geomicrobiology Journal* **28**: 418-429.

Spain, A.M., Peacock, A.D., Istok, J.D., Elshahed, M.S., Najar, F.Z., Roe, B.A. et al. (2007) Identification and Isolation of a Castellaniella Species Important during Biostimulation of an Acidic Nitrate- and Uranium-Contaminated Aquifer. *Applied and Environmental Microbiology* **73**: 4892-4904.

Tang, G., Watson, D.B., Wu, W.-M., Schadt, C.W., Parker, J.C., and Brooks, S.C. (2013) U(VI) Bioreduction with Emulsified Vegetable Oil as the Electron Donor – Model Application to a Field Test. *Environmental Science & Technology* **47**: 3218-3225.

Tavares, P., Pereira, A.S., Moura, J.J.G., and Moura, I. (2006) Metalloenzymes of the denitrification pathway. *Journal of Inorganic Biochemistry* **100**: 2087-2100.

Ter Braak, C.J. (1986) Canonical correspondence analysis: a new eigenvector technique for multivariate direct gradient analysis. *Ecology* **67**: 1167-1179.

Thavamani, P., Malik, S., Beer, M., Megharaj, M., and Naidu, R. (2012) Microbial activity and diversity in long-term mixed contaminated soils with respect to polyaromatic hydrocarbons and heavy metals. *Journal of environmental management* **99**: 10-17.

Thorgersen, M.P., Lancaster, W.A., Vaccaro, B.J., Poole, F.L., Rocha, A.M., Mehlhorn, T. et al. (2015) Molybdenum availability is key to nitrate removal in contaminated groundwater environments. *Applied and environmental microbiology*: AEM. 00917-00915.

Thorpe, C.L., Law, G.T.W., Boothman, C., Lloyd, J.R., Burke, I.T., and Morris, K. (2012) The Synergistic Effects of High Nitrate Concentrations on Sediment Bioreduction. *Geomicrobiology Journal* **29**: 484-493.

Van Nostrand, J.D., Wu, W.M., Wu, L., Deng, Y., Carley, J., Carroll, S. et al. (2009a) GeoChip-based analysis of functional microbial communities during the reoxidation of a bioreduced uranium-contaminated aquifer. *Environmental Microbiology* **11**: 2611-2626.

Van Nostrand, J.D., Wu, L., Wu, W.-M., Huang, Z., Gentry, T.J., Deng, Y. et al. (2011) Dynamics of microbial community composition and function during in-situ bioremediation of a uranium-contaminated aquifer. *Applied and environmental microbiology*: AEM. 01981-01910.

Van Nostrand, J.D., Wu, W.M., Wu, L., Deng, Y., Carley, J., Carroll, S. et al. (2009b) GeoChip-based analysis of functional microbial communities during the reoxidation of a bioreduced uranium-contaminated aquifer. *Environ Microbiol* **11**: 2611-2626.

Van Sickle, J. (1997) Using mean similarity dendrograms to evaluate classifications. *Journal of Agricultural, Biological, and Environmental Statistics*: 370-388.

Wang, Q., Garrity, G.M., Tiedje, J.M., and Cole, J.R. (2007) Naive Bayesian classifier for rapid assignment of rRNA sequences into the new bacterial taxonomy. *Applied and environmental microbiology* **73**: 5261-5267.

Ward, M.H. (2005) Workgroup report: drinking-water nitrate and health—recent findings and research needs. *Environmental health perspectives* **113**: 1607.

Watson, D., Kostka, J., Fields, M., and Jardine, P. (2004) The Oak Ridge field research center conceptual model.

Wu, L., Liu, X., Schadt, C.W., and Zhou, J. (2006a) Microarray-based analysis of subnanogram quantities of microbial community DNAs by using whole-community genome amplification. *Applied and Environmental Microbiology* **72**: 4931-4941.

Wu, W.-M., Carley, J., Gentry, T., Ginder-Vogel, M.A., Fienen, M., Mehlhorn, T. et al. (2006b) Pilot-scale in situ bioremedation of uranium in a highly contaminated aquifer. 2. Reduction of U (VI) and geochemical control of U (VI) bioavailability. *Environmental science & technology* **40**: 3986-3995.

Yan, T., Fields, M.W., Wu, L., Zu, Y., Tiedje, J.M., and Zhou, J. (2003) Molecular diversity and characterization of nitrite reductase gene fragments (nirK and nirS) from nitrate-and uranium-contaminated groundwater. *Environmental microbiology* **5**: 13-24.

Yarbrough, J., Rake, J., and Eagon, R. (1980) Bacterial inhibitory effects of nitrite: inhibition of active transport, but not of group translocation, and of intracellular enzymes. *Applied and Environmental Microbiology* **39**: 831-834.

Zhang, P., Van Nostrand, J.D., He, Z., Chakraborty, R., Deng, Y., Curtis, D. et al. (2015) A Slow-Release Substrate Stimulates Groundwater Microbial Communities for Long-Term in Situ Cr(VI) Reduction. *Environmental Science & Technology* **49**: 12922-12931.

Zhang, P., He, Z., Van Nostrand, J.D., Qin, Y., Deng, Y., Wu, L. et al. (2017) Dynamic Succession of Groundwater Sulfate-Reducing Communities during Prolonged Reduction of Uranium in a Contaminated Aquifer. *Environmental Science & Technology* **51**: 3609-3620.

Zhou, J., Liu, W., Deng, Y., Jiang, Y.-H., Xue, K., He, Z. et al. (2013) Stochastic assembly leads to alternative communities with distinct functions in a bioreactor microbial community. *Mbio* **4**: e00584-00512.

Zhou, J., Deng, Y., Zhang, P., Xue, K., Liang, Y., Van Nostrand, J.D. et al. (2014) Stochasticity, succession, and environmental perturbations in a fluidic ecosystem. *Proceedings of the National Academy of Sciences*: 201324044.

Zumft, W.G. (1997) Cell biology and molecular basis of denitrification. *Microbiology and Molecular Biology Reviews* **61**: 533-616.

Chapter 3 – Figure legends

Figure 1. Normalized signal intensity representing the relative abundance for detected N cycling genes. Significant differences identified between means are indicated by different letters. Calculation based on ANOVA followed by Fisher's LSD test. N cycling categories: A) Anammox; B) Denitrification; C) Assimilatory N Reduction; D) Nitrification; E) Ammonification; F) Dissimilatory N Reduction; G) Nitrogen Fixation.

Figure 2. Normalized signal intensity representing the relative abundance for detected S cycling genes. Significant differences identified between means are indicated by different letters. Calculation based on ANOVA followed by Fisher's LSD test. N cycling categories: A) DMSP degradation; B) Sulfide Oxidation; C) Adenylylsulfate reductase; D) Sulfite Reduction; E) Sulfur Oxidation.

Figure 3. Normalized signal intensity representing the relative abundance for detected genes influencing electron transfer. Significant differences identified between means are indicated by different letters. Calculation based on ANOVA followed by Fisher's LSD.

Figure 4. Canonical correspondence analysis (CCA) using (A) taxonomic composition and (B) functional gene profiles from wells surveyed. Environmental variables were selected using forward selection procedure and variance inflation factors (VIFs < 20) calculated during CCA procedure. Environmental variables included: Eh, Redox potential; DO, Dissolved oxygen; DIC, Dissolved Inorganic Carbon; DOC, Dissolved Organic Carbon; Na, Sodium; pH, Mn, Manganese; Ca, Calcium; S^{2-}, Sulfide; NO_3^-, Nitrate; SO_4^{2-}, Sulfate; SO_4^{2-}.

Figure 1A.

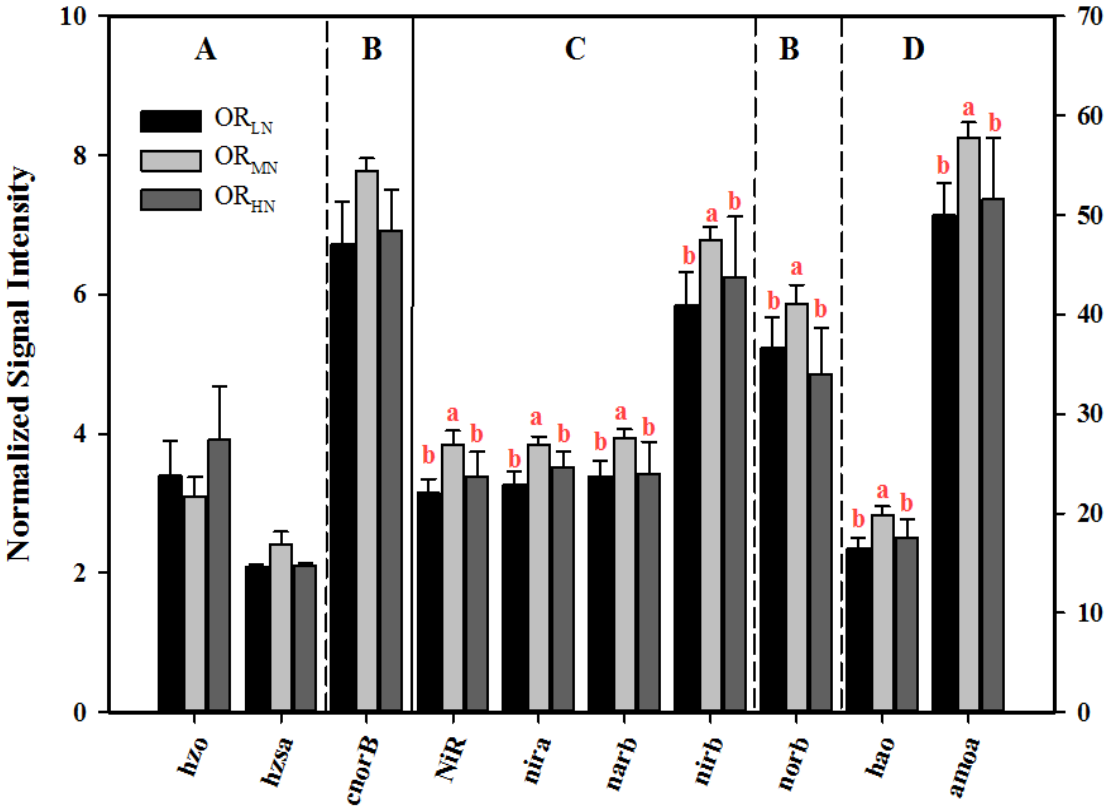
Normalized Signal Intensity
A
B
C
B
D
OR_LN
OR_MN
OR_HN
hzo
hzsa
cnorB
NiR
nira
narb
nirb
norb
hao
amoa

Figure 1B.

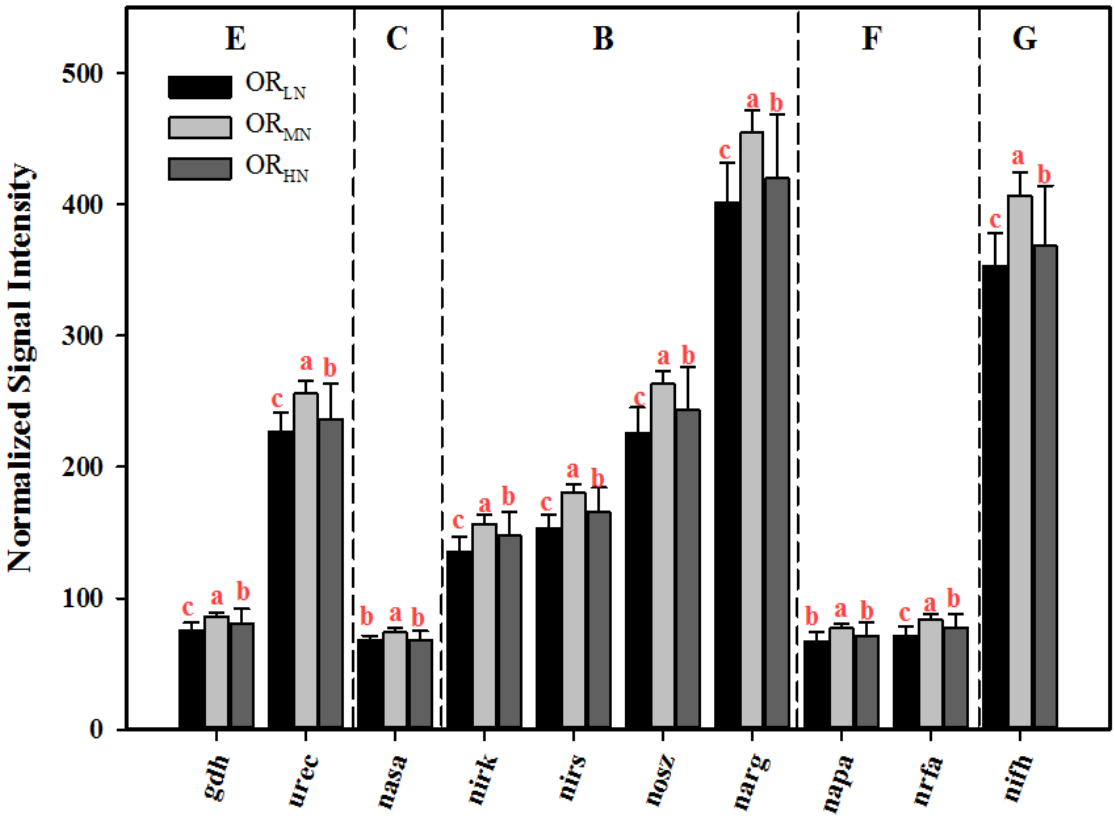
E
C
B
F
G
OR_LN
OR_MN
OR_HN
Normalized Signal Intensity
0
100
200
300
400
500
gdh
urec
nasa
nirk
nirs
nosz
narg
napa
nrfa
nifh

Figure 2.

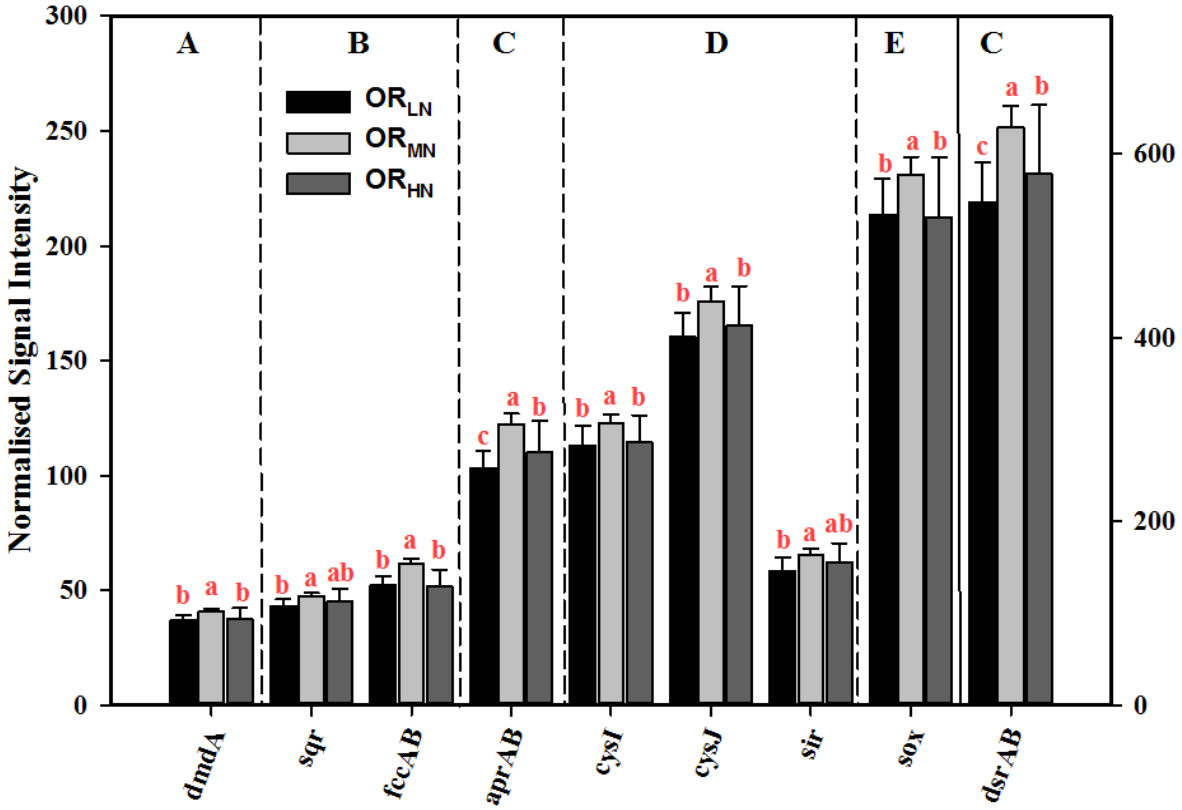
A
B
C
D
E
C
OR_LN
OR_MN
OR_HN
Normalised Signal Intensity
300
250
200
150
100
50
0
600
400
200
0
dmdA
sqr
fccAB
aprAB
cysI
cysJ
sir
sox
dsrAB

Figure 3.

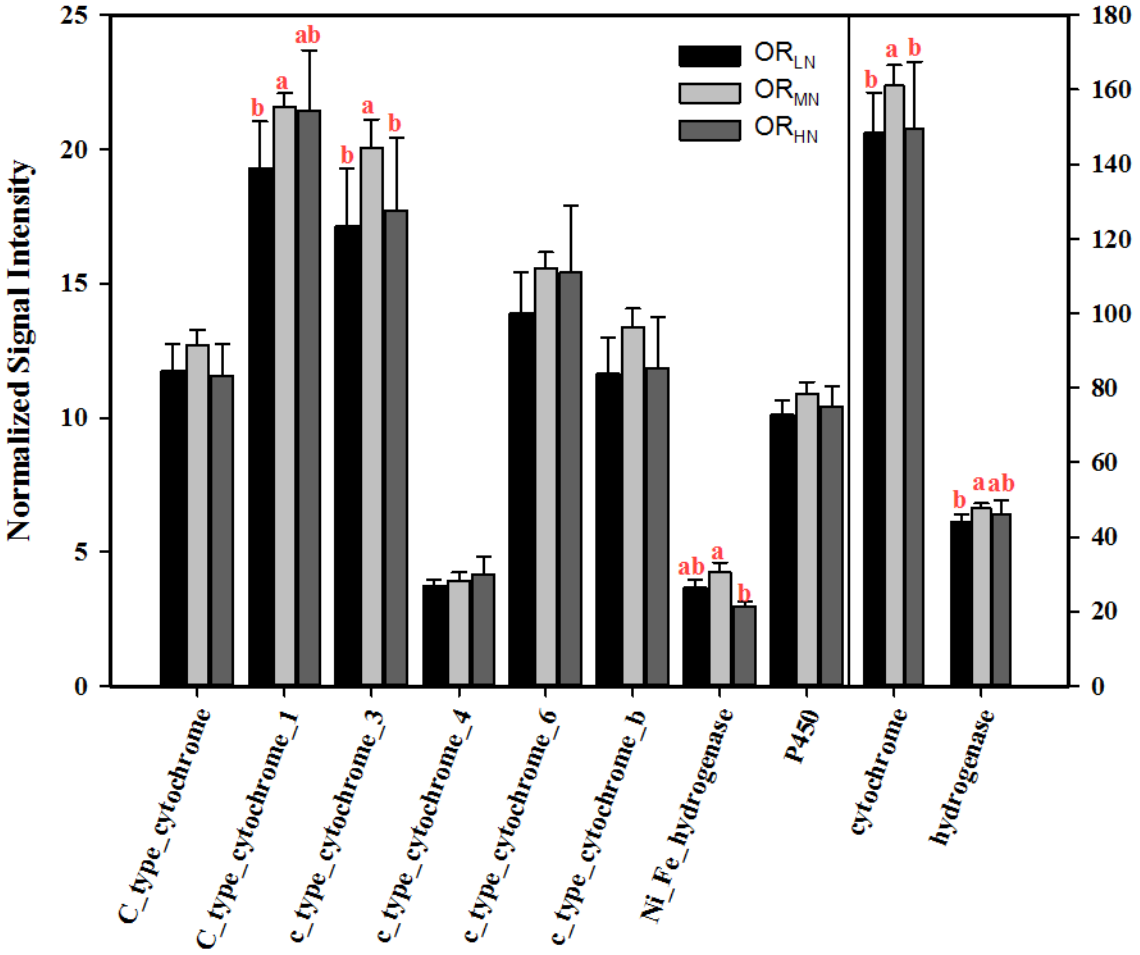
Normalized Signal Intensity
25
20
15
10
5
0
180
160
140
120
100
80
60
40
20
0
OR_LN
OR_MN
OR_HN
b
a
ab
b
a
b
b
a
b
ab
a
b
b
a b
b
a ab
C_type_cytochrome
C_type_cytochrome_1
c_type_cytochrome_3
c_type_cytochrome_4
c_type_cytochrome_6
c_type_cytochrome_b
Ni_Fe_hydrogenase
P450
cytochrome
hydrogenase

Figure 4A.

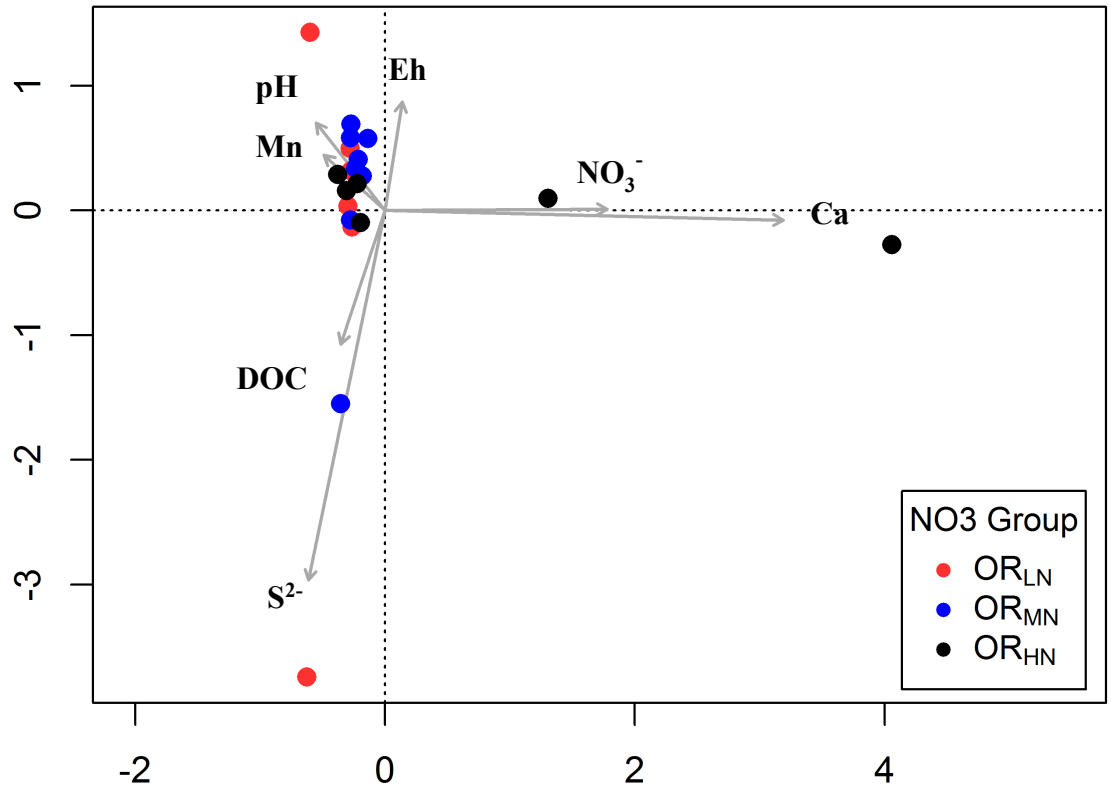

Figure 4B.

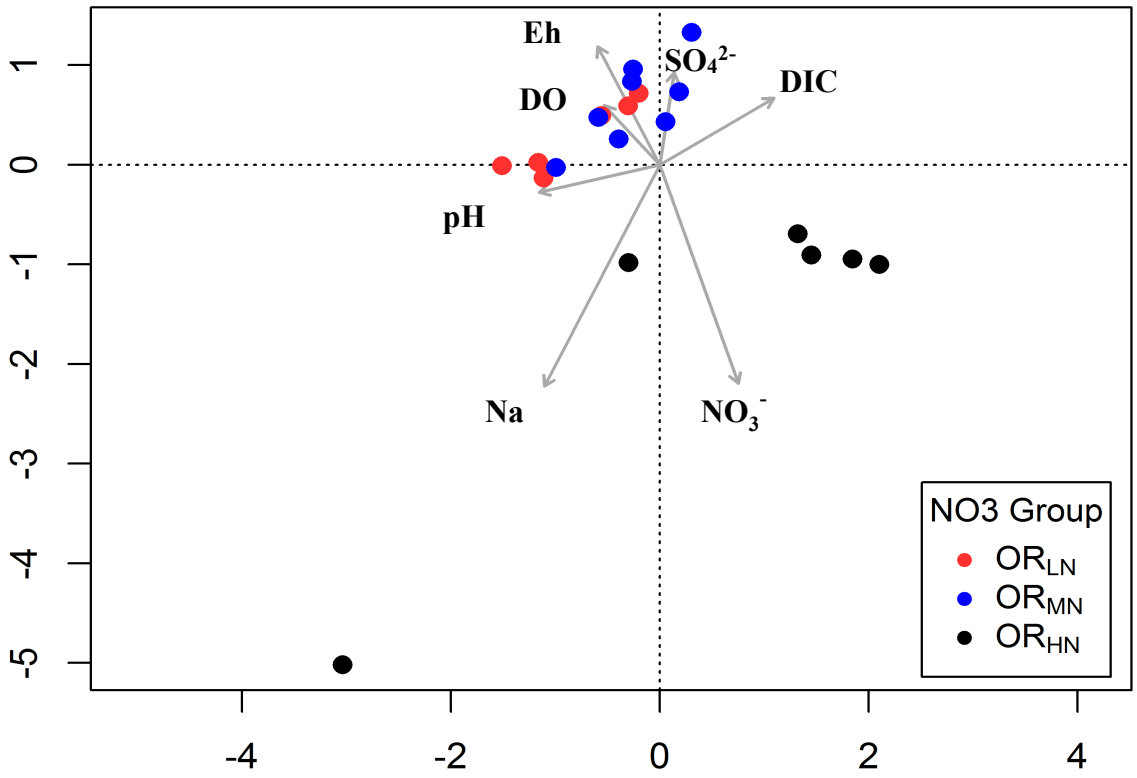
Eh
DO
pH
Na
SO_4^{2-}
DIC
NO_3^-
NO3 Group
OR_{LN}
OR_{MN}
OR_{HN}
1
0
-1
-2
-3
-4
-5
-4
-2
0
2
4

Chapter 3

Table 1.

Summary of nonparametric multivariate dissimilarity tests of functional gene and 16S rRNA gene profiles between pairs of treatments. MRPP, multiresponse permutation procedures; Adonis, permutational multivariate analysis of variance using distance matrices; ANOISM, analysis of similarity. Distances calculated are based on Bray-Curtis index. P values < 0.1 are in bold.

Dataset	Comparison	Sample set	MRPP		Adonis		ANOSIM	
			δ	p	R	p	F	p
GeoChip	OR_{LN} OR_{MN}	14 samples	0.169	**0.008**	0.288	**0.016**	2.711	**0.015**
	OR_{LN} OR_{HN}	12 samples	0.209	**0.076**	0.176	**0.04**	1.350	0.197
	OR_{MN} OR_{HN}	19 samples	0.196	**0.054**	0.190	**0.049**	1.635	**0.087**
16s rRNA gene sequencing	OR_{LN} OR_{MN}	14 samples	0.885	0.185	0.031	0.279	1.142	0.18
	OR_{LN} OR_{HN}	12 samples	0.879	**0.003**	0.402	**0.009**	1.731	**0.003**
	OR_{MN} OR_{HN}	14 samples	0.864	**0.009**	0.369	**0.009**	1.957	**0.01**

Supplemental material

Table S1.

Indices capturing measures of α diversity for both functional genes detected by GeoChip and taxonomic profiles determined by 16S rRNA amplicon sequencing. ± indicate standard error.

Dataset	Indices	OR_{LN}	OR_{MN}	OR_{HN}
GeoChip	Probe number	52300 ± 3458	58636 ± 1896	54111 ± 6220
	Shannon	10.84 ± 0.066	10.96 ± 0.033	10.84 ± 0.142
	Simpson	0.999980 ± 0.0000013	0.999982 ± 0.0000006	0.9999793 ± 0.0000035
	Evenness	0.99948 ± 0.0000839	0.999393 ± 0.0000576	0.999466 ± 0.0000529
16s rRNA gene sequencing	OTUs	1104 ± 251	1109 ± 206	1313 ± 266
	Shannon	4.253 ± 0.626	4.101 ± 0.503	4.587 ± 0.465
	Simpson	0.875 ± 0.061	0.871 ± 0.075	0.935 ± 0.025
	Evenness	0.607 ± 0.076	0.585 ± 0.061	0.647 ± 0.045

Table S2.

Gene overlap among sampling wells. [a] Numbers and percentages not in italic or bold indicate functional genes or OTUs that overlapped between two treatment groups. [b] Total number of functional genes or OTUs detected in treatment group. [c] Numbers and percentages in bold and italic are unique functional genes or OTUs detected in each treatment group.

Well Group	No. (%) of overlapping OTUs[a]		
	OR_{LN} (4,247)[b]	OR_{MN} (4,981)	OR_{HN} (4,497)
OR_{LN}	***1,256(29.57%)*** [c]	2,604(39.31%)	1,752(25.05%)
OR_{MN}		***1,383(27.76%)***	2,359(33.13%)
OR_{HN}			***1,751(38.93%)***
Well Group	No. (%) of overlapping genes[a]		
	OR_{LN} (63,139)[b]	OR_{MN} (71,345)	OR_{HN} (68,046)
OR_{LN}	***1,387(2.20%)*** [c]	60,647(82.14%)	59,531(83.08%)
OR_{MN}		***5,088(7.13%)***	64,036(84.98%)
OR_{HN}			***2,905(4.27%)***

Table S3.

Mean values for groundwater geochemical variables collected from wells in OR_{LN}, OR_{MN} and OR_{HN} groups. DIC, dissolved inorganic carbon; DOC, dissolved organic carbon.

Geochemical variable		OR_{LN}	OR_{MN}	OR_{HN}
Cations (mg/L)	Ag	0.009	0.010	0.018
	Al	0.039	0.068	0.790
	As	0.005	0.007	0.009
	Ba	0.180	0.108	4.013
	Be	0.037	0.039	0.046
	Bi	0.022	0.017	0.008
	Ca	60.599	142.815	1268.599
	Cd	0.003	0.003	0.006
	Co	0.003	0.004	0.013
	Cr	0.004	0.005	0.012
	Cu	0.022	0.008	0.049
	Fe	0.179	0.015	1.096
	Ga	0.012	0.008	0.126
	K	2.305	2.753	12.856
	Li	0.132	0.045	0.201
	Mg	25.284	32.639	87.059
	Mn	0.795	0.423	3.048
	Na	29.178	22.669	281.075
	Ni	0.010	0.030	0.057
	Pb	0.003	0.003	0.004
	Se	0.007	0.007	0.007
	Sr	0.238	0.275	9.615
	U	0.027	0.186	0.213
	Zn	0.047	0.051	0.073
Anions (mg/L)	Cl	35.208	53.9949	41.64249
	NO_3	0.36293	38.4013	2214.95
	SO_4	33.2624	145.81	23.13896
	S^{2-}	0.054	0.03463	0.0135
Carbon (mg/L)	DIC	49.48	65.9788	64.69833
	DOC	1.12267	9.77638	1.972667
Gases (mM)	CH_4	0.00333	0	0.008333
	CO_2	2.75167	3.48375	3.835
	N_2O	0	0	0.215
	DO	1.64167	0.875	0.338333
Other	Eh (mV)	203.5	187.75	79.16667
	pH	6.94833	6.855	6.855
	Temperature (°C)	14.7883	18.0425	16.26333

Chapter 3 – Supplementary figure legends

Figure S1. GPS co-ordinates of the 20 wells at OR-IFRC. Color intensity indicates the NO_3 concentration measured in the groundwater. Low, < 1mgL^{-}; High, > 100mg/L^{-}.

Figure S2. Mean values for A) acridine orange direct cell counts (AODC) and B) DNA yield for wells grouped in OR_{LN}, OR_{MN} and OR_{HN} groups. DNA yield represents amount recovered from biomass harvested from 4 liters of groundwater.

Figure S3. Detrended correspondence analysis (DCA) of all (A) functional genes and (B) 16S rRNA amplicon sequences detected in the groundwater samples in each of the treatment groups. OR_{LN} (< 1 mg/L^{-1} NO_3^-), OR_{MN} (10-100 mg/L^{-1} NO_3^-), OR_{HN} (>100 mg/L^{-1} NO_3^-).

Figure S4. Detrended correspondence analysis (DCA) of (A) *cytochrome c* gene sequences representing dissimilatory metal reducing bacteria (DMRB), (B) *nirK/S* gene sequences representing denitrifying bacteria (NRB) and (C) *dsrAB* gene sequences representing dissimilatory sulfate reducing bacteria (SRB). OR_{LN} (< 1 mg/L^{-1} NO_3^-), OR_{MN} (10-100 mg/L^{-1} NO_3^-), OR_{HN} (>100 mg/L^{-1} NO_3^-).

Figure S5. Normalized signal intensity representing the relative abundance for detected C cycling genes. Significant differences identified between means are indicated by different letters. Calculation based on ANOVA followed by Fisher's LSD test. C degradation gene categories: A) Cellulose, B) Chitin, C) Cutin, D) Glyoxylate Cycle, E) Hemicellulose, F) Lignin, G) Pectin, H) Starch, I) Vanillin/Lignin, J) Camphor, K) Inulin, L) Terpenes.

Figure S6. Normalized signal intensity representing the relative abundance for detected *dsrAB* sequences determined to differ significantly between treatments. Signal intensities represent the sum of the gene sequences detected from each organism. Significant differences identified

between means are indicated by different letters. Calculation based on ANOVA followed by Fisher's LSD test.

Figure S7. Normalized signal intensity representing the relative abundance for detected *cytochrome c* sequences determined to differ significantly between treatments. Signal intensities represent the sum of the gene sequences detected from each organism. Significant differences identified between means are indicated by different letters. Calculation based on ANOVA followed by Fisher's LSD test.

Figure S8. Normalized signal intensity representing the relative abundance for detected *hydrogenase* sequences determined to differ significantly between treatments. Signal intensities represent the sum of the gene sequences detected from each organism. Significant differences identified between means are indicated by different letters. Calculation based on ANOVA followed by Fisher's LSD test.

Figure S9. Variance partitioning analysis (VPA) of environmental variables analyzed by CCA explaining relative effect of variables on A) functional gene content and B) taxonomic composition across samples grouped by NO_3. Circles represent the effects of variables by partitioning out the effects of other variables. Values between circles represent combined effect of circle on either side.

Figure S10. Relative abundance of OTUs identified at >1% mean RA across samples in OR_{LN}, OR_{MN} and OR_{HN} wells. OTU_17, OTU_2, OTU_211 and OTU_4 were detected at >1% RA in more than one treatment group. Taxonomic levels presented: OTU; Genus; Order

Figure S11. Relative abundance of 16s rRNA sequences at class level determined to be present at >1% RA in OR_{LN}, OR_{MN} and OR_{HN} groups of wells.

Figure S1.

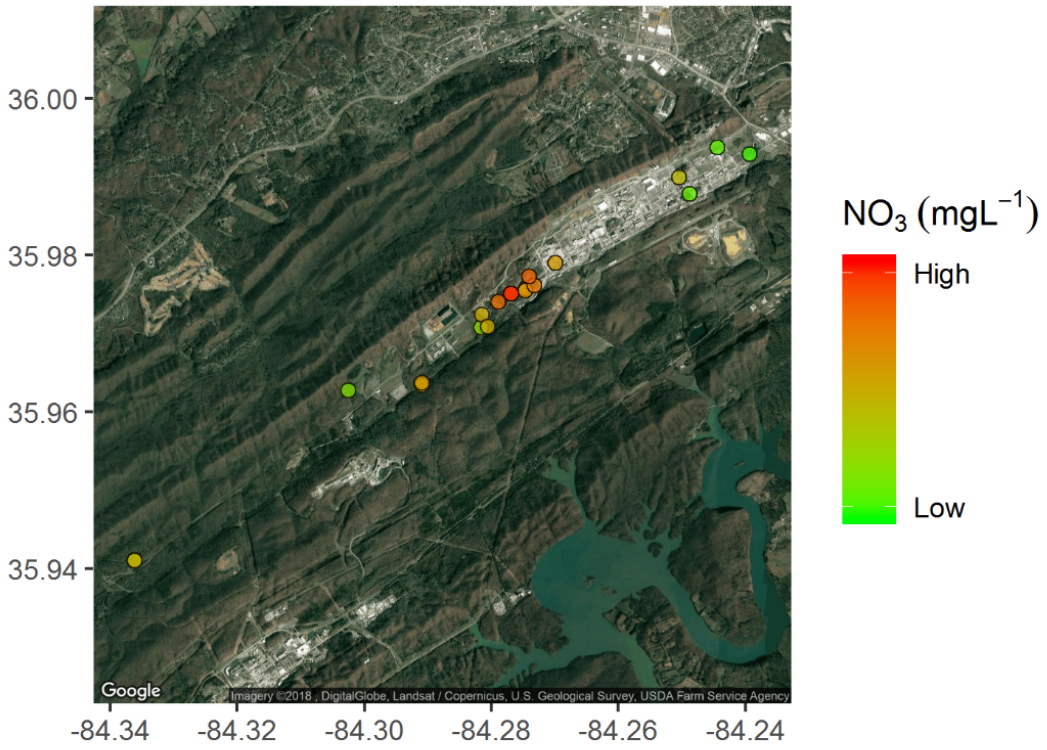
36.00
35.98
35.96
35.94
-84.34
-84.32
-84.30
-84.28
-84.26
-84.24
Google
Imagery ©2018 , DigitalGlobe, Landsat / Copernicus, U.S. Geological Survey, USDA Farm Service Agency
NO3 (mgL−1)
High
Low

Figure S2A.

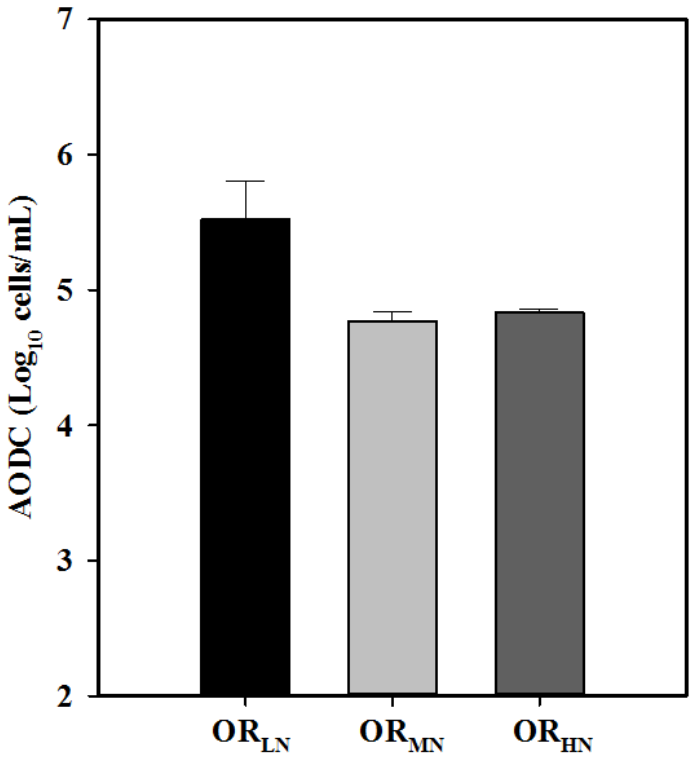

Figure S2B.

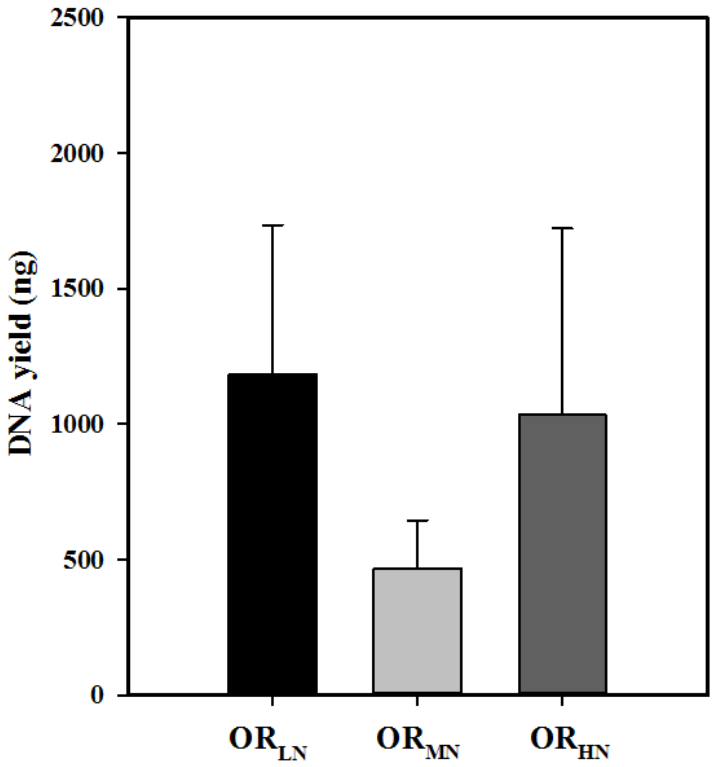

Figure S3A.

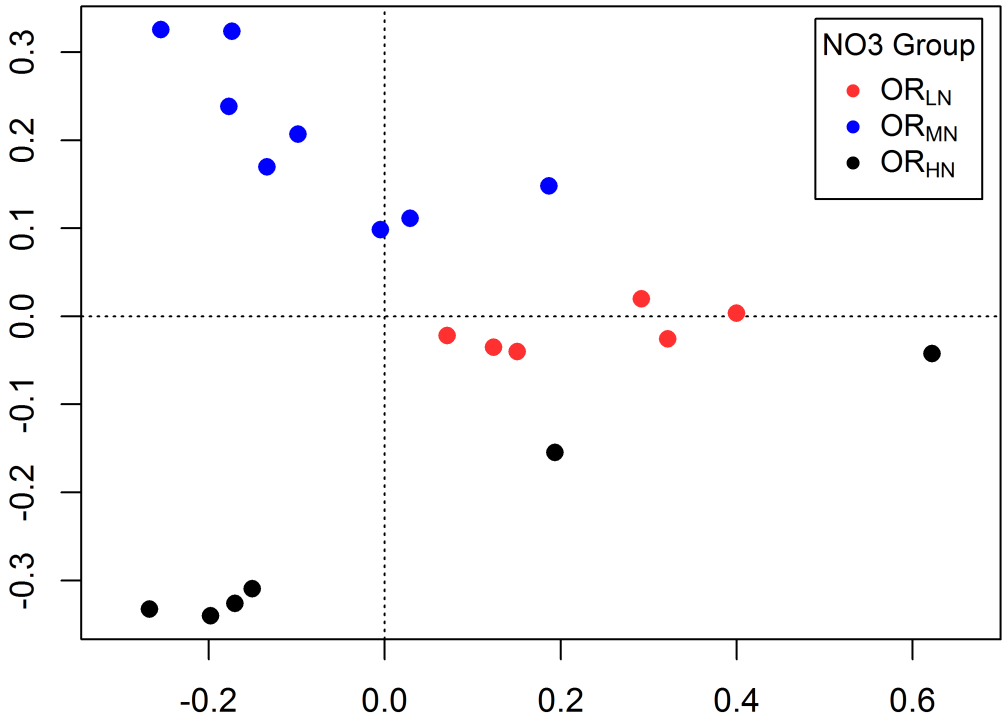

Figure S3B.

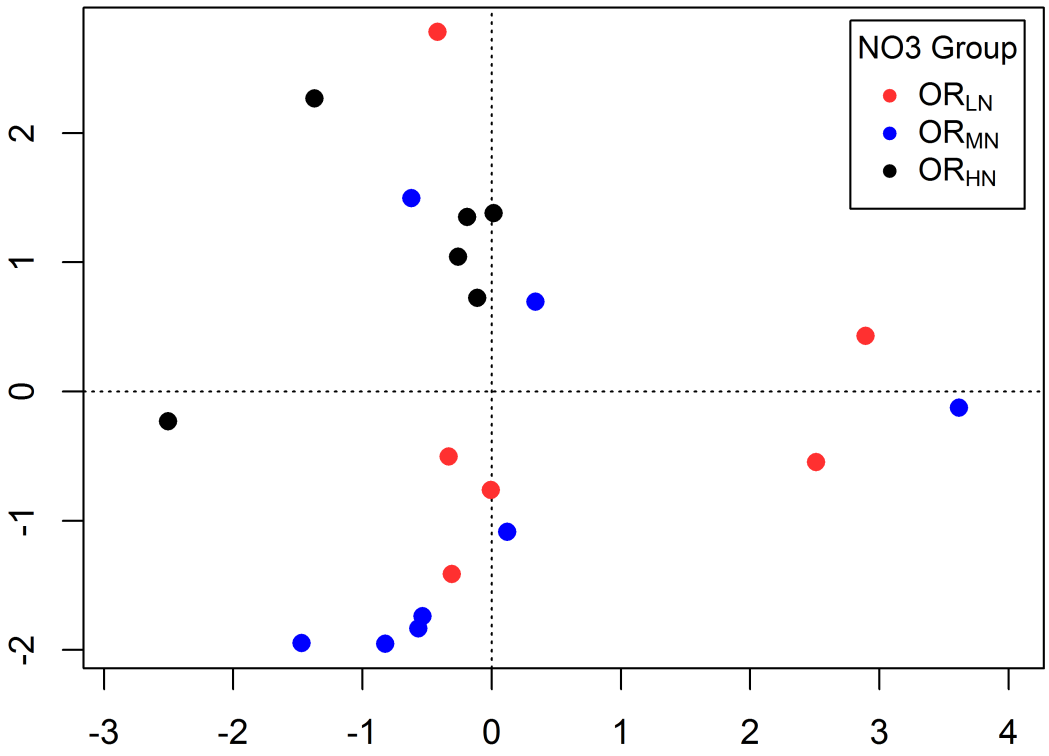

Figure S4A.

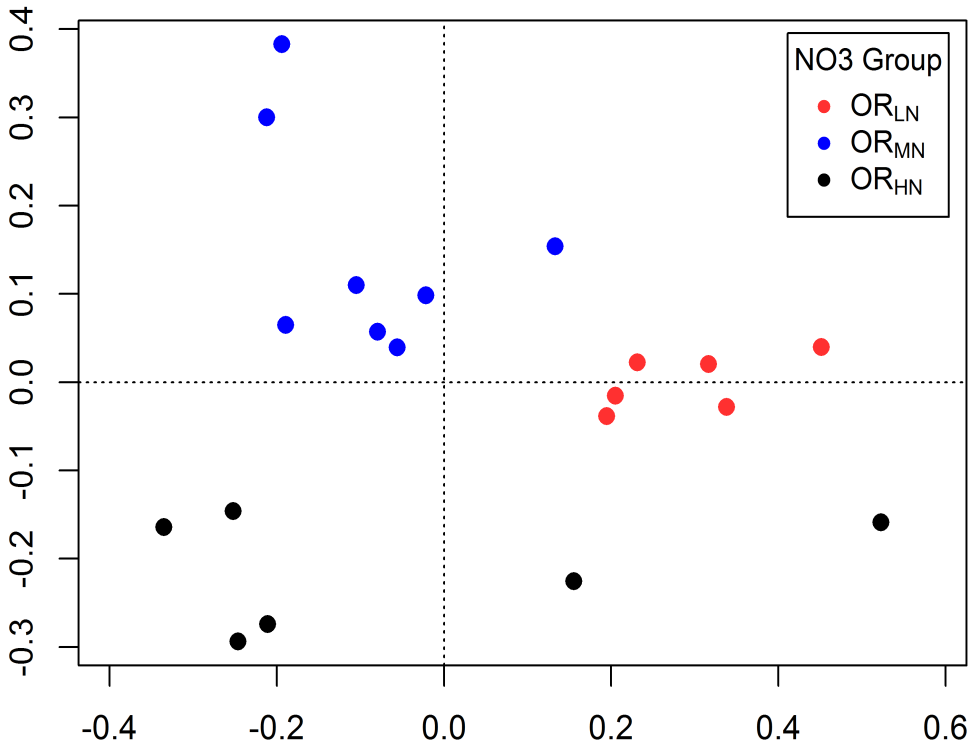

Figure S4B.

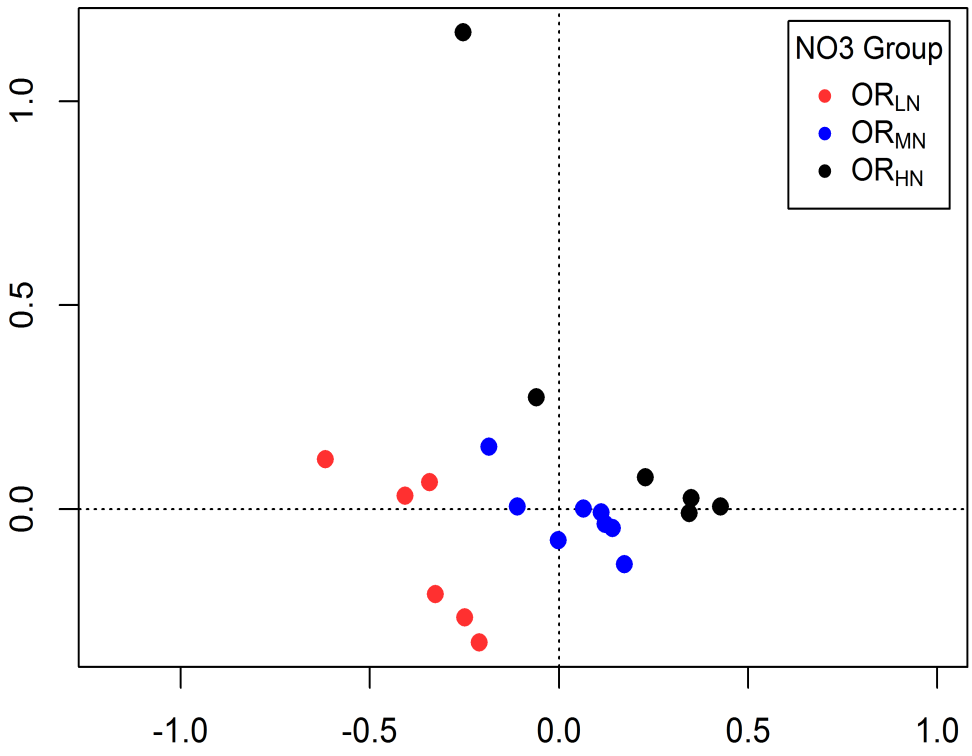

Figure S4C.

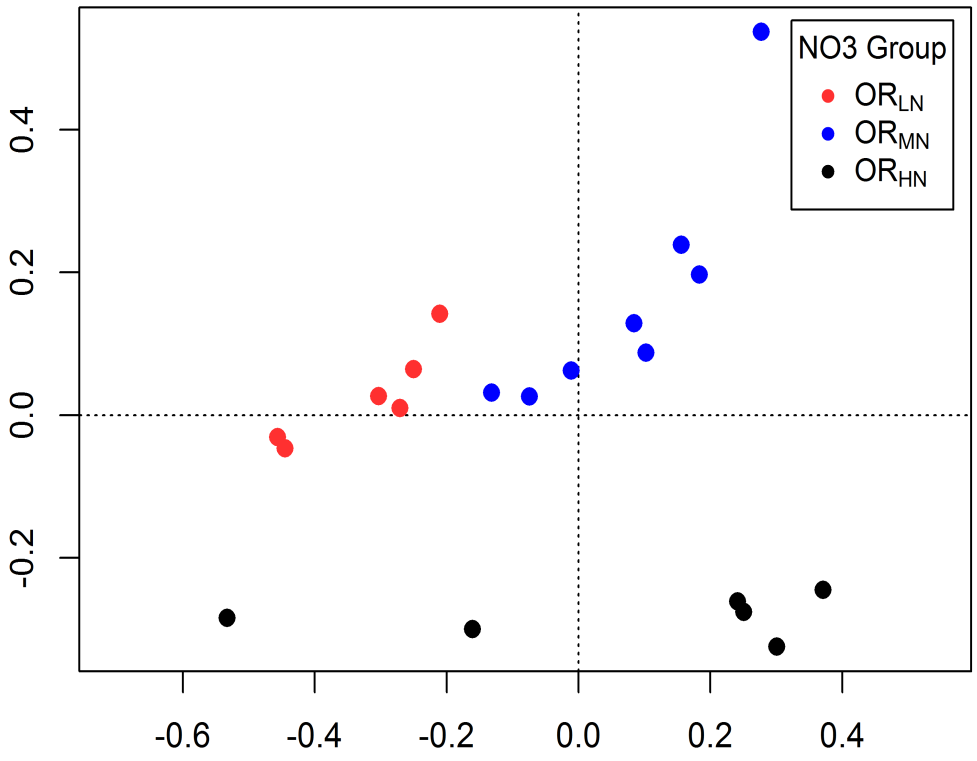

Figure S5A.

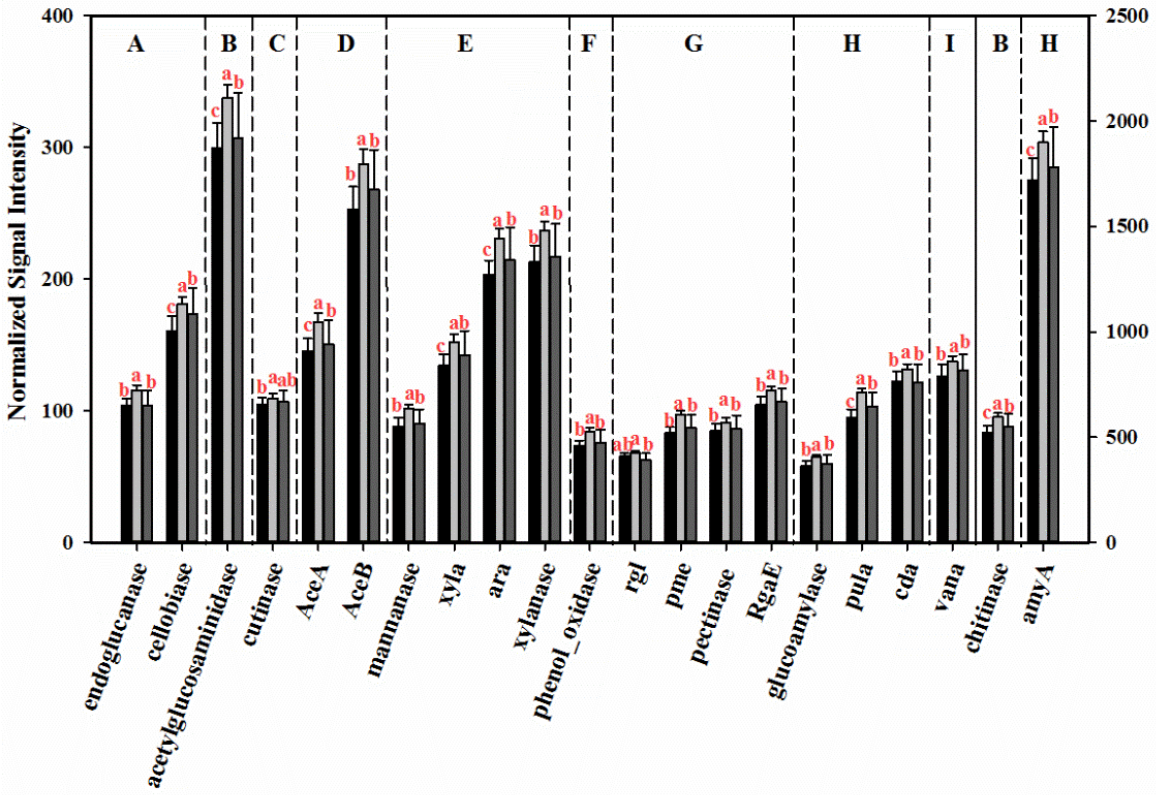
Normalized Signal Intensity
400
300
200
100
0
2500
2000
1500
1000
500
0
A
B
C
D
E
F
G
H
I
B
H
endoglucanase
cellobiase
acetylglucosaminidase
cutinase
AceA
AceB
mannanase
xyla
ara
xylanase
phenol_oxidase
rgl
pme
pectinase
RgaE
glucoamylase
pula
cda
vana
chitinase
amyA

Figure S5B.

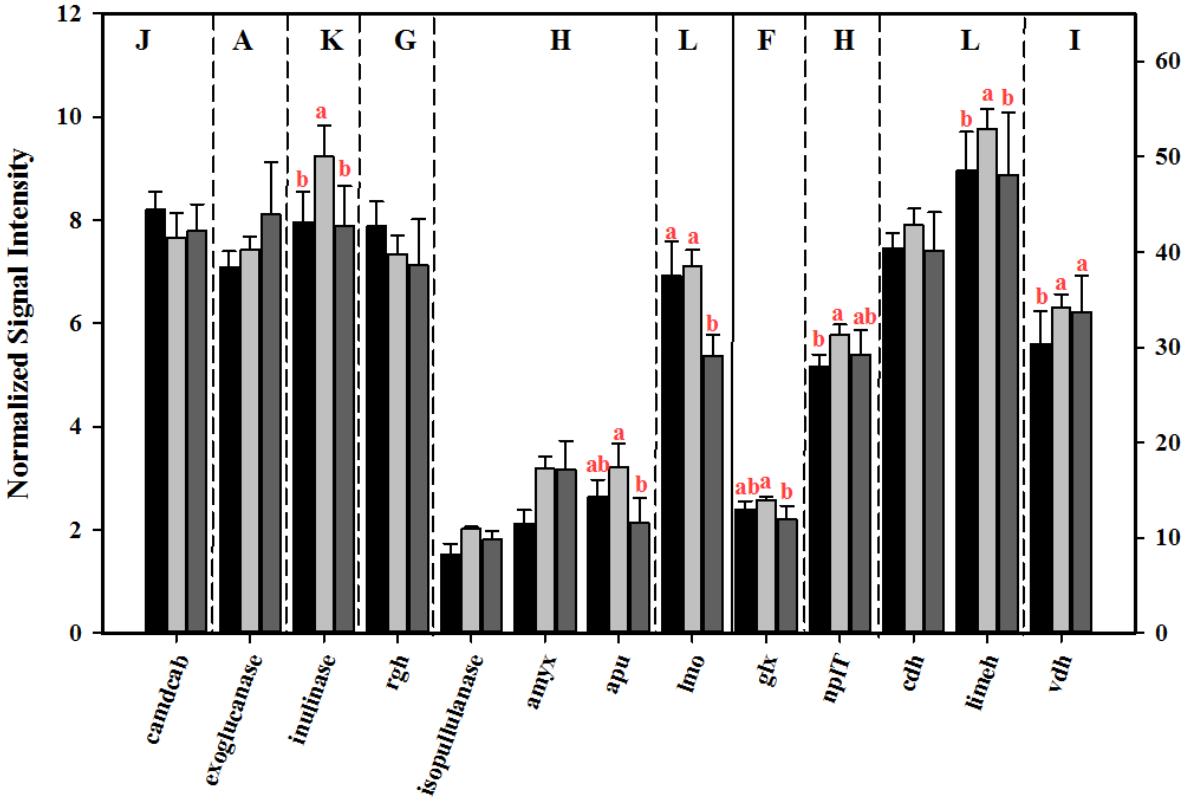
Normalized Signal Intensity
J
A
K
G
H
L
F
H
L
I
camdcab
exoglucanase
inulinase
rgh
isopullulanase
amyx
apu
lmo
glx
nplT
cdh
limeh
vdh

Figure S6.

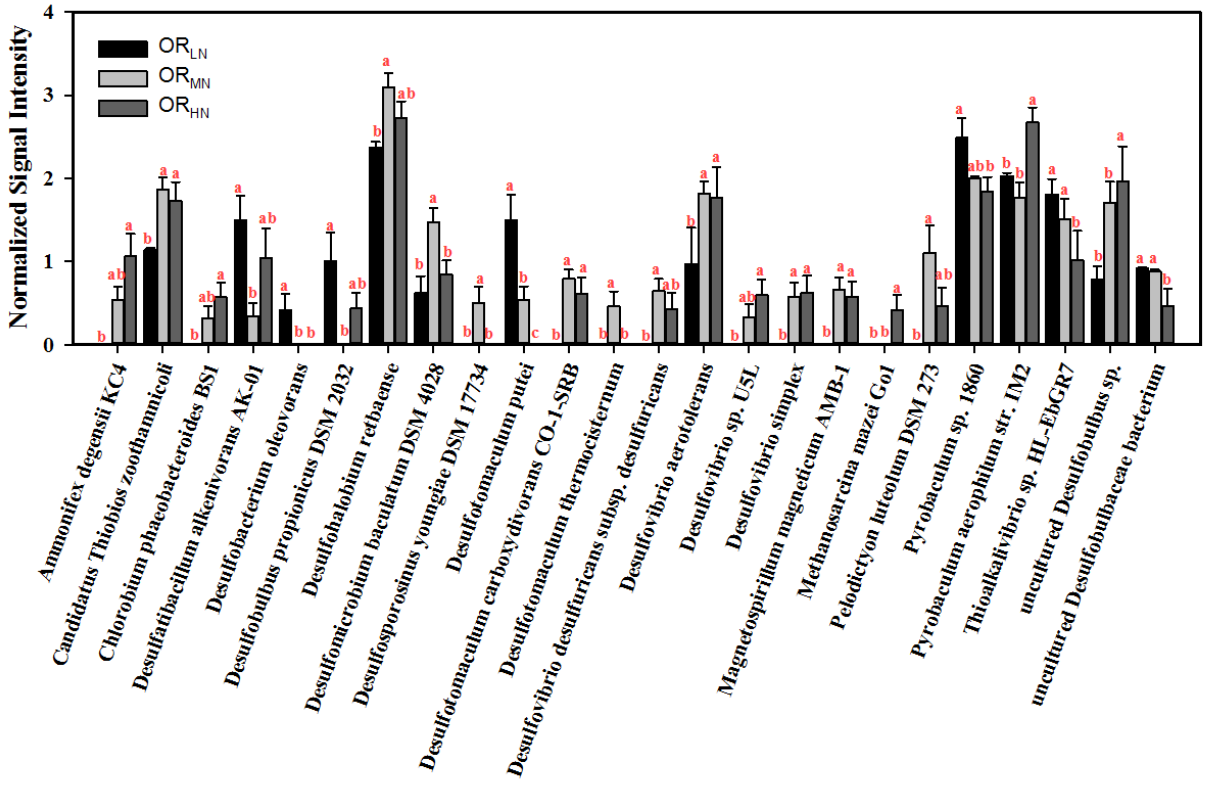
Normalized Signal Intensity
OR_LN
OR_MN
OR_HN
Ammonifex degensii KC4
Candidatus Thiobios zoothamnicoli
Chlorobium phaeobacteroides BS1
Desulfatibacillum alkenivorans AK-01
Desulfobacterium oleovorans
Desulfobulbus propionicus DSM 2032
Desulfohalobium retbaense
Desulfomicrobium baculatum DSM 4028
Desulfosporosinus youngiae DSM 17734
Desulfotomaculum putei
Desulfotomaculum carboxydivorans CO-1-SRB
Desulfotomaculum thermocisternum
Desulfovibrio desulfuricans subsp. desulfuricans
Desulfovibrio aerotolerans
Desulfovibrio sp. U5L
Desulfovibrio simplex
Magnetospirillum magneticum AMB-1
Methanosarcina mazei Go1
Pelodictyon luteolum DSM 273
Pyrobaculum sp. 1860
Pyrobaculum aerophilum str. IM2
Thioalkalivibrio sp. HL-EbGR7
uncultured Desulfobulbus sp.
uncultured Desulfobulbaceae bacterium

Figure S7.

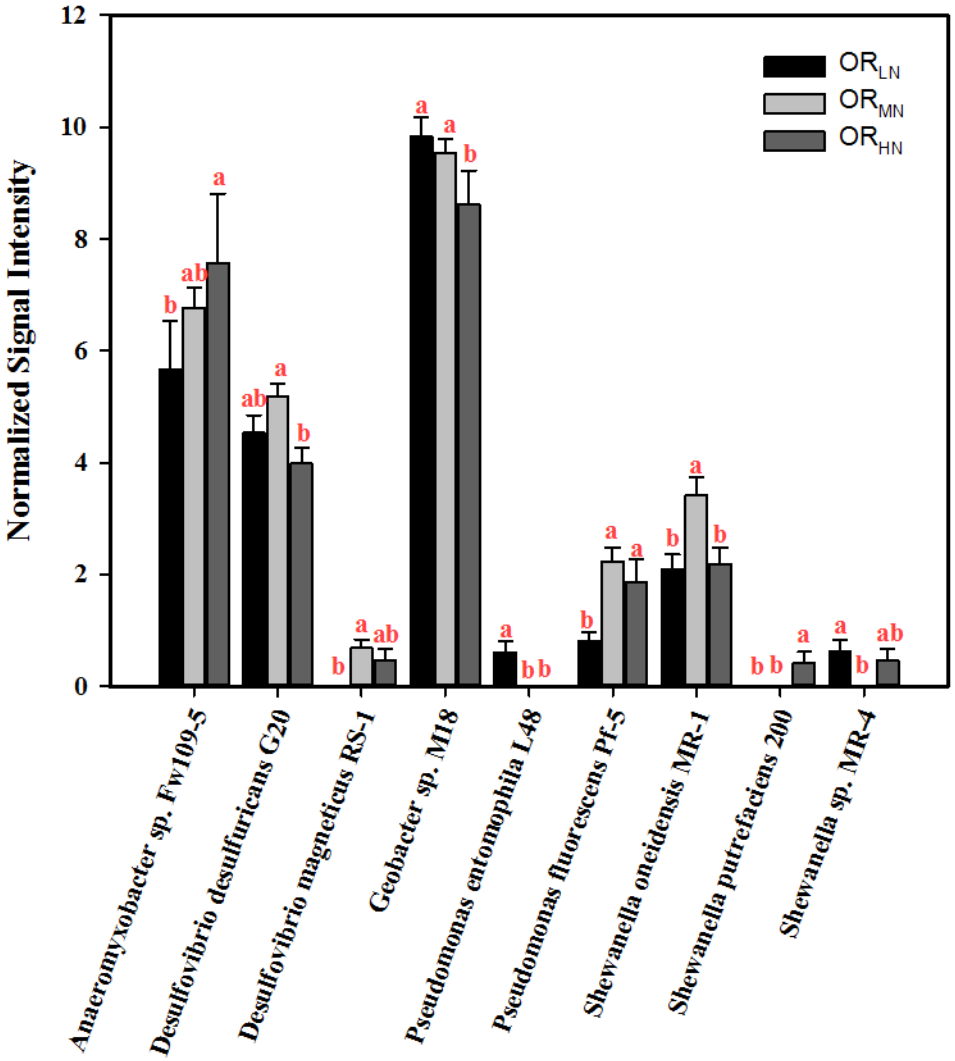
Normalized Signal Intensity
12
10
8
6
4
2
0
OR_LN
OR_MN
OR_HN
a
ab
b
Anaeromyxobacter sp. Fw109-5
Desulfovibrio desulfuricans G20
Desulfovibrio magneticus RS-1
Geobacter sp. M18
Pseudomonas entomophila L48
Pseudomonas fluorescens Pf-5
Shewanella oneidensis MR-1
Shewanella putrefaciens 200
Shewanella sp. MR-4

Figure S8.

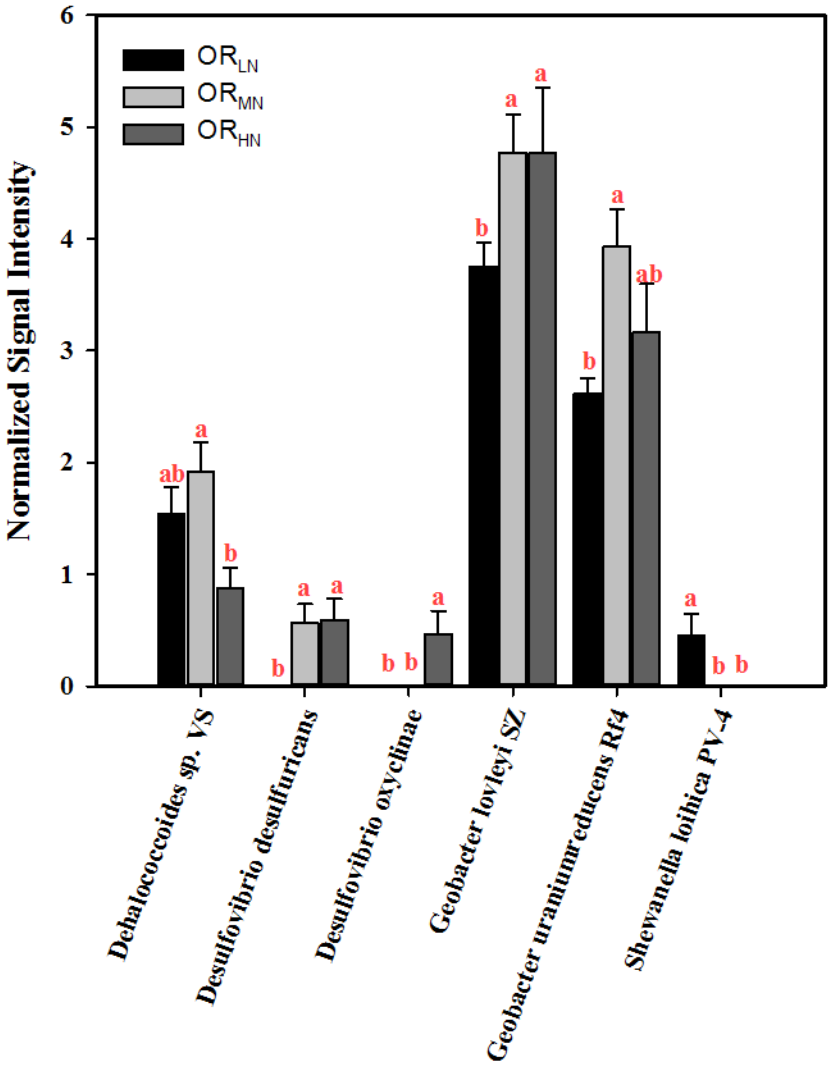
Normalized Signal Intensity
0
1
2
3
4
5
6
OR_LN
OR_MN
OR_HN
ab
a
b
b
a
a
b b
a
b
a
a
b
a
ab
a
b b
Dehalococcoides sp. VS
Desulfovibrio desulfuricans
Desulfovibrio oxyclinae
Geobacter lovleyi SZ
Geobacter uraniumreducens Rf4
Shewanella loihica PV-4

Figure S9A.

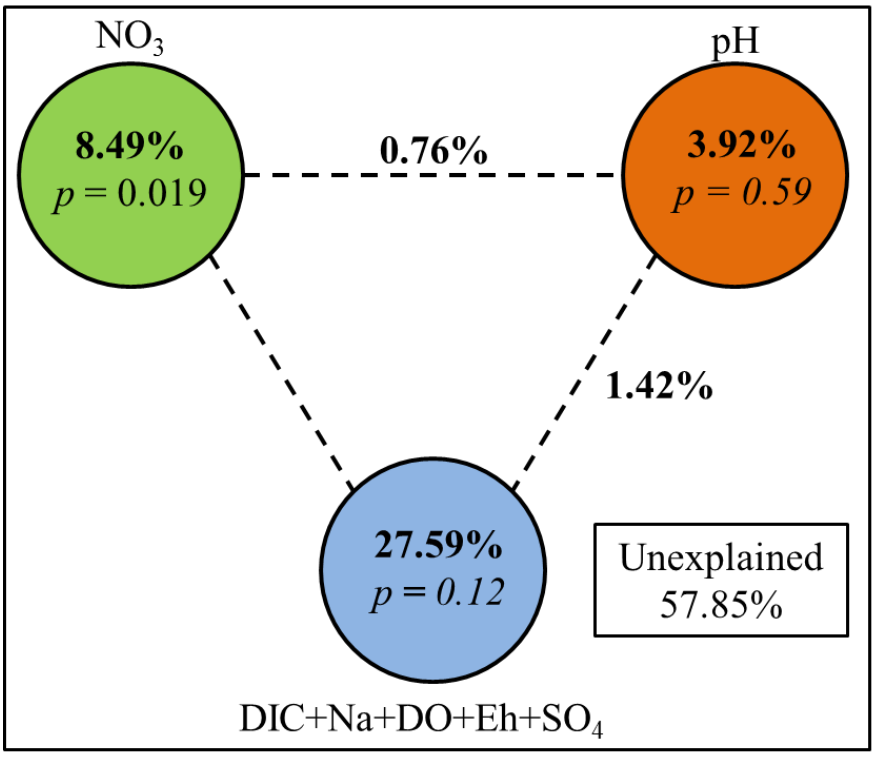
NO3
pH
8.49%
p = 0.019
0.76%
3.92%
p = 0.59
1.42%
27.59%
p = 0.12
Unexplained
57.85%
DIC+Na+DO+Eh+SO4

Figure S9B.

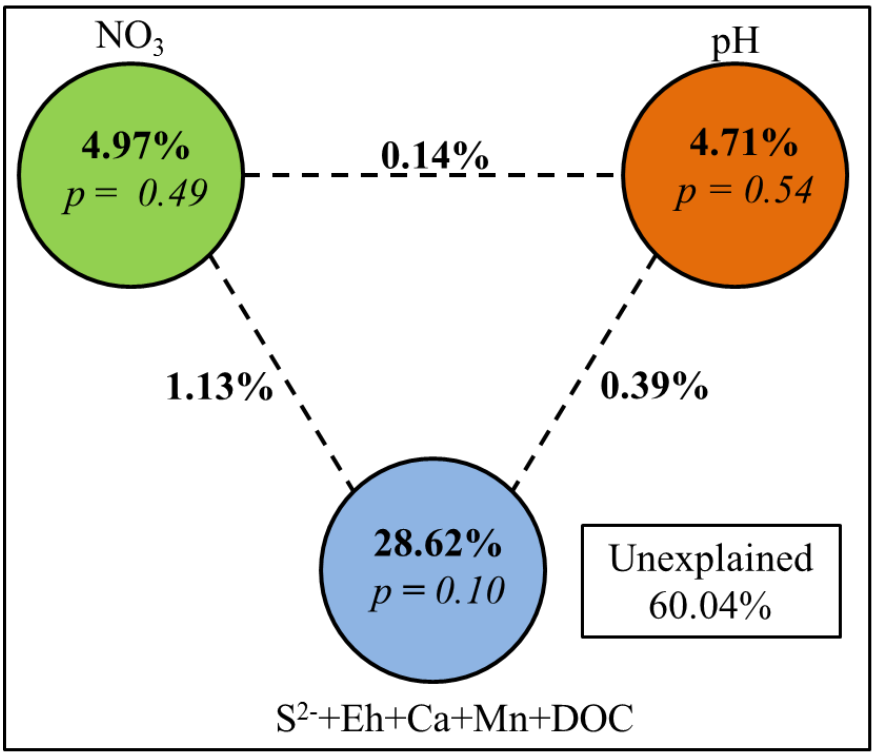
NO3
pH
4.97%
p = 0.49
0.14%
4.71%
p = 0.54
1.13%
0.39%
28.62%
p = 0.10
Unexplained
60.04%
S2-+Eh+Ca+Mn+DOC

Figure S10.

Taxonomy	OR_{LN}	OR_{MN}	OR_{HN}
OTU_26; Unclassified; Unclassified	1.41	0.46	0.15
OTU_2878; Pseudomonas; Gammaproteobacteria	3.50	0.94	0.05
OTU_3; Nitrosopumilus; Nitrosopumilales	9.68	0.07	0.09
OTU_346; Sideroxydans; Betaproteobacteria	1.00	0.08	0.07
OTU_35; Sediminibacterium; Sphingobacteriia	2.40	0.69	0.02
OTU_6; Unclassified; Gammaproteobacteria	8.92	0.00	0.00
OTU_7; Unclassified; Unclassified	2.48	0.02	0.00
OTU_85; Unclassified; Gammaproteobacteria	1.05	0.06	0.01
OTU_10; Massilia; Betaproteobacteria	0.55	2.64	0.05
OTU_11; Unclassified; Unclassified	0.04	3.56	0.01
OTU_12; Arthrobacter; Actinobacteria	0.13	1.97	0.07
OTU_16; Unclassified; Unclassified	0.01	1.27	0.01
OTU_18; Unclassified; Betaproteobacteria	0.00	1.10	0.00
OTU_19; Undibacterium; Betaproteobacteria	0.03	1.70	0.00
OTU_20; Cupriavidus; Betaproteobacteria	0.42	1.95	0.03
OTU_2034; Brevundimonas; Alphaproteobacteria	0.31	2.32	0.43
OTU_22; Malikia; Betaproteobacteria	0.13	1.39	0.02
OTU_38; Afipia; Alphaproteobacteria	0.53	1.20	0.08
OTU_3802; Roseateles; Betaproteobacteria	0.74	1.82	0.11
OTU_41; Unclassified; Betaproteobacteria	0.12	1.09	0.66
OTU_8; Rhodopseudomonas; Alphaproteobacteria	0.17	3.61	0.01
OTU_1; Sideroxydans; Betaproteobacteria	0.60	0.65	8.92
OTU_13; Unclassified; Unclassified	0.03	0.12	1.76
OTU_14; Unclassified; Deltaproteobacteria	0.00	0.01	1.82
OTU_15; Pseudomonas; Gammaproteobacteria	0.07	0.06	2.62
OTU_1515; Unclassified; Betaproteobacteria	0.46	0.93	1.21
OTU_21; Unclassified; Unclassified	0.00	0.00	1.12
OTU_23; Nitrosospira; Betaproteobacteria	0.05	0.15	1.10
OTU_24; Unclassified; Gammaproteobacteria	0.01	0.02	1.28
OTU_25; Unclassified; Unclassified	0.00	0.00	1.08
OTU_27; Gp6; Acidobacteria_Gp6	0.00	0.01	1.19
OTU_32; Nitrosospira; Betaproteobacteria	0.71	0.33	2.01
OTU_43; Unclassified; Unclassified	0.00	0.07	2.18
OTU_5; Unclassified; Unclassified	0.00	0.22	3.87
OTU_9; Unclassified; Unclassified	0.01	0.03	4.55
OTU_17; Unclassified; Betaproteobacteria	2.01	0.23	1.05
OTU_2; Unclassified; Unclassified	1.20	10.10	0.00
OTU_211; Unclassified; Betaproteobacteria	1.16	0.82	1.77
OTU_4; Brevundimonas; Alphaproteobacteria	1.03	7.56	0.04

Figure S11.

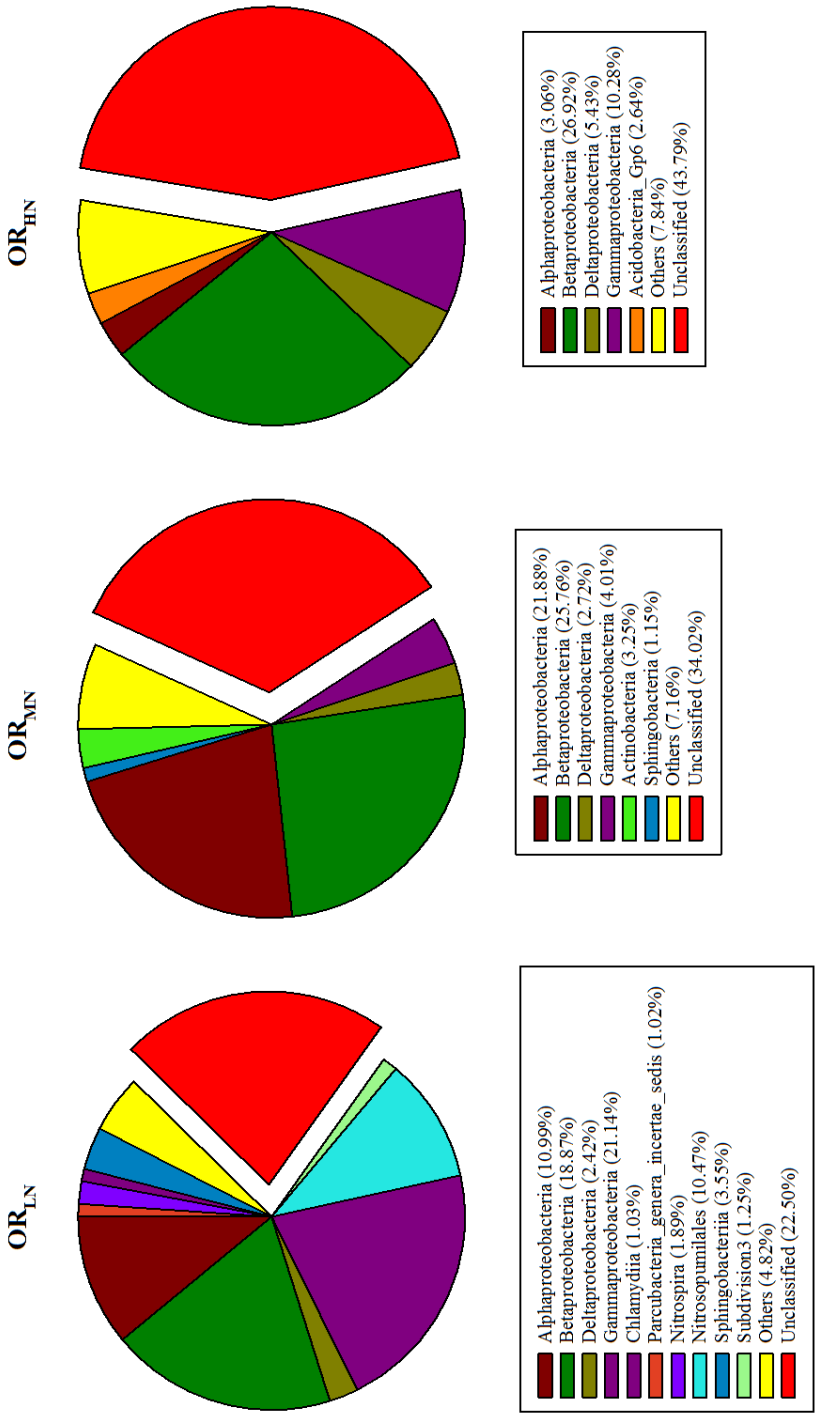
OR_HN
Alphaproteobacteria (3.06%)
Betaproteobacteria (26.92%)
Deltaproteobacteria (5.43%)
Gammaproteobacteria (10.28%)
Acidobacteria_Gp6 (2.64%)
Others (7.84%)
Unclassified (43.79%)
OR_MN
Alphaproteobacteria (21.88%)
Betaproteobacteria (25.76%)
Deltaproteobacteria (2.72%)
Gammaproteobacteria (4.01%)
Actinobacteria (3.25%)
Sphingobacteria (1.15%)
Others (7.16%)
Unclassified (34.02%)
OR_LN
Alphaproteobacteria (10.99%)
Betaproteobacteria (18.87%)
Deltaproteobacteria (2.42%)
Gammaproteobacteria (21.14%)
Chlamydiia (1.03%)
Parcubacteria_genera_incertae_sedis (1.02%)
Nitrospira (1.89%)
Nitrosopumilales (10.47%)
Sphingobacteriia (3.55%)
Subdivision3 (1.25%)
Others (4.82%)
Unclassified (22.50%)

CHAPTER 4: pH and groundwater microbial communities at the OR-IFRC: alkaline conditions reveal enhanced microbial functional potential.

Introduction

Microbes are highly adaptable and our understanding of their ubiquity in natural environments has been enhanced by high throughput techniques in microbial ecology (Keller and Zengler, 2004). While a suite of environmental factors in conjunction with stochastic processes contribute to governing microbial community assembly, pH is one of the most environmental important factors that defines natural microbial communities (Rousk et al., 2009; Inskeep et al., 2010). This finding can be linked to the fact that pH exerts a strong influence on both cell function and geochemistry and therefore plays an important role in the microbiology of any ecosystem (Madshus, 1988; Bigham et al., 1996; Kalbitz et al., 2000; Krulwich et al., 2011) . The Oak Ridge Integrated Field Research Center (OR-IFRC) has lent itself to the study of subsurface microbial communities owing to the unique nature of mixed waste contaminants occurring in the subsurface (Watson et al., 2004a). Given the hazards posed to the environment following the identification of a subsurface contaminant plume emanating from the former S-3 ponds, research has centered on mitigating the spread of radionuclides (uranium, Tc-99 and Th-230) and other heavy metals in the subsurface. Natural attenuation through microbial bio-reduction, has proved a feasible approach to sequester radionucleotides provided conditions in the subsurface are favorable for microbial growth (Wu et al., 2006b; Gihring et al., 2011; Van Nostrand et al., 2011). One major barrier to the successful implementation of field bio-reduction is the extremely acidic pH in highly contaminated areas, with preconditioning of subsurface conditions identified as a necessary prerequisite prior to microbial bioproduction occurring in the subsurface (Wu et al., 2006c; Tang et al., 2013c). While the effect of high nitrate, acidic pH and toxic metals in unison restrict microbial function in highly contaminated areas, oligotrophic conditions due to the limited availability of electron donors and acceptors in aquifer

environments define the limited microbial activity in these terrestrial ecosystems (Griebler and Lueders, 2009).

The most acidic pH levels are seen in areas adjoining the former S-3 ponds. The main contributor to the low pH in the subsurface being the infiltration of liquid nitric acid uranium refining wastes which have seeped through the S-3 unlined surface impoundments (Brooks, 2001; Watson et al., 2004a). The ponds received approximately 10 million liters/year before efforts were made to neutralize and reduce nitrate levels prior to their eventual capping in 1988. The groundwater in the underlying aquifer at the OR-IFRC can fall into the alkaline pH range (> pH 7.0) as a result of the diverse lithologic composition. Cation exchange and reactions driving silicate hydrolysis have been attributed as possible mechanisms for the production of alkaline Na-HCO_3 groundwater at the site (Toran and Saunders, 1999). Very few studies have examined the functional potential of microbial communities under acidic conditions in the field at the OR-IFRC and of the work has focused on evaluating functional potential over the course of field experiments involving bio-stimulation or using microcosms. During field treatments incorporating bio-stimulation of the subsurface microbial community, increased microbial activity is associated with circumneutral pH along with readily metabolizable carbon sources and the removal of inhibitory levels of nitrate (Wu et al., 2006c; Cardenas et al., 2008; Van Nostrand et al., 2011). Work using microcosms has identified the progression of terminal electron accepting processes (TEAPs) to coincide with increases in pH or to be enhanced at circumneutral pH (Michalsen et al., 2006; Edwards et al., 2007). Efforts focusing on microbial function under alkaline conditions in the subsurface haven't been explored at the OR-IFRC given the focus on microbiology in highly contaminated areas. However, microbial activity related to TEAPs involving the utilization of NO_3, Fe(III) and SO_4 in has been identified in the study of alkaline aquifers in Hanford, WA(Stevens et al., 1993). In addition, these TEAPs have also been

documented to occur in microcosms evaluating alkali-tolerant communities evaluated for their application in the remediation of alkaline wastes (Rizoulis et al., 2012). While these processes can occur at alkaline pH there are limits given the observed decreases in free energy yields as pH increases beyond pH 8.0 (Rizoulis et al., 2012).

Amplicon sequencing of the 16S rRNA gene and functional genes (*dsrAB*, *nirK/S*) have been used to study the composition of microbial communities important to natural attenuation efforts at the OR-IFRC (Spain and Krumholz, 2011; Zhang et al., 2017b). The GeoChip functional gene array has primarily been employed to trace microbial functional potential primarily during field experiments evaluating how subsurface respond during and after treatment (Van Nostrand et al., 2009a; Van Nostrand et al., 2011). In this study we specifically utilize a combination of 16S rRNA gene sequencing and the functional gene array (GeoChip 5.0) to address i) How does groundwater pH spanning acidic, circumneutral and alkaline pH influence community functional gene composition and abundance when accounting for the effects of other stressors (high NO_3, high Uranium)? ii) What is the taxonomic composition of these communities? and iii) What are the environmental factors in addition to the pH which influence the taxonomic and functional gene profiles across the wells sampled in this study?

Materials and methods

Procedures for nucleic acid extraction, sample processing for GeoChip 5.0 hybridization, 16S rRNA gene amplicon sequencing and statistical analysis are described in detail in Chapter 3.

Sample Selection

For this study, a subset of the wells from the 100 well survey conducted previously (Smith et al., 2015, Zhou et al., 2018), were selected which covered a gradient in pH and for which data was

available from both the GeoChip 5.0 functional gene array and from 16S rRNA gene sequencing datasets. These wells were selected such that each had NO_3 less that 10 mgL^{-1} at the time of sampling and were distributed among three groups- OR_A (pH < 6.0, 5 wells), OR_{CN} (pH 7.0 – 8.0, 10 wells) and OR_{ALK} (pH > 9.0, 9 wells) (Table S3, Figure S1).

Results

Groundwater Microbial Composition and Structure

Cell counts determined by the AODC method revealed similar readings with no significant differences observed between OR_A, OR_{CN} and OR_{ALK} wells, average DNA yield (total DNA recovered from 4 liters groundwater) was highest from group OR_{ALK} (Figure S2). α diversity estimates using 16S rRNA sequencing data revealed a marginally significant ($p < 0.1$) difference between the OR_{CN} and OR_{ALK} wells for the Shannon index and a significant ($p < 0.05$) difference in OTU richness between these wells (Table S1). However, when comparing α diversity estimates using probes detected on the functional gene array, no significant differences were observed between treatments for the probe richness or the Shannon, Simpson and Peilou indices. While strong clustering of samples was absent in treatment groups (Figure S2), significant differences were observed between OR_A – OR_{ALK} and OR_{CN} – OR_{ALK} comparisons based on dissimilatory tests (MRPP, Adonis and ANOSIM) using the component of 16S rRNA gene sequences detected in these wells (Table 1). DCA ordination plots based on functional genes detected, revealed clustering of samples assigned to the OR_A and OR_{CN} wells while those in the OR_{ALK} wells formed a cluster (Figure S3). In addition, dissimilarity tests using all functional genes detected in the treatment groups revealed significant differences between all three treatments. Ordination using genes identifying NRB, and DMRB did not yield a clear separation or grouping of samples based on treatment group; however the SRB, were seen to cluster based

on the three treatment groups (Figure S4). The highest percentage of unique OTUs (47.92%) were detected in the OR_{CN} wells while the OR_A wells had the least number of unique OTUs (15.17%) (Table S2). Between 17 – 40% of the OTUs detected were shared between the treatment groups with the OR_A and OR_{CN} wells sharing 40% of their taxonomic composition. 76 – 85% of the functional genes detected were shared between treatments (Table S2). The OR_A wells had the fewest unique functional genes (<1%) while the OR_{CN} wells had the highest number of unique functional genes at 7.17% of those detected. Between 15 – 24% of the OTUs detected across the three groups could not accurately be assigned to a taxonomic class. Eleven taxonomic classes comprising *Acidobacteria_Gp2*, *Acidobacteria_Gp3*, *Acidobacteria_Gp5*, *Alphaproteobacteria*, *Chlaymdiia*, *Microgenomates*, *Nitrososphaerales*, *Pacearchaeota Incertae Sedia AR13*, *Planctomycetia*, *Spartobacteria* and *Spirochaetia* were found to differ significantly between at least two of the treatment groups (Figure S11). Most of these taxa were present at <1% in the samples across the treatment groups. Of those taxonomic classes that were detected at >1% RA, *Alphaproteobacteria* (18.77%) and *Chlamydiia* (1.03%) were present at the highest relative abundance in the OR_A wells. *Pacearchaeota Incertae Sedia AR13* and *Planctomycetia* were found to have the highest relative abundance in OR_{CN} wells however these taxa were at <1% RA of those detected. Similarly, while *Microgenomates_genera_incertae_sedis* and *Spartobacteria* were at significantly higher relative abundance in OR_A and OR_{CN} wells they made up <1% of those taxonomic classes identified in these wells. Twelve OTUs comprised >1% RA of those detected in OR_A wells and 6 of these were assigned to *Dechloromoas* (OTU_2; 12.65%), *Variovirax* (OTU_25; 2.38%), *Sediminibacterium* (OTU_18; 2.05%), *Reyranella* (OTU_23; 1.83%), *Acidobacteria* _Gp24(OTU_33; 1.44%), and *Paludibacter* (OTU_52; 1.02%). Two OTUs belonged to *Brevundimonas* (OTU_5; 3.85% and OTU_4115; 2.20%) and the remaining 4 OTUs (OTU_1, OTU_15, OTU_26 and OTU_36 were 'Unclassified' at the

OTU level. Of the 10 OTUs detected at >1% RA in OR_{CN} wells, 3 were assigned to *Streptococcus* (OTU_3; 8.49%), *Acinetobacter* (OTU_24; 1.80%), *Brevundimonas* (OTU_5; 1.58%). Two OTUs were classified as *Pseudonomas*(OTU_20; 2.08% and OTU_2139,1.54%) and 5 (OTU_6, OTU_8, OTU_10, OTU_41 and OTU_588) could not be assigned a genus. Finally in the OR_A wells, 19 OTUs were detected at >1% RA. *Thiobacillus* (OTU_13; 8.98%), *Nitrospira*(OTU_12; 6.01%), *Hydrogenophaga* (OTU_19; 5.12%), *Aridibacter* (OTU_17; 1.59%), *Truepera* (OTU_42; 1.16%), *Bradyrhizobium* (OTU_46; 1.09%) and *Brevundimonas* (OTU_5; 1.01%) could be assigned taxonomy to the genus level and the other 10 OTUs (OTU_4, OTU_7, OTU_8, OTU_9, OTU_11, OTU_16, OTU_21, OTU_28, OTU_29, OTU_43 were 'Unclassified' at the genus level (Figure S10).

Changes in Functional Genes Involved in Important Microbial Processes

C Cycling Genes

Genes responsible for the breakdown of labile and recalcitrant organic carbon were detected in the microbial community (Figure S5). From a total of 8549 bacterial and archaeal probes representing 35 genes, 17(48%) were detected at highest abundance in the OR_{ALK} wells and were significantly different ($p < 0.05$) between at least two treatment groups. Of these genes, *amyA*, *cellobiase*, *chitinase, endoglucanase, xylA* and *xylanase* had lowest relative abundance in the OR_A wells. *acetylglucosaminidase, cda, exoglucanase, mannase, pme and pulA* were seen to have similar functional potentials in the OR_{CN} and OR_{ALK} wells. *ara, aceA, phenol oxidase, vdh and glucoamylase* had enriched functional potential in the OR_{ALK} wells. Methane cycling was studied using 84 probes covering methanogenesis and 70 probes targeting methane oxidation genes and both processes had least functional potential in the OR_A wells. *mcrA* was identified to

have similar relative abundance in OR_{CN} and OR_{ALK} wells. *pmoA* also followed this trend while *mmox* genes had highest relative abundance in OR_{ALK} wells.

N Cycling Genes

Genes responsible for N cycling processes were found to increase in relative abundance from OR_A to OR_{ALK} treatment groups (Figure 1). 11 genes were found to be significantly different between at least two treatment groups. Assimilatory nitrate reductase *nirA*, dissimilatory nitrate reductase *nrfA*, denitrification pathway genes *nirS*, *nosZ* and *nifH* encoding dinitrogen reductase were found to have the lowest functional potential in OR_A wells. Sequences representing nitrate reductase (*narG*), nitric oxide reductase (*norB*) and nitrite reductase (*nirK*) involved in the denitrification pathway did not differ in relative abundance between OR_A and OR_{CN} wells. *nasA*, *nir* and *ureC* encoding reductases driving assimilatory N reduction and the urease gene also followed this trend.

S Cycling Genes

Six genes involved in sulfur metabolism were identified to significantly ($p < 0.05$) differ in relative abundance between at least two groups (Figure 2). A key enzyme in dissimilatory sulfate reduction, *aprAB* encoding dissimilatory adenosine-5'-phospho-sulfate reductase*, sir* and *cysI/J* encoding sulfite reductases and *fccAB* encoding a sulfide dehydrogenase had the highest functional potential in OR_{ALK} wells. 896 probes representing *dsrAB* sequences were identified in the samples. OR_A wells had the lowest relative abundance for these sequences and they were enriched in both OR_{CN} and OR_{ALK} wells. The *sox* gene which codes and enzyme for a H_2S oxidizing also followed the same trend from OR_A to OR_{ALK}. Analysis of 869 probes targeting *dsrAB* like sequences revealed 8 genera to be significantly different between at least two

treatment groups. *dsrAB* like sequences belonging to *Desulfovibrio,* were enriched in both OR_A and OR_{ALK} wells while those from *Desulfatibacillum, Geobacter* and *Thioalkalivibrio* were enriched in both OR_{CN} and OR_{ALK} wells. *Acetohalobium, Ammonifix, Desulforhabdus,* and *Thioalkalivibrio* were only enriched in OR_{ALK} wells. *dsrAB* sequences from *Magnetospirillum* were detected at highest relative abundance in OR_A and OR_{ALK} wells.

Genes Involved in Metal Reduction

Cytochrome c and some *hydrogenase* genes are known to be involved in the reduction of metals. *cytochrome c* sequences were lower in relative abundance in OR_A wells while *hydrogenase* sequences were lower in both OR_A and OR_{ALK} wells respectively (Figure 3). Analysis of 211 *cytochrome* sequences from known metal reducing general that differed significantly between at least two treatment groups revealed *Geobacter* to be depleted in OR_A wells. Sequences from *Anaeromyxobacter* were enriched in OR_{ALK} wells and those from *Pseudomonas* were enriched in both OR_A and OR_{ALK} wells. *hydrogenase* like sequences from *Geobacter* were found to be enriched in OR_{CN} and OR_{ALK} wells.

Influence of Groundwater Geochemistry on Microbial Community Structure

8 geochemical variables were identified to have the strongest influence on the subsurface microbial community based on functional gene composition (Figure 4B). These were, DO (VIF = 3.07), pH (VIF = 2.96), Eh (VIF = 2.09), Ca (VIF = 1.87), Al (VIF = 1.82), DIC (VIF = 1.72), SO_4 (VIF = 1.67) and Zn (VIF = 2.97). Together, these variables were able to explain 35.97% of the variation in functional gene abundance seen across the three treatments ($p < 0.05$). The first axis accounted for 10.7% while the second axis accounted for 8.32% of the explained variation respectively. Eh, Zn and DO exerted a strong influence in the OR_A wells. Ca and SO_4 had the

strongest influence in the OR_{CN} samples while pH, Al and Na were seen to exert the strongest influence in the OR_{ALK} wells. Partitioning of explanatory variables to determine the contribution of pH alone revealed Al, Zn and Ca contributed to variation in functional gene content (Figure S9A). 7 environmental variables were selected to explain the taxonomic composition of the microbial community (Figure 4A). DIC (VIF = 1.70), pH (VIF = 2.01), Al (VIF = 1.50), SO_4 (VIF = 1.75), Ca (VIF = 2.12), NO_3 (VIF = 1.18) and Mn (VIF = 1.97) contributed to explaining 38.17% of the variation in OTUs ($p < 0.001$) detected across the treatment groups. The first axis accounted for 7.0 % while the second axis accounted for 6.17% of the variation in taxonomic composition across the wells. Variance partitioning to separate out the contribution of pH indicated that NO_3 accounted for a slightly larger percentage of variation in taxonomic composition across the wells (Figure S9).

Discussion

Both deterministic and stochastic factors contribute to defining the microbial composition in any given environment. pH is an important environmental variable that influences microbial diversity, abundance and function, and this has been described in studies spanning a range of ecosystems including grasslands, coastal habitats, agricultural systems and contaminated environments (Rousk et al., 2009; Lu et al., 2012; Bai et al., 2013; Yang et al., 2013). In this study we examined the subsurface microbial taxonomic composition and functional potential across a gradient in pH at the OR-IFRC. We found shifts in both the taxonomic and functional composition from samples representing acidic, circumneutral and alkaline conditions in the subsurface while α diversity was not seen to change in samples assigned to these treatments. Overall, the functional potential for genes across most categories detected was negatively influenced by acidic pH. While few of the previous studies at the OR-IFRC explore how

gradients in pH, NO_3 and U(VI) influence microbial composition across the site, a previous study identified inverse relationships between contamination and both functional potential and diversity (Wu et al., 2006). However, the contaminated wells in question were characterized by high nitrate and low pH and each well was studied individually without replicates for treatment conditions. In a similar way, a 16S rRNA molecular survey also identified this inverse relationship between contamination and microbial diversity in sediments from contaminated (acidic pH) and background (neutral pH) wells (Akob et al., 2007).

The greater numbers of unique OTUs and functional genes in the OR_{CN} and OR_{ALK} wells support the taxonomic and functional differences identified when these groups were compared to OR_A wells. The larger taxonomic overlap between OR_A and OR_{CN} wells likely contributes to the insignificant differences in taxonomic composition observed between these two well groups. Previous studies examining functional gene overlap and taxonomic composition have also reported samples more similar in geochemistry to be more similar in terms of their microbial composition (Gihring et al., 2011; Zhang et al., 2015b). Of the classified genera determined to be present at >1% across the treatment groups, *Dechloromoas Sediminibacterium, Variovorax* and genera belonging to the metabolically diverse *Acidobacteria* have been previously identified at the OR-IFRC (Barns et al., 2007; Cardenas et al., 2008; Bollmann et al., 2010; Chourey et al., 2013). The genus *Reyranella* has been identified in oligotrophic environments (Parfenova et al., 2013), *Paludibacter* is a genus known to be capable of fermentation and has been identified in an aquifer environment (Kuppardt et al., 2014) and members belonging to the genus *Acinetobacer* are capable of degrading hydrocarbons (Vanbroekhoven et al., 2004). Species classified as *Brevundimonas*, *Thiobacillus* and *Pseudomonas* have all been described as playing key roles to denitrification at the OR-IFRC (Cardenas et al., 2010; Gihring et al., 2011; Spain and Krumholz, 2011). *Nitrospira* and *Bradyrhizobium* species are implicated as important players in N cycling

given their capability for nitrite oxidation and denitrification respectively while *Hydrogenophaga* species are known to drive hydrogen oxidation (Daims et al., 2015, Hwang et al., 2006, Torres et al., 2011). The detection of *Truepera* sequences in the OR_{ALK} wells can be attributed to its association with alkaline environments (Tiago and Veríssimo, 2013). Though no significant differences between OTUs present at >1% RA were identified it is notable that the overlap between these abundant OTUs is minimal. Only OTU_5 was present above 1% RA in all three treatment groups. Therefore, it is reasonable to conclude that different players could be responsible for nutrient cycling and mediating energy exchange in the wells.

The reduced functional potential in the OR_A samples can be explained by the energy investment needed to counter the damage of intracellular biomolecules (e.g. proteins and nucleic acids) caused by increased intracellular H^+ concentration (Madshus, 1988; Beales, 2004). As a result, maintaining intracellular pH is vital under acidic conditions as imbalances in pH homeostasis can affect physiology by negatively influencing DNA transcription and enzyme activity. However, the active mechanisms employed to counter the intracellular influx of protons which include proton efflux systems, organic acid degradation, synthesis of acid resistant membrane components, decarboxylase enzymes and molecular chaperons involved in protein refolding (Cronan, 2002; Stancik et al., 2002; Baker-Austin and Dopson, 2007) require the investment of energy under the prevailing conditions. While the investment of maintenance energy in combating acid stress in subsurface environments is less examined, the positive correlation between bacterial biomass and pH and decreased bacterial activity under acidic conditions is well documented in soils (Blagodatskaya and Anderson, 1999; Bååth and Anderson, 2003). Furthermore, the increased bacterial respiration rate post acid challenge is implicated as evidence of fulfilling the energy requirements for cell maintenance functions (Anderson and Domsch, 1993). While the potential to degrade a broad range of labile and recalcitrant carbon was detected

across the treatments, DOC and TEAs (NO_3 and SO_4) were low in OR_A wells. Additionally, the availability of DOC in soils has been identified to be negatively influenced by pH (Kalbitz et al., 2000) . Therefore, having to meet maintenance energy requirements at low pH in an oligotrophic setting is a plausible explanation for reduced functional potential in the OR_A wells.

Remediation efforts in the most contaminated areas at the OR-IFRC have focused on optimizing growth conditions for NRB, SRB and DMRB to promote succession of TEAPs which ultimately generates anaerobic conditions favoring bio-reduction (Van Nostrand et al., 2011; Tang et al., 2013; Wu et al., 2006). Our findings indicate similar functional potentials for denitrification at low and circumneutral pH ranges at the OR-IFRC. Previous work at using microcosms established with OR-IFRC sediments monitoring TEAPs at low pH revealed denitrification to proceed in acidic microcosms, albeit at a lower rate compared to microcosms established at circumneutral pH (Shelobolina et al., 2003; Edwards et al., 2006). Furthermore, denitrifying species were present when characterizing metabolically active members in the same sediment (Akob et al., 2007). Biological denitrification has also been determined to proceed at lower rates in other studies using unbuffered microcosms established from acidified sediments (Thorpe et al., 2012).

Since SO_4 is not a contaminant of concern, the study of sulfate reducing populations at the OR-IFRC has primarily focused on their diversity and activity during bio-reduction experiments. Through the analysis of *dsrAB* gene sequences recovered from contaminated and uncontaminated wells revealed their ubiquitous distribution across the site (Bagwell et al., 2006). Given that nitrate is a thermodynamically more favorable electron acceptor, sulfate reduction in contaminated sediments is observed to proceed freely given the availability of electron donors and nitrate consumption either by denitrification or removal via pre-treatment (Van Nostrand et al., 2011; Tang et al., 2013). While nitrate levels in the acidic wells incorporated in this study

were low compared to highly contaminated areas, the increased toxicity of H_2S and organic acids at low pH could be an explanation for the overall reduced functional potential based on *dsrAB* sequences (Koschorreck, 2008). The study of active SRBs at alkaline pH has predominantly focused on hypersaline soda lake environments, with their activity documented at pH > 9.0 (Foti et al., 2007; Sorokin et al., 2008). While SRB activity has not been profiled under alkaline conditions at the OR-IFRC, the above findings lend support for the increased functional potential we observed in alkaline wells. However definite conclusions regarding the activity of these populations cannot be drawn based on signal intensity data from target functional genes.

The study of metal reducing bacteria has been of great interest given their role in controlling the mobility of toxic metals and radionuclides in groundwater at sites like the OR-IFRC (Wall, 2006). Research into the activity of these populations has identified that at the OR-IFRC, pretreatment is necessary to induce more permissive growth conditions prior to significant metal sequestration occurring in the subsurface. Overall, these findings pinpoint high nitrate and highly acidic pH to inhibit microbial activity, with active biological metal reduction occurring after the removal of nitrate and at circumneutral pH (Wu et al., 2006c; Van Nostrand et al., 2011). Given the carbon limited nature of the aquifer, the addition of readily metabolizable electron donors are also important in influencing the activity of species driving dissimilatory metal reduction or through indirect reduction (e.g. via electron transfer from hydrogenases) as a result of metabolic activity under prevailing conditions (Madden et al., 2007). The reduced functional potential of known metal reducing species previously described to bring about metal reduction, indicates that lower pH restricts the capacity for metal reduction across the gradient examined in this study.

pH was found to exert a stronger influence compared to NO_3 and SO_4 on both the taxonomic and functional microbial populations across the OR_A, OR_{CN} and OR_{ALK} wells. pH, NO_3 and SO_4 have been identified as important in explaining the variation seen in subsurface microbial populations

during active bio-reduction phases at the OR-IFRC (Van Nostrand et al., 2011). Their importance stemming from the changes in the concentrations of these anions during the succession of TEAPs in the subsurface. While NO_3 and SO_4 did contribute to the variation in the subsurface community based on taxonomic and functional gene data, it is notable that they influenced the subsurface microbial community to a lesser degree. The lower concentration of these TEAs is reflected in the small size of their vectors (Figure 4A) compared to the other environmental factors. The Al-mediated disruption of cell function is greater at acidic pH given the more prevalent Al^{3+} ions which contribute to the loss of membrane fluidity, increased oxidative stress and reduced ATP synthesis (Auger et al., 2013). The average concentration of Al in the OR_A and OR_{ALK} wells was similar ($0.10 mg/L^{-1}$), thus Al^{3+} is likely to have been more toxic in the OR_A wells and its toxicity in OR_{ALK} wells would depend on the amount that was bioavailable. The strong influence of higher DIC and pH on OR_{ALK} samples can be explained by the finding that dissolution of carbonate minerals and silicate hydrolysis can occur as a result of bicarbonate driven reactions which increase groundwater alkalinity (Toran and Saunders, 1999). Overall, the portion of unexplained variation given the subset of variables selected, is higher than findings from previous studies at the OR-IFRC (Waldron et al., 2009; Xu et al., 2010). The portion of unaccounted variation can be attributed to stochastic processes, unmeasured variables (subsurface lithology, age of groundwater, etc.) and the inability to measure effects arising from the interaction of geochemical variables, which both contribute to influencing microbial communities (Zhou et al., 2014).

We analyzed the taxonomic (~ 7,200 OTUs) and functional (~ 75,000 probes) profiles of groundwater communities collected from the OR-IFRC across a gradient in pH covering acidic, circumneutral and alkaline pH and identified distinct patterns in the functional potential and taxonomic composition. The highest functional potential for genes driving C, N and S cycling as

well as electron transfer processes were under conditions in alkaline wells while the lowest functional potential were observed in wells with acidic pH. Additionally, taxonomic composition was markedly different across each of the treatment groups with a large proportion of OTUs found to occur at low abundance. Groundwater geochemistry varied across the pH gradient with heterogeneity in metals, carbon and redox conditions also governing community composition and function. However further studies examining process rates and microbial activity across spatial and temporal scales are required to confirm the complex responses to subsurface conditions across pH gradients at the OR-IFRC.

Acknowledgements

Dr. Ping Zhang completed the MDA and processing of genomic DNA for GeoChip 5.0 hybridization and 16S rRNA gene amplicon sequencing via the Illumina MiSeq platform. Dr. Joy Van Nostrand provided valuable assistance in selecting wells used in this study. This work was funded by a grant from the U.S Department of Energy, ENIGMA Scientific Focus Area Program.

References

Akob, D.M., Mills, H.J., and Kostka, J.E. (2007) Metabolically active microbial communities in uranium-contaminated subsurface sediments. *FEMS Microbiology Ecology* **59**: 95-107.

Anderson, T.-H., and Domsch, K.H. (1993) The metabolic quotient for CO2 (qCO2) as a specific activity parameter to assess the effects of environmental conditions, such as ph, on the microbial biomass of forest soils. *Soil Biology and Biochemistry* **25**: 393-395.

Auger, C., Han, S., Appanna, V.P., Thomas, S.C., Ulibarri, G., and Appanna, V.D. (2013) Metabolic reengineering invoked by microbial systems to decontaminate aluminum: Implications for bioremediation technologies. *Biotechnology Advances* **31**: 266-273.

Bååth, E., and Anderson, T.H. (2003) Comparison of soil fungal/bacterial ratios in a pH gradient using physiological and PLFA-based techniques. *Soil Biology and Biochemistry* **35**: 955-963.

Bai, S., Li, J., He, Z., Van Nostrand, J.D., Tian, Y., Lin, G. et al. (2013) GeoChip-based analysis of the functional gene diversity and metabolic potential of soil microbial communities of mangroves. *Applied Microbiology and Biotechnology* **97**: 7035-7048.

Baker-Austin, C., and Dopson, M. (2007) Life in acid: pH homeostasis in acidophiles. *Trends in Microbiology* **15**: 165-171.

Beales, N. (2004) Adaptation of microorganisms to cold temperatures, weak acid preservatives, low pH, and osmotic stress: a review. *Comprehensive Reviews in Food science and Food safety* **3**: 1-20.

Bigham, J., Schwertmann, U., and Pfab, G. (1996) Influence of pH on mineral speciation in a bioreactor simulating acid mine drainage. *Applied geochemistry* **11**: 845-849.

Blagodatskaya, E.V., and Anderson, T.-H. (1999) Adaptive responses of soil microbial communities under experimental acid stress in controlled laboratory studies. *Applied Soil Ecology* **11**: 207-216.

Brooks, S.C. (2001) Waste characteristics of the former S-3 ponds and outline of uranium chemistry relevant to NABIR Field Research Center studies. *NABIR Field Research Center, Oak Ridge, Tenn*.

Cardenas, E., Wu, W.-M., Leigh, M.B., Carley, J., Carroll, S., Gentry, T. et al. (2008) Microbial Communities in Contaminated Sediments, Associated with Bioremediation of Uranium to Submicromolar Levels. *Applied and Environmental Microbiology* **74**: 3718-3729.

Cronan, J.E., Jr. (2002) Phospholipid modifications in bacteria. *Curr Opin Microbiol* **5**: 202-205.

Edwards, L., Küsel, K., Drake, H., and Kostka, J.E. (2007) Electron flow in acidic subsurface sediments co-contaminated with nitrate and uranium. *Geochimica et Cosmochimica Acta* **71**: 643-654.

Foti, M., Sorokin, D.Y., Lomans, B., Mussman, M., Zacharova, E.E., Pimenov, N.V. et al. (2007) Diversity, Activity, and Abundance of Sulfate-Reducing Bacteria in Saline and Hypersaline Soda Lakes. *Applied and Environmental Microbiology* **73**: 2093-2100.

Gihring, T.M., Zhang, G., Brandt, C.C., Brooks, S.C., Campbell, J.H., Carroll, S. et al. (2011) A limited microbial consortium is responsible for extended bio-reduction of uranium in a contaminated aquifer. *Applied and Environmental Microbiology*: AEM. 00220-00211.

Griebler, C., and Lueders, T. (2009) Microbial biodiversity in groundwater ecosystems. *Freshwater Biology* **54**: 649-677.

Inskeep, W.P., Rusch, D.B., Jay, Z.J., Herrgard, M.J., Kozubal, M.A., Richardson, T.H. et al. (2010) Metagenomes from High-Temperature Chemotrophic Systems Reveal Geochemical Controls on Microbial Community Structure and Function. *PLOS ONE* **5**: e9773.

Kalbitz, K., Solinger, S., Park, J.-H., Michalzik, B., and Matzner, E. (2000) CONTROLS ON THE DYNAMICS OF DISSOLVED ORGANIC MATTER IN SOILS: A REVIEW. *Soil Science* **165**: 277-304.

Keller, M., and Zengler, K. (2004) Tapping into microbial diversity. *Nature Reviews Microbiology* **2**: 141.

Koschorreck, M. (2008) Microbial sulphate reduction at a low pH. *FEMS Microbiology Ecology* **64**: 329-342.

Krulwich, T.A., Sachs, G., and Padan, E. (2011) Molecular aspects of bacterial pH sensing and homeostasis. *Nature Reviews Microbiology* **9**: 330.

Lu, Z., He, Z., Parisi, V.A., Kang, S., Deng, Y., Van Nostrand, J.D. et al. (2012) GeoChip-Based Analysis of Microbial Functional Gene Diversity in a Landfill Leachate-Contaminated Aquifer. *Environmental Science & Technology* **46**: 5824-5833.

Madden, A.S., Smith, A.C., Balkwill, D.L., Fagan, L.A., and Phelps, T.J. (2007) Microbial uranium immobilization independent of nitrate reduction. *Environmental Microbiology* **9**: 2321-2330.

Madshus, I.H. (1988) Regulation of intracellular pH in eukaryotic cells. *Biochemical journal* **250**: 1.

Michalsen, M.M., Goodman, B.A., Kelly, S.D., Kemner, K.M., McKinley, J.P., Stucki, J.W., and Istok, J.D. (2006) Uranium and Technetium Bio-Immobilization in Intermediate-Scale Physical Models of an In Situ Bio-Barrier. *Environmental Science & Technology* **40**: 7048-7053.

Rizoulis, A., Steele, H., Morris, K., and Lloyd, J. (2012) The potential impact of anaerobic microbial metabolism during the geological disposal of intermediate-level waste. *Mineralogical Magazine* **76**: 3261-3270.

Rousk, J., Brookes, P.C., and Bååth, E. (2009) Contrasting Soil pH Effects on Fungal and Bacterial Growth Suggest Functional Redundancy in Carbon Mineralization. *Applied and Environmental Microbiology* **75**: 1589-1596.

Sorokin, D.Y., Tourova, T.P., Mußmann, M., and Muyzer, G. (2008) Dethiobacter alkaliphilus gen. nov. sp. nov., and Desulfurivibrio alkaliphilus gen. nov. sp. nov.: two novel representatives of reductive sulfur cycle from soda lakes. *Extremophiles* **12**: 431-439.

Spain, A.M., and Krumholz, L.R. (2011) Nitrate-reducing bacteria at the nitrate and radionuclide contaminated Oak Ridge Integrated Field Research Challenge site: a review. *Geomicrobiology Journal* **28**: 418-429.

Stancik, L.M., Stancik, D.M., Schmidt, B., Barnhart, D.M., Yoncheva, Y.N., and Slonczewski, J.L. (2002) pH-dependent expression of periplasmic proteins and amino acid catabolism in Escherichia coli. *J Bacteriol* **184**: 4246-4258.

Stevens, T., McKinley, J., and Fredrickson, J.K. (1993) Bacteria associated with deep, alkaline, anaerobic groundwaters in southeast Washington. *Microbial Ecology* **25**: 35-50.

Tang, G., Watson, D.B., Wu, W.-M., Schadt, C.W., Parker, J.C., and Brooks, S.C. (2013) U (VI) bio-reduction with emulsified vegetable oil as the electron donor–model application to a field test. *Environmental science & technology* **47**: 3218-3225.

Toran, L.E., and Saunders, J.A. (1999) Modeling alternative paths of chemical evolution of Na-HCO3-type groundwater near Oak Ridge, Tennessee, USA. *Hydrogeology Journal* **7**: 355-364.

Van Nostrand, J.D., Wu, W.M., Wu, L., Deng, Y., Carley, J., Carroll, S. et al. (2009) GeoChip-based analysis of functional microbial communities during the reoxidation of a bioreduced uranium-contaminated aquifer. *Environmental Microbiology* **11**: 2611-2626.

Van Nostrand, J.D., Wu, L., Wu, W.-M., Huang, Z., Gentry, T.J., Deng, Y. et al. (2011) Dynamics of microbial community composition and function during in-situ bioremediation of a uranium-contaminated aquifer. *Applied and environmental microbiology*: AEM. 01981-01910.

Waldron, P.J., Wu, L., Nostrand, J.D.V., Schadt, C.W., He, Z., Watson, D.B. et al. (2009) Functional Gene Array-Based Analysis of Microbial Community Structure in Groundwaters with a Gradient of Contaminant Levels. *Environmental Science & Technology* **43**: 3529-3534.

Watson, D., Kostka, J., Fields, M., and Jardine, P. (2004) The Oak Ridge field research center conceptual model. *NABIR Field Research Center, Oak Ridge, TN*.

Wu , L., Liu, X., Schadt, C.W., and Zhou, J. (2006) Microarray-Based Analysis of Subnanogram Quantities of Microbial Community DNAs by Using Whole-Community Genome Amplification. *Applied and Environmental Microbiology* **72**: 4931-4941.

Wu, W.-M., Carley, J., Fienen, M., Mehlhorn, T., Lowe, K., Nyman, J. et al. (2006a) Pilot-scale in situ bioremediation of uranium in a highly contaminated aquifer. 1. Conditioning of a treatment zone. *Environmental science & technology* **40**: 3978-3985.

Wu, W.-M., Carley, J., Gentry, T., Ginder-Vogel, M.A., Fienen, M., Mehlhorn, T. et al. (2006b) Pilot-scale in situ bioremedation of uranium in a highly contaminated aquifer. 2. Reduction of U (VI) and geochemical control of U (VI) bioavailability. *Environmental science & technology* **40**: 3986-3995.

Xu, M., Wu, W.-M., Wu, L., He, Z., Van Nostrand, J.D., Deng, Y. et al. (2010) Responses of microbial community functional structures to pilot-scale uranium in situ bioremediation. *The Isme Journal* **4**: 1060.

Yang, Y., Gao, Y., Wang, S., Xu, D., Yu, H., Wu, L. et al. (2013) The microbial gene diversity along an elevation gradient of the Tibetan grassland. *The Isme Journal* **8**: 430.

Zhang, P., He, Z., Van Nostrand, J.D., Qin, Y., Deng, Y., Wu, L. et al. (2017) Dynamic Succession of Groundwater Sulfate-Reducing Communities during Prolonged Reduction of Uranium in a Contaminated Aquifer. *Environmental Science & Technology* **51**: 3609-3620.

Zhang, P., Wu, W.-M., Van Nostrand, J.D., Deng, Y., He, Z., Gihring, T. et al. (2015) Dynamic succession of groundwater functional microbial communities in response to emulsified vegetable oil amendment during sustained in situ U(VI) reduction. *Applied and Environmental Microbiology*.

Zhou, J., Deng, Y., Zhang, P., Xue, K., Liang, Y., Van Nostrand, J.D. et al. (2014) Stochasticity, succession, and environmental perturbations in a fluidic ecosystem. Proceedings of the National Academy of Sciences: 201324044.

Barns, S.M., Cain, E.C., Sommerville, L., and Kuske, C.R. (2007) Acidobacteria Phylum Sequences in Uranium-Contaminated Subsurface Sediments Greatly Expand the Known Diversity within the Phylum. Applied and Environmental Microbiology **73**: 3113-3116.

Bollmann, A., Palumbo, A.V., Lewis, K., and Epstein, S.S. (2010) Isolation and physiology of bacteria from contaminated subsurface sediments. Applied and environmental microbiology **76**: 7413-7419.

Cardenas, E., Wu, W.-M., Leigh, M.B., Carley, J., Carroll, S., Gentry, T. et al. (2010) Significant association between sulfate-reducing bacteria and uranium-reducing microbial communities as revealed by a combined massively parallel sequencing-indicator species approach. Applied and environmental microbiology **76**: 6778-6786.

Cardenas, E., Wu, W.-M., Leigh, M.B., Carley, J., Carroll, S., Gentry, T. et al. (2008) Microbial Communities in Contaminated Sediments, Associated with Bioremediation of Uranium to Submicromolar Levels. Applied and Environmental Microbiology **74**: 3718-3729.

Chourey, K., Nissen, S., Vishnivetskaya, T., Shah, M., Pfiffner, S., Hettich, R.L., and Löffler, F.E. (2013) Environmental proteomics reveals early microbial community responses to biostimulation at a uranium- and nitrate-contaminated site. PROTEOMICS **13**: 2921-2930.

Daims, H., Lebedeva, E.V., Pjevac, P., Han, P., Herbold, C., Albertsen, M. et al. (2015) Complete nitrification by Nitrospira bacteria. Nature **528**: 504.

Gihring, T.M., Zhang, G., Brandt, C.C., Brooks, S.C., Campbell, J.H., Carroll, S. et al. (2011) A Limited Microbial Consortium Is Responsible for Extended Bioreduction of Uranium in a Contaminated Aquifer. Applied and Environmental Microbiology **77**: 5955-5965.

Hwang, C., Wu, W.-M., Gentry, T.J., Carley, J., Carroll, S.L., Schadt, C. et al. (2006) Changes in bacterial community structure correlate with initial operating conditions of a field-scale denitrifying fluidized bed reactor. Applied Microbiology and Biotechnology **71**: 748-760.

Kuppardt, A., Kleinsteuber, S., Vogt, C., Lüders, T., Harms, H., and Chatzinotas, A. (2014) Phylogenetic and Functional Diversity Within Toluene-Degrading, Sulphate-Reducing Consortia Enriched from a Contaminated Aquifer. Microbial Ecology **68**: 222-234.

Parfenova, V.V., Gladkikh, A.S., and Belykh, O.I. (2013) Comparative analysis of biodiversity in the planktonic and biofilm bacterial communities in Lake Baikal. Microbiology **82**: 91-101.

Spain, A.M., and Krumholz, L.R. (2011) Nitrate-reducing bacteria at the nitrate and radionuclide contaminated Oak Ridge Integrated Field Research Challenge site: a review. Geomicrobiology Journal **28**: 418-429.

Tiago, I., and Veríssimo, A. (2013) Microbial and functional diversity of a subterrestrial high pH groundwater associated to serpentinization. Environmental Microbiology **15**: 1687-1706.

Torres, M.J., Bueno, E., Mesa, S., Bedmar, E.J., and Delgado, M.J. (2011) Emerging complexity in the denitrification regulatory network of Bradyrhizobium japonicum. In: Portland Press Limited.

Vanbroekhoven, K., Ryngaert, A., Wattiau, P., De Mot, R., and Springael, D. (2004) Acinetobacter diversity in environmental samples assessed by 16S rRNA gene PCR–DGGE fingerprinting. FEMS microbiology ecology **50**: 37-50.

Akob, D.M., Mills, H.J., and Kostka, J.E. (2007) Metabolically active microbial communities in uranium-contaminated subsurface sediments. *FEMS Microbiology Ecology* **59**: 95-107.

Bagwell, C.E., Liu, X., Wu, L., and Zhou, J. (2006) Effects of legacy nuclear waste on the compositional diversity and distributions of sulfate-reducing bacteria in a terrestrial subsurface aquifer. *FEMS microbiology ecology* **55**: 424-431.

Edwards, L., Küsel, K., Drake, H., and Kostka, J.E. (2007) Electron flow in acidic subsurface sediments co-contaminated with nitrate and uranium. *Geochimica et Cosmochimica Acta* **71**: 643-654.

Shelobolina, E.S., Sullivan, S.A., O'Neill, K.R., Nevin, K.P., and Lovley, D.R. (2004) Isolation, Characterization, and U(VI)-Reducing Potential of a Facultatively Anaerobic, Acid-Resistant Bacterium from Low-pH, Nitrate- and U(VI)-Contaminated Subsurface Sediment and Description of Salmonella subterranea sp. nov. *Applied and Environmental Microbiology* **70**: 2959-2965.

Thorpe, C.L., Law, G.T.W., Boothman, C., Lloyd, J.R., Burke, I.T., and Morris, K. (2012) The Synergistic Effects of High Nitrate Concentrations on Sediment Bioreduction. *Geomicrobiology Journal* **29**: 484-493.

Chapter 4 – Figure legends

Figure 1. Normalized signal intensity representing the relative abundance for detected N cycling genes. Significant differences identified between means are indicated by different letters. Calculation based on ANOVA followed by Fisher's LSD test. N cycling categories: A) Anammox; B) Denitrification; C) Assimilatory N Reduction; D) Nitrification; E) Ammonification; F) Dissimilatory N Reduction; G) Nitrogen Fixation.

Figure 2. Normalized signal intensity representing the relative abundance for detected S cycling genes. Significant differences identified between means are indicated by different letters. Calculation based on ANOVA followed by Fisher's LSD test. N cycling categories: A) DMSP degradation; B) Sulfide Oxidation; C) adenylylsulfate reductase; D) Sulfite Reduction; E) Sulfur Oxidation.

Figure 3. Normalized signal intensity representing the relative abundance for detected genes influencing electron transfer. Significant differences identified between means are indicated by different letters. Calculation based on ANOVA followed by Fisher's LSD test.

Figure 4. Canonical correspondence analysis (CCA) using (A) taxonomic composition and (B) functional gene profiles from wells surveyed. Environmental variables were selected using forward selection procedure and variance inflation factors (VIFs < 20) calculated during CCA procedure. Environmental variables included: Eh, Redox potential; DO, Dissolved oxygen; DIC, Dissolved Inorganic Carbon; DOC, Dissolved Organic Carbon; Na, Sodium; pH, Mn, Manganese; Ca, Calcium; S^{2-}, Sulfide; NO_3^-, Nitrate; SO_4^{2-}, Sulfate.

Figure 1A.

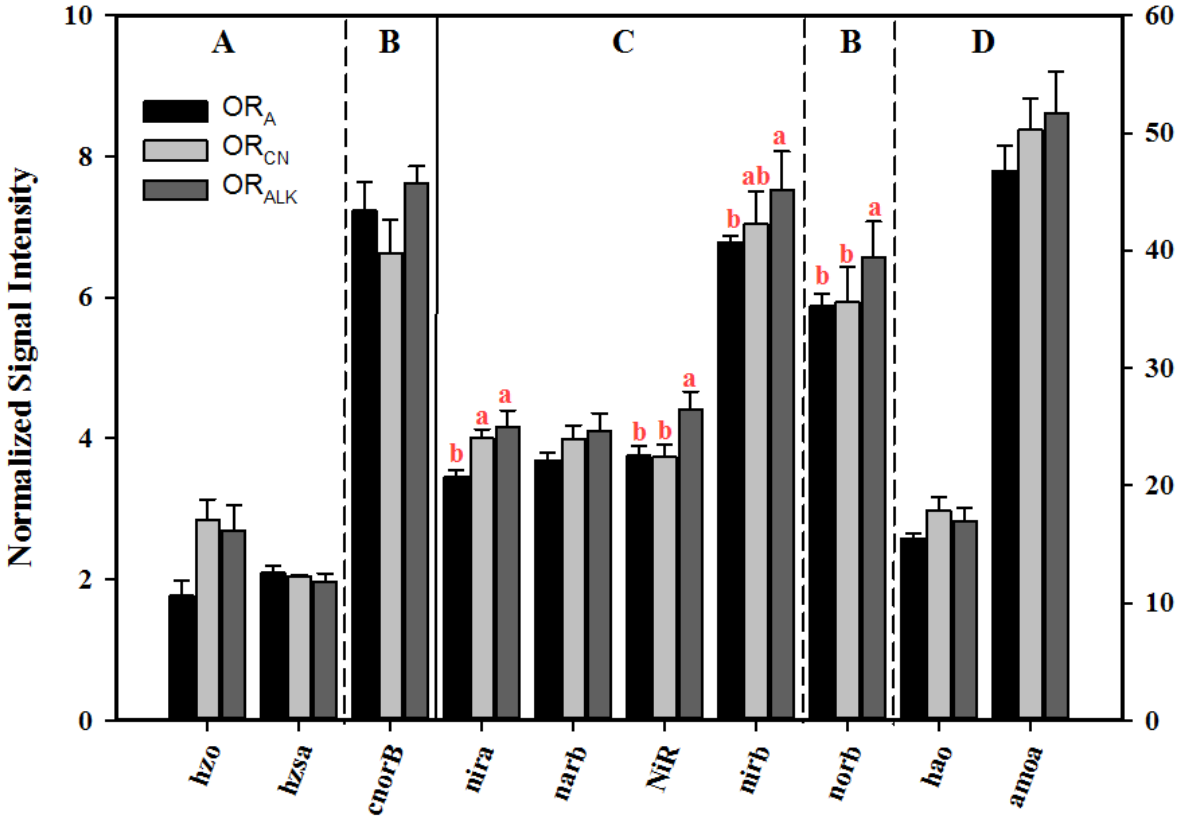
Normalized Signal Intensity
A
B
C
B
D
OR_A
OR_CN
OR_ALK
hzo
hzsa
cnorB
nira
narb
NiR
nirb
norb
hao
amoa

Figure 1B.

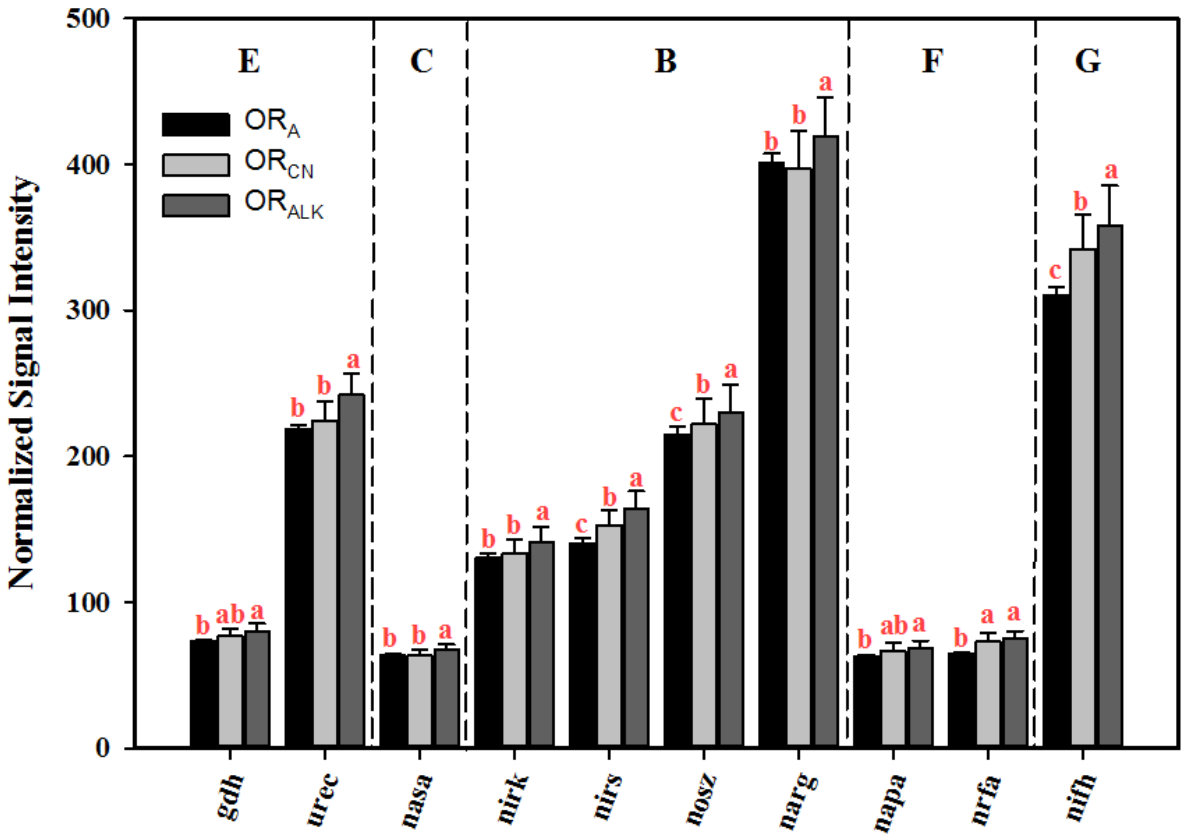
Normalized Signal Intensity
500
400
300
200
100
0
E
C
B
F
G
OR_A
OR_CN
OR_ALK
gdh
urec
nasa
nirk
nirs
nosz
narg
napa
nrfa
nifh

Figure 2.

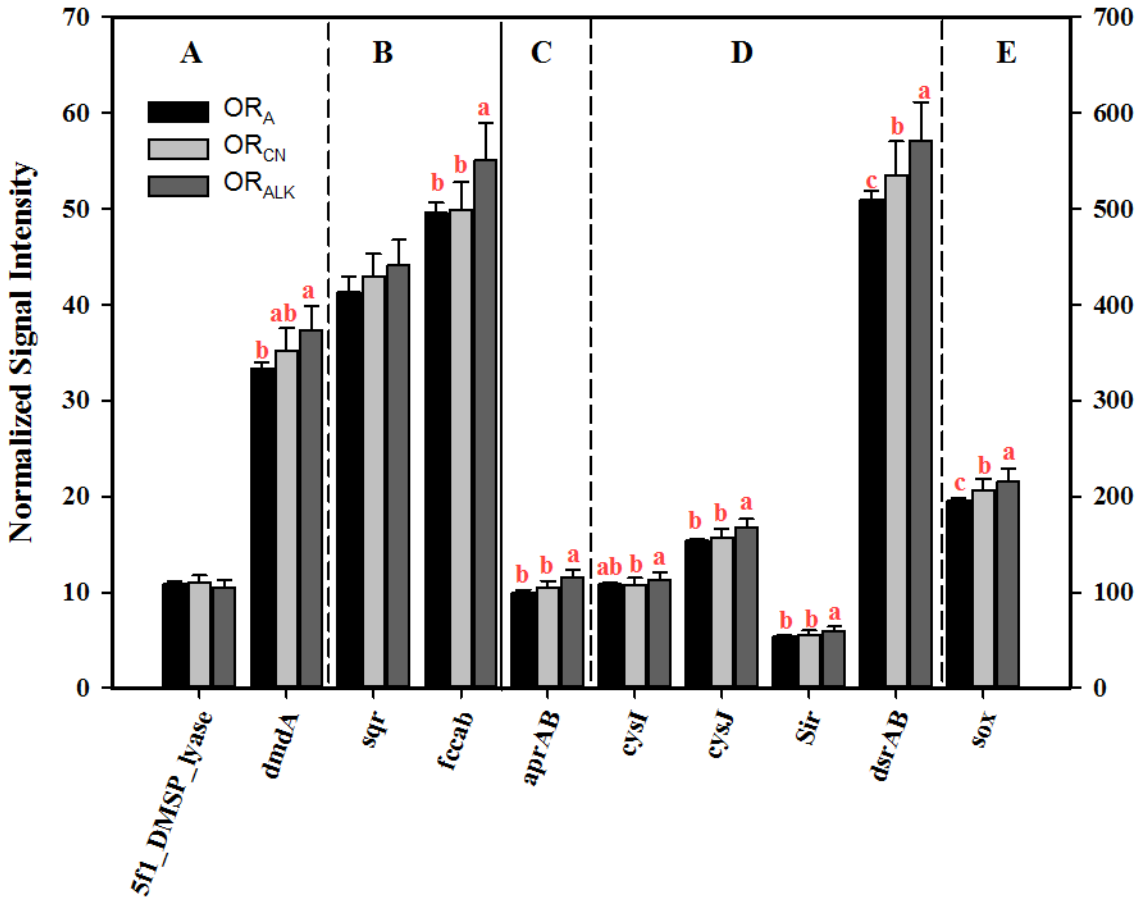
Normalized Signal Intensity
70
60
50
40
30
20
10
0
700
600
500
400
300
200
100
0
A
B
C
D
E
OR_A
OR_CN
OR_ALK
5fl_DMSP_lyase
dmdA
sqr
fccab
aprAB
cysI
cysJ
Sir
dsrAB
sox

Figure 3.

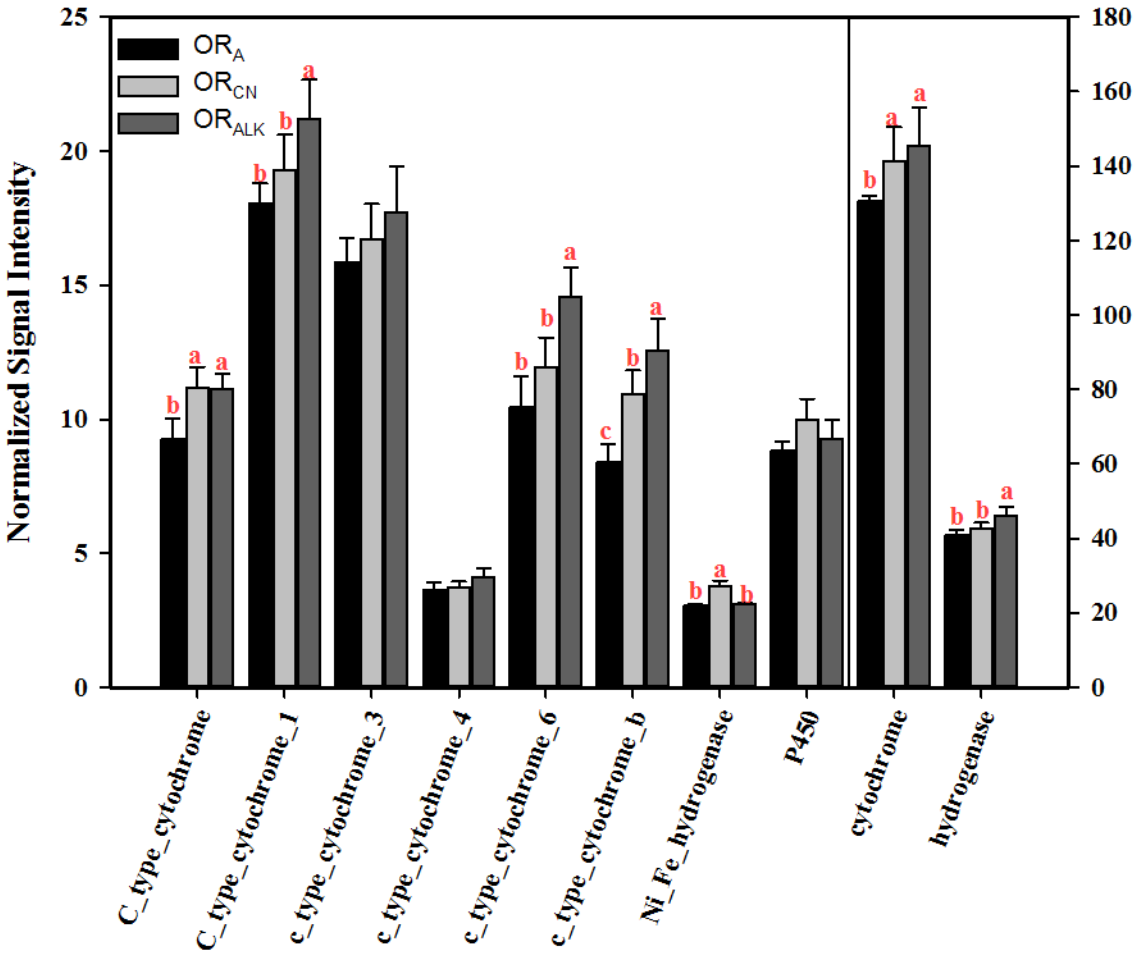
Normalized Signal Intensity
OR_A
OR_CN
OR_ALK
C_type_cytochrome
C_type_cytochrome_1
c_type_cytochrome_3
c_type_cytochrome_4
c_type_cytochrome_6
c_type_cytochrome_b
Ni_Fe_hydrogenase
P450
cytochrome
hydrogenase

Figure 4A.

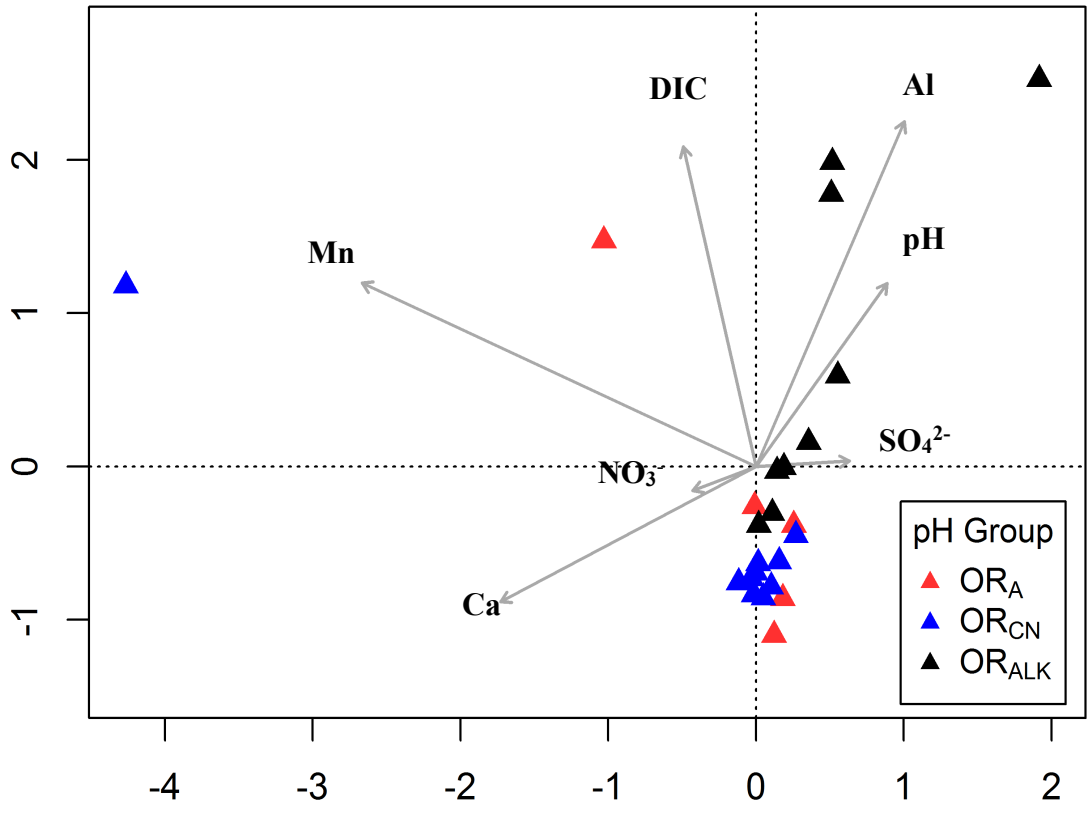

Figure 4B.

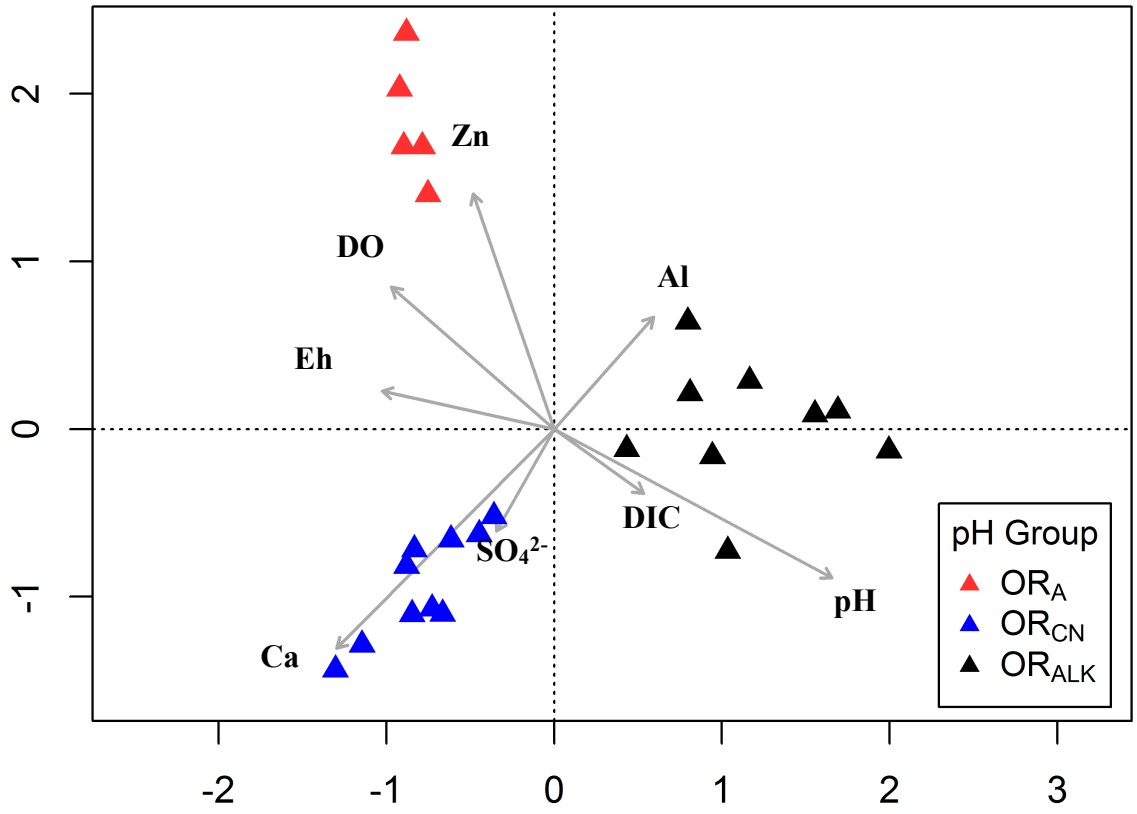

Chapter 4

Table 1.

Summary of nonparametric multivariate dissimilarity tests of functional gene and 16S rRNA gene profiles between pairs of treatment groups. MRPP, multiresponse permutation procedures; Adonis, permutational multivariate analysis of variance using distance matrices; ANOISM, analysis of similarity. Distances calculated are based on Bray-Curtis index. P values < 0.1 are in bold.

Dataset	Comparison		Sample set	MRPP		Adonis		ANOSIM	
				δ	p	R	p	F	p
GeoChip	OR_A	OR_{CN}	15 samples	0.192	**0.005**	0.135	0.158	2.149	**0.03**
	OR_A	OR_{ALK}	14 samples	0.178	**0.007**	0.241	**0.061**	2.481	**0.02**
	OR_{CN}	OR_{ALK}	19 samples	0.209	**0.052**	0.082	**0.087**	1.670	0.12
16s rRNA gene sequencing	OR_A	OR_{CN}	15 samples	0.885	0.157	0.031	0.306	1.142	0.17
	OR_A	OR_{ALK}	14 samples	0.879	**0.006**	0.402	**0.006**	1.731	**0.01**
	OR_{CN}	OR_{ALK}	19 samples	0.864	**0.01**	0.369	**0.01**	1.957	**0.004**

Supplemental material

Table S1.

Indices capturing measures of α diversity for both functional genes detected by GeoChip and taxonomic profiles determined by 16S rRNA amplicon sequencing. ± indicate standard error. Differences between means from two treatments were tested using ANOVA. Different letters denote significant difference. **, $p < 0.05$; * $p < 0.1$

Dataset	Indices	OR_A	OR_{CN}	OR_{ALK}
GeoChip	Probe number	49168 ± 589	51503 ± 2969	53642 ± 3298
	Shannon	10.796 ± 0.01	10.827 ± 0.06	10.866 ± 0.06
	Simpson	0.99997937 ± 0.0000003	0.99997966 ± 0.0000014	0.99998043 ± 0.0000014
	Evenness	0.999394 ± 0.0000712	0.9995472 ± 0.0000456	0.999402 ± 0.0000362
16s rRNA gene sequencing	OTUs **	921 ± 420 ^{ab}	1225 ± 387 ^{a}	361 ± 120 ^{b}
	Shannon *	3.836 ± 0.81 ^{ab}	4.276 ± 1.352 ^{a}	2.729 ± 0.909 ^{b}
	Simpson	0.837 ± 0.071	0.861 ± 0.272	0.813 ± 0.271
	Evenness	0.570 ± 0.087	0.604 ± 0.191	0.464 ± 0.154

Table S2.

Gene overlap among sampling wells. [a] Numbers and percentages not in italic or bold indicate functional genes or OTUs that overlapped between two treatment groups. [b] Total number of functional genes or OTUs detected in treatment group. [c] Numbers and percentages in bold and italic are unique functional genes or OTUs detected in each treatment group**.**

Well Group	No. (%) of overlapping OTUs[a]		
	OR_A (3,303)[b]	OR_{CN} (6,108)	OR_{ALK} (1,556)
OR_A	***499(15.17%)*** [c]	2729(40.84%)	755(18.39%)
OR_{CN}		***2927(47.92%)***	1132(17.33%)
OR_{ALK}			***349(22.42%)***
Well Group	No. (%) of overlapping genes[a]		
	OR_A (55,655)[b]	OR_{CN} (69,500)	OR_{ALK} (68,731)
OR_A	***546(0.98%)*** [c]	54405(76.90%)	54247(77.34%)
OR_{CN}		***4987(7.17%)***	63656(85.36%)
OR_{ALK}			***4371(6.36%)***

Table S3.

Mean values for groundwater geochemical variables collected from wells in OR_A, OR_{CN} and OR_{ALK} groups. DIC, dissolved inorganic carbon; DOC, dissolved organic carbon.

Geochemical variable		OR_A	OR_{CN}	OR_{ALK}
Cations (mg/L)	Ag	0.01	0.01	0.01
	Al	0.11	0.03	0.11
	As	0.01	0.01	0.01
	Ba	0.39	0.23	0.12
	Be	0.04	0.04	0.04
	Bi	0.01	0.02	0.01
	Ca	15.14	73.12	7.36
	Cd	0.00	0.00	0.00
	Co	0.02	0.00	0.00
	Cr	0.01	0.01	0.01
	Cu	0.05	0.02	0.02
	Fe	0.07	0.35	0.01
	Ga	0.02	0.01	0.01
	K	2.60	2.33	4.18
	Li	0.05	0.10	0.15
	Mg	38.82	27.95	43.13
	Mn	0.61	0.38	0.02
	Na	27.74	26.18	202.21
	Ni	0.04	0.02	0.02
	Pb	0.00	0.00	0.00
	Se	0.01	0.01	0.01
	Sr	0.10	0.34	0.24
	U	0.01	0.03	0.01
	Zn	0.14	0.04	0.05
Anions (mg/L)	Cl^-	66.30	38.57	36.20
	NO_3	9.26	2.88	1.64
	SO_4	9.96	33.55	20.29
	S^{2-}	0.02	0.01	0.30
Gases (mM)	CH_4	0.01	0.00	0.04
	CO_2	2.87	2.10	3304.33
	DO	3.72	1.20	0.20
	N_2O	0.00	0.00	0.00
Carbon (mg/L)	DIC	16.89	55.94	78.81
	DOC	0.72	4.57	1.04
Others	pH	5.05	7.26	9.62
	Eh (mV)	316.60	250.30	57.00
	Temperature (°C)	14.86	16.37	14.38

Chapter 4 – Supplementary figure legends

Figure S1. Locations of the 24 wells at the OR-IFRC based on GPS co-ordinates. Color intensity indicates the pH concentration measured in the groundwater. Acidic, < pH 6.0; Alkaline, > pH 8.0.

Figure S2. Mean values for A) acridine orange direct cell counts (AODC) and B) DNA yield for wells grouped in OR_A, OR_B and OR_C groups. DNA yield represents amount recovered from biomass harvested from 4 liters of groundwater.

Figure S3. Detrended correspondence analysis (DCA) of all (A) functional genes and (B) 16S rRNA amplicon sequences detected in groundwater samples from each treatment groups. OR_A (pH < 6.0), OR_{CN} (pH 7.0 - 7.9), OR_{ALK} (pH > 9.0).

Figure S4. Detrended correspondence analysis (DCA) of (A) *cytochrome c* gene sequences representing dissimilatory metal reducing bacteria (DMRB), (B) *nirK/S* gene sequences representing denitrifying bacteria (NRB) and (C) *dsrAB* gene sequences representing dissimilatory sulfate reducing bacteria (SRB). OR_A (pH < 6.0), OR_{CN} (pH 7.0 – 7.9), OR_{ALK} (pH > 9.0).

Figure S5. Normalized signal intensity representing the relative abundance for detected C cycling genes. Significant differences identified between means are indicated by different letters. Calculation based on ANOVA followed by Fisher's LSD test. C degradation gene categories: A) Cellulose, B) Chitin, C) Cutin, D) Glyoxylate Cycle, E) Hemicellulose, F) Lignin, G) Pectin, H) Starch, I) Vanillin/Lignin, J) Camphor, K) Inulin, L) Terpenes.

Figure S6. Normalized signal intensity representing the relative abundance for detected *dsrAB* sequences determined to differ significantly between treatments. Signal intensities represent the sum of the gene sequences detected from each organism. Significant differences identified between means are indicated by different letters. Calculation based on ANOVA followed by Fisher's LSD test.

Figure S7. Normalized signal intensity representing the relative abundance for detected *cytochrome c* sequences determined to differ significantly between treatments. Signal intensities represent the sum of the gene sequences detected from each organism. Significant differences identified between means are indicated by different letters. Calculation based on ANOVA followed by Fisher's LSD test.

Figure S8. Normalized signal intensity representing the relative abundance for detected *hydrogenase* sequences determined to differ significantly between treatments. Signal intensities represent the sum of the gene sequences detected from each organism. Significant differences identified between means are indicated by different letters. Calculation based on ANOVA followed by Fisher's LSD test.

Figure S9. Variance partitioning analysis (VPA) of environmental variables analyzed by CCA explaining relative effect of environmental variables on A) functional gene content and B) taxonomic composition across samples grouped by pH. Circles represent the effects of variables by partitioning out the effects of other variables. Values between circles represent combined effect of circle on either side.

Figure S10. Relative abundance of OTUs identified at >1% mean RA across samples in OR_A, OR_{CN} and OR_{ALK} wells. OTU_8 and OTU_5 were detected at >1% RA in more than one treatment group. Taxonomic levels presented: OTU; Genus; Order.

Figure S11. Relative abundance of 16s rRNA sequences at class level determined to be present at >1% RA in OR_A, OR_{CN} and OR_{ALK} groups of wells.

Figure S1.

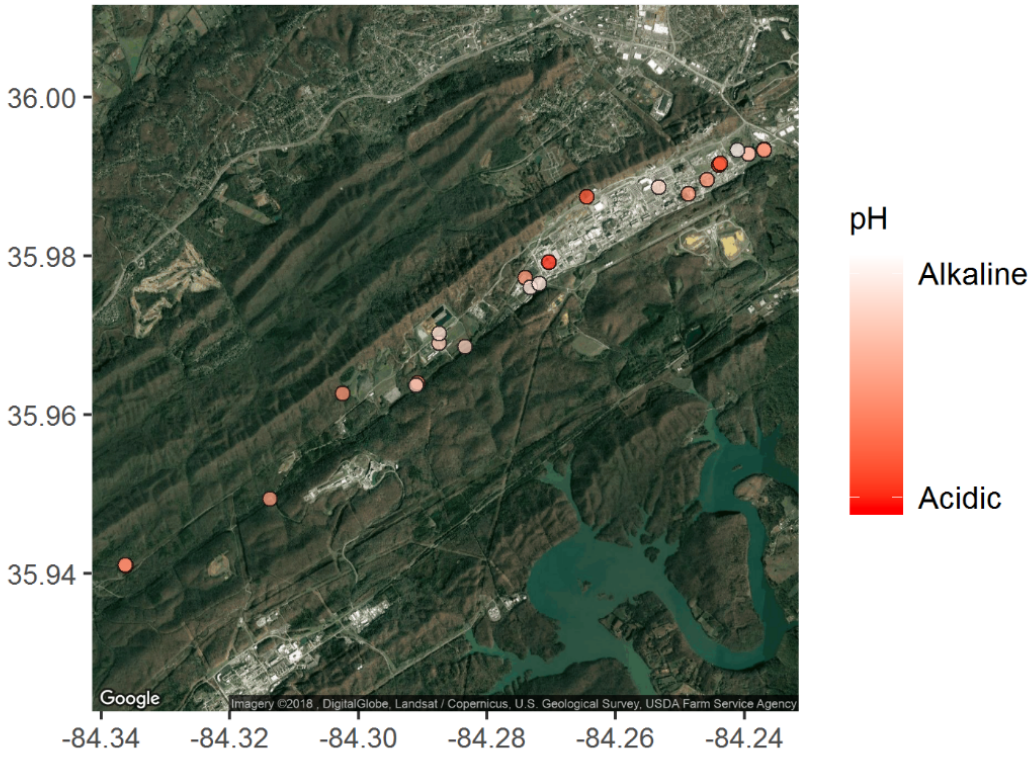
36.00
35.98
35.96
35.94
-84.34
-84.32
-84.30
-84.28
-84.26
-84.24
Google
Imagery ©2018 , DigitalGlobe, Landsat / Copernicus, U.S. Geological Survey, USDA Farm Service Agency
pH
Alkaline
Acidic

Figure S2A.

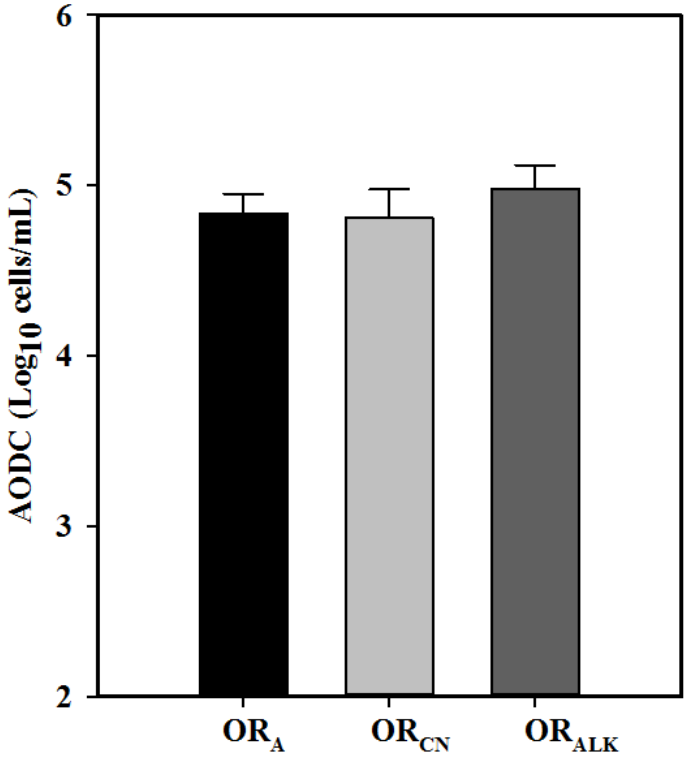

Figure S2B.

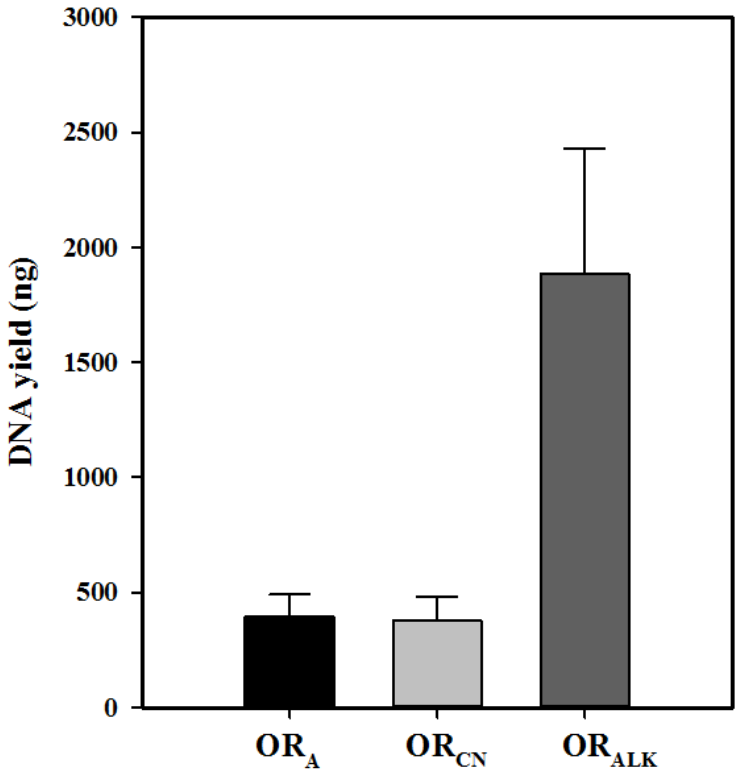

Figure S3A.

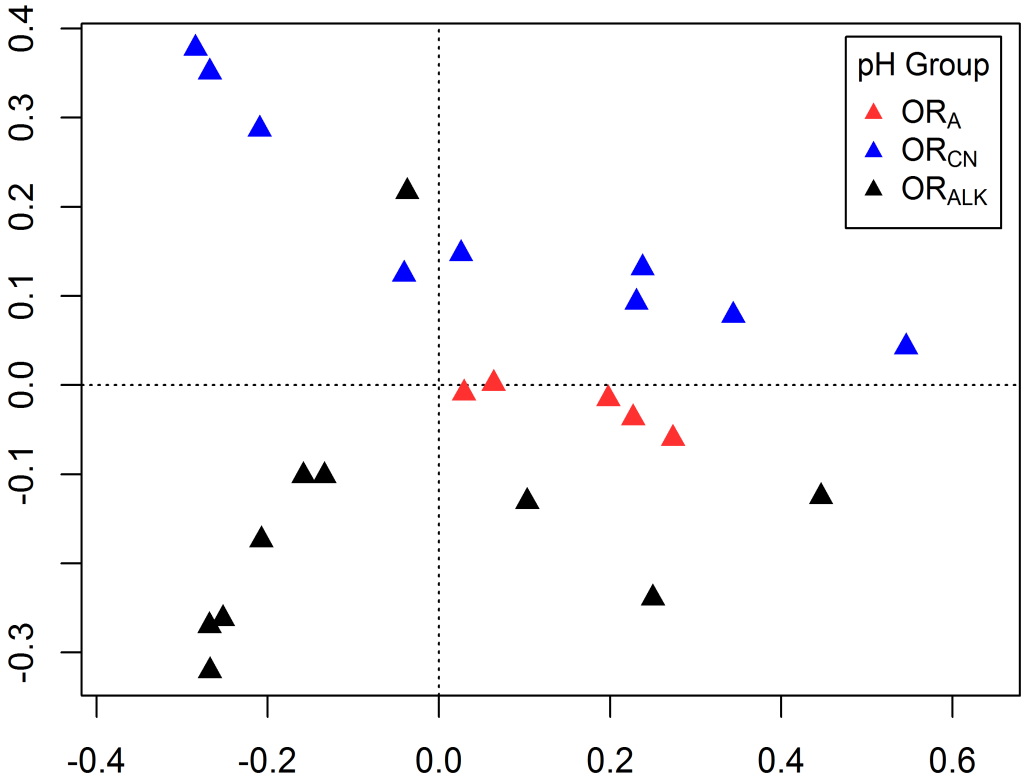

Figure S3B.

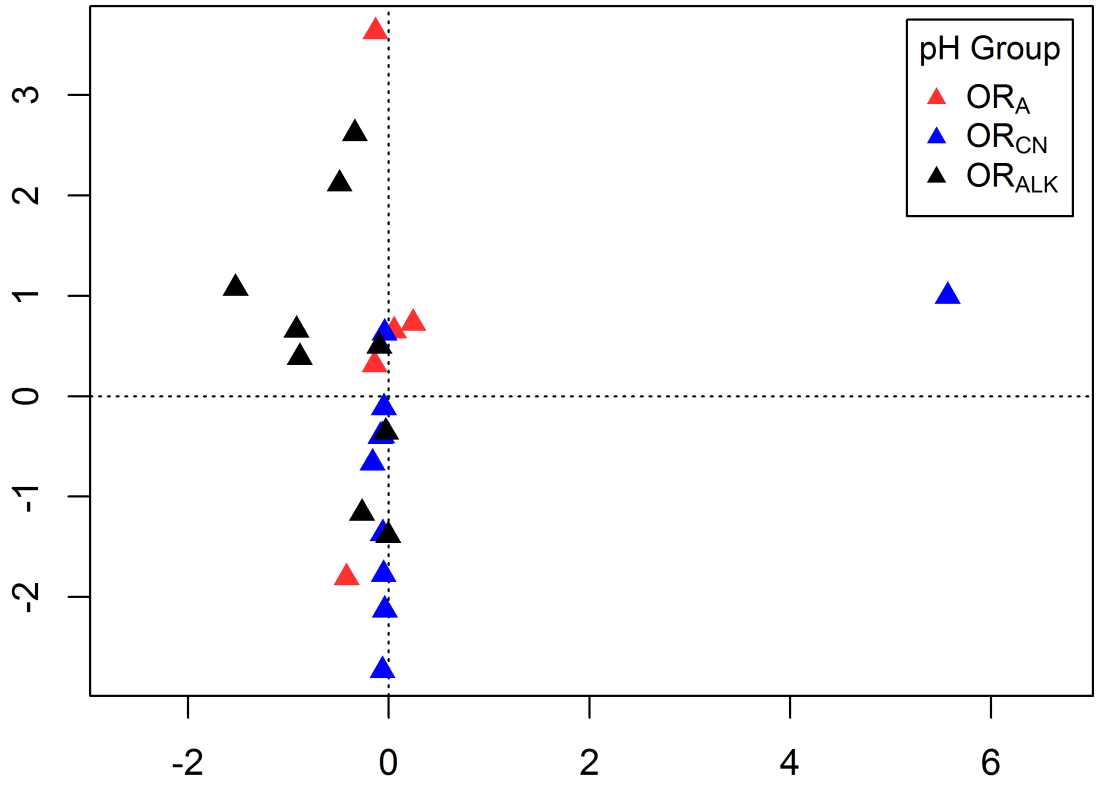

Figure S4A.

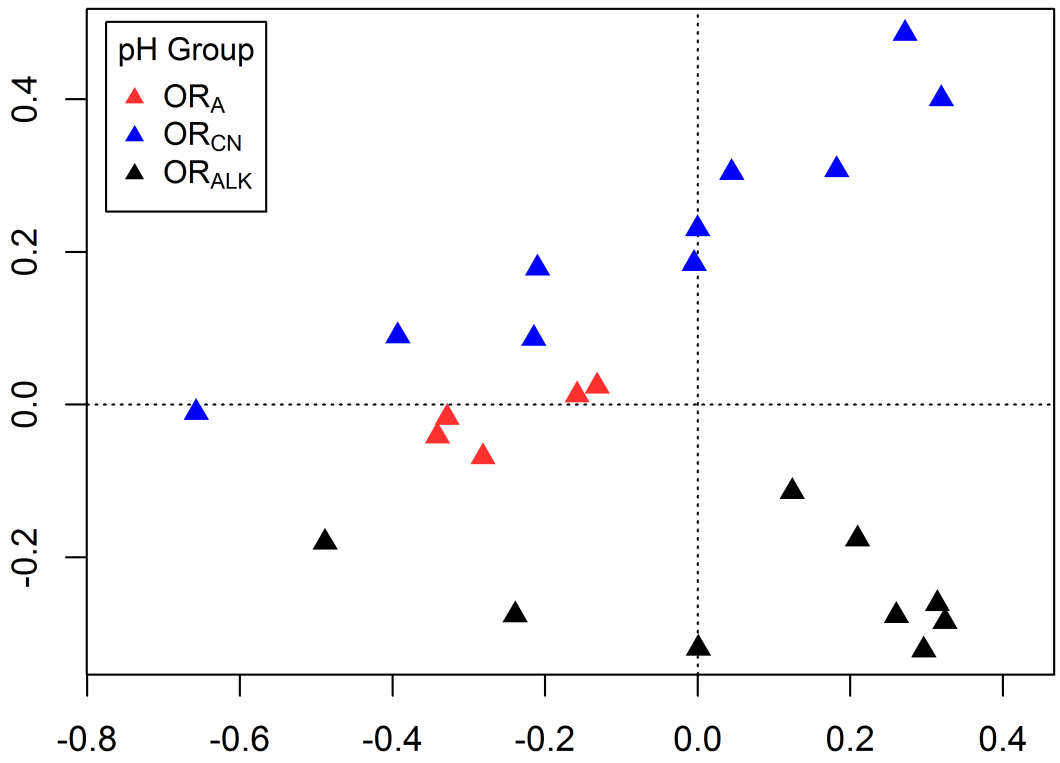

Figure S4B.

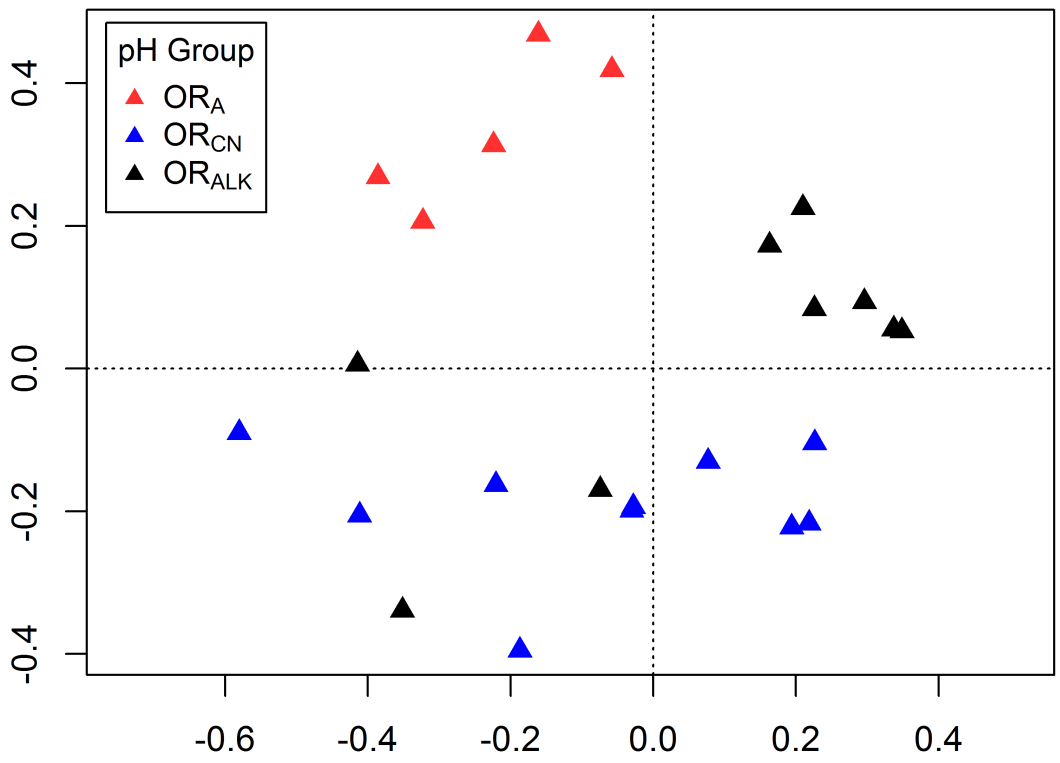

Figure S4C.

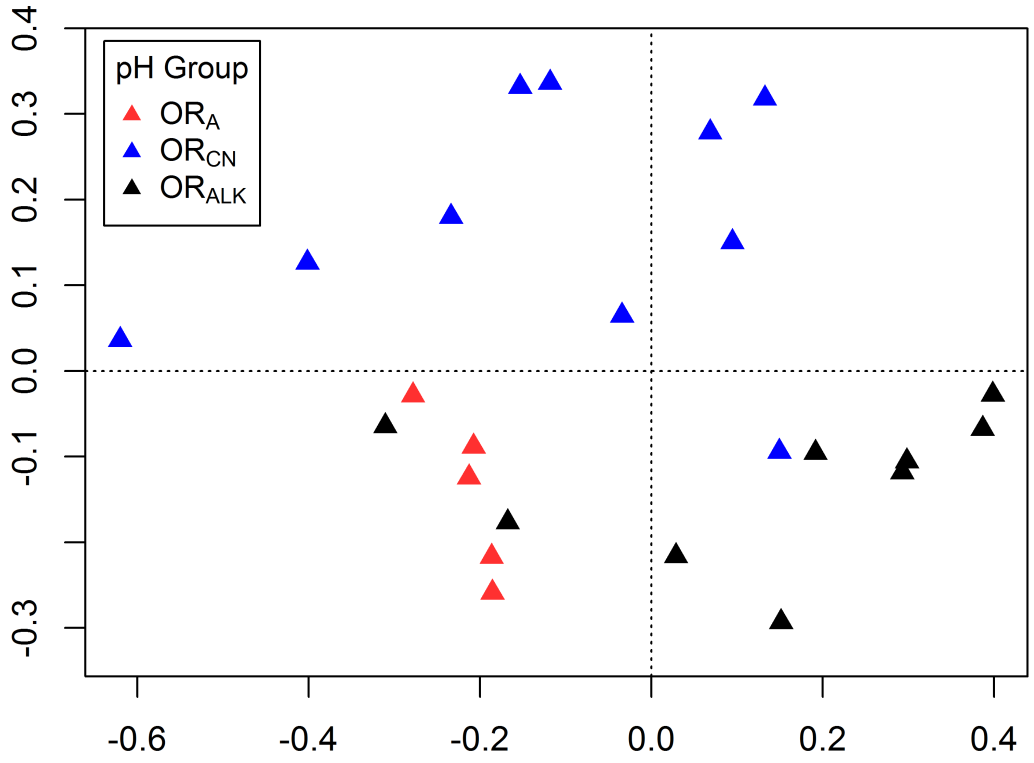

Figure S5A.

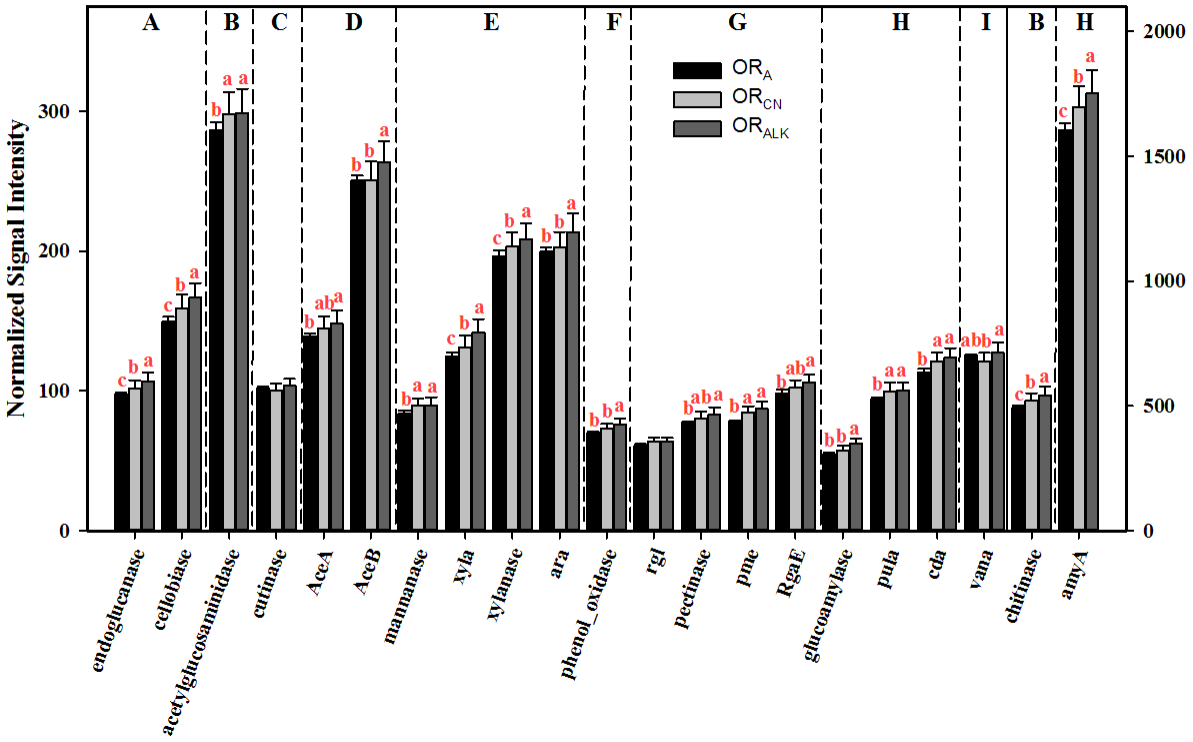
A
B
C
D
E
F
G
H
I
B
H
OR_A
OR_CN
OR_ALK
Normalized Signal Intensity
0
100
200
300
0
500
1000
1500
2000
endoglucanase
cellobiase
acetylglucosaminidase
cutinase
AceA
AceB
mannanase
xyla
xylanase
ara
phenol_oxidase
rgl
pectinase
pme
RgaE
glucoamylase
pula
cda
vana
chitinase
amyA

Figure S5B.

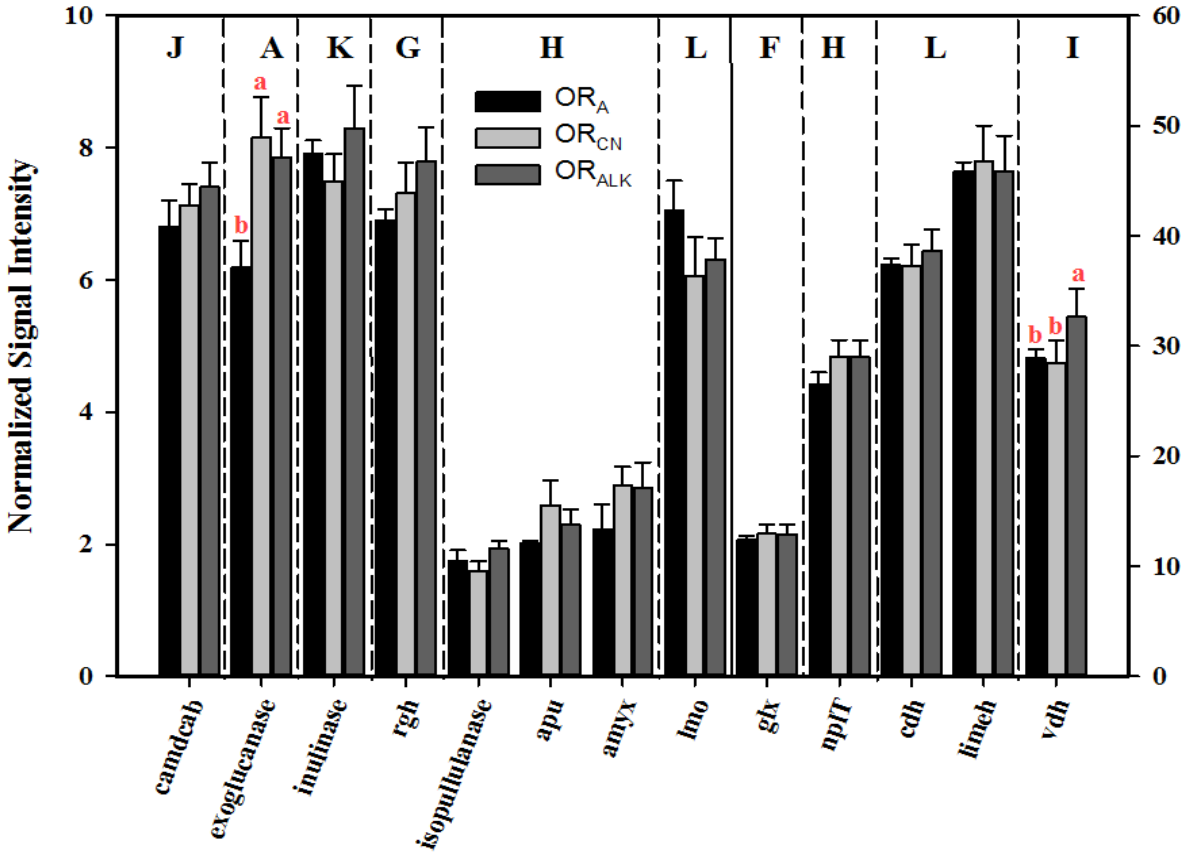
Normalized Signal Intensity
J
A
K
G
H
L
F
H
L
I
OR_A
OR_CN
OR_ALK
a
a
b
b
b
a
camdcab
exoglucanase
inulinase
rgh
isopullulanase
apu
amyx
lmo
glx
nplT
cdh
limeh
vdh

Figure S6.

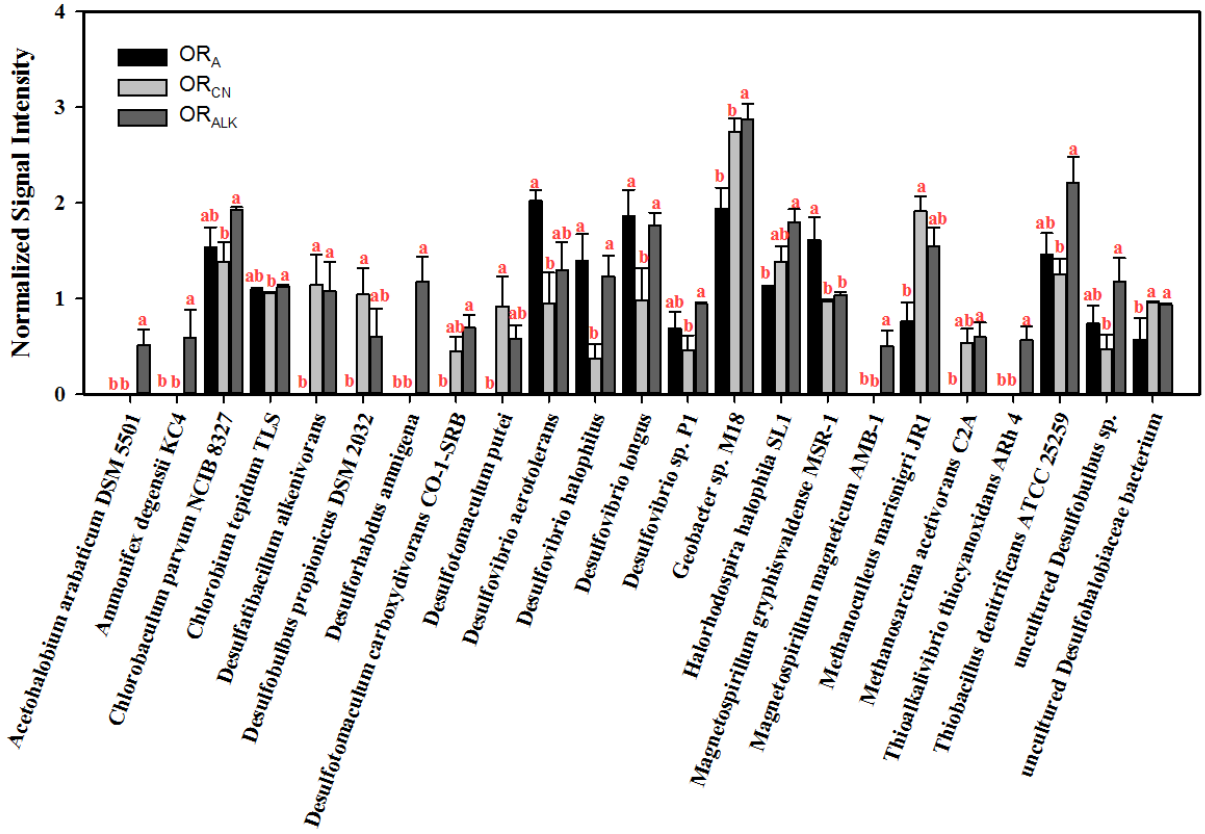
Normalized Signal Intensity
OR_A
OR_CN
OR_ALK
0
1
2
3
4
Acetohalobium arabaticum DSM 5501
Ammonifex degensii KC4
Chlorobaculum parvum NCIB 8327
Chlorobium tepidum TLS
Desulfatibacillum alkenivorans
Desulfobulbus propionicus DSM 2032
Desulforhabdus amnigena
Desulfotomaculum carboxydivorans CO-1-SRB
Desulfotomaculum putei
Desulfovibrio aerotolerans
Desulfovibrio halophilus
Desulfovibrio longus
Desulfovibrio sp. P1
Geobacter sp. M18
Halorhodospira halophila SL1
Magnetospirillum gryphiswaldense MSR-1
Magnetospirillum magneticum AMB-1
Methanoculleus marisnigri JR1
Methanosarcina acetivorans C2A
Thioalkalivibrio thiocyanoxidans ARh 4
Thiobacillus denitrificans ATCC 25259
uncultured Desulfobulbus sp.
uncultured Desulfohalobiaceae bacterium

Figure S7.

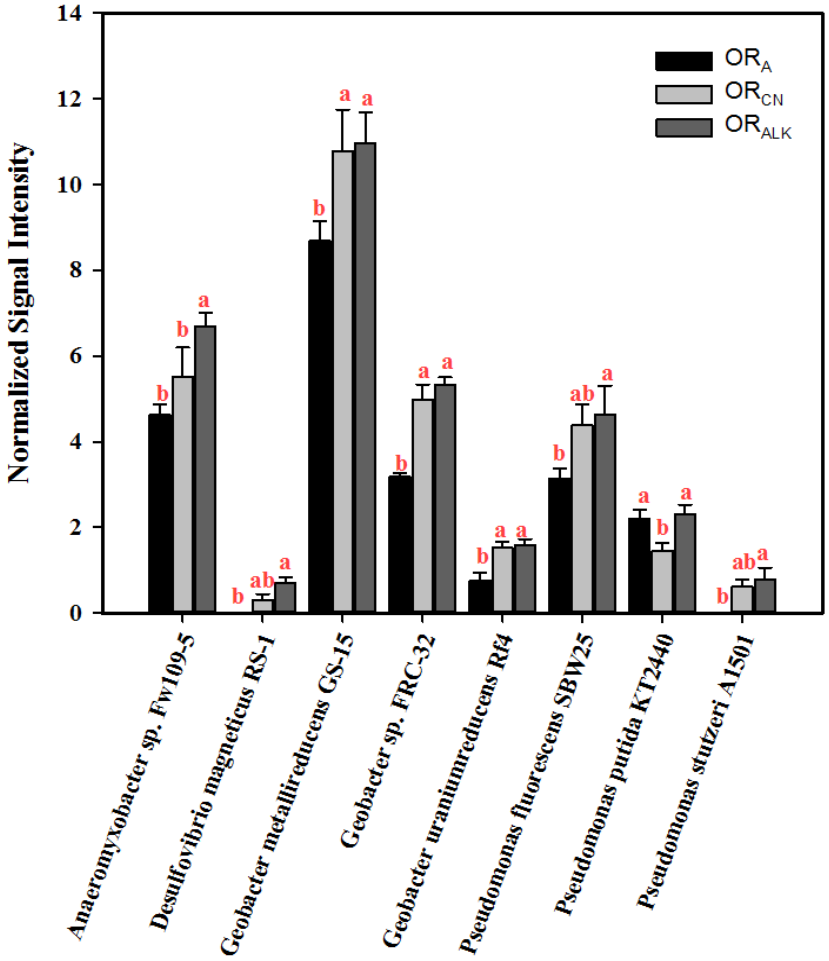
Normalized Signal Intensity
14
12
10
8
6
4
2
0
OR_A
OR_CN
OR_ALK
Anaeromyxobacter sp. Fw109-5
Desulfovibrio magneticus RS-1
Geobacter metallireducens GS-15
Geobacter sp. FRC-32
Geobacter uraniumreducens Rf4
Pseudomonas fluorescens SBW25
Pseudomonas putida KT2440
Pseudomonas stutzeri A1501

Figure S8.

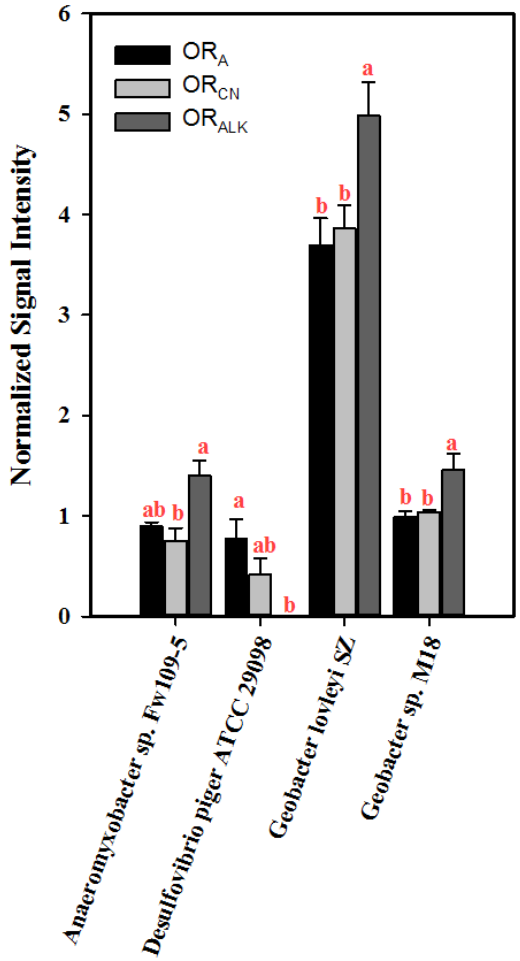
Normalized Signal Intensity
0
1
2
3
4
5
6
OR_A
OR_CN
OR_ALK
ab b a
a ab b
b b a
b b a
Anaeromyxobacter sp. Fw109-5
Desulfovibrio piger ATCC 29098
Geobacter lovleyi SZ
Geobacter sp. M18

Figure S9A.

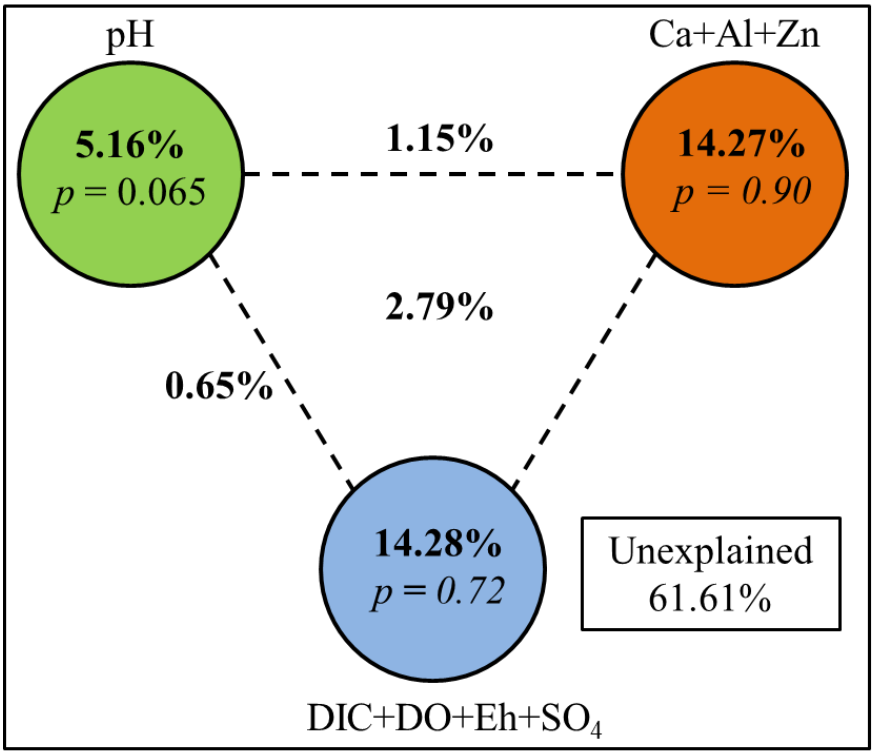
pH
Ca+Al+Zn
5.16%
p = 0.065
1.15%
14.27%
p = 0.90
2.79%
0.65%
14.28%
p = 0.72
Unexplained
61.61%
DIC+DO+Eh+SO4

Figure S9B.

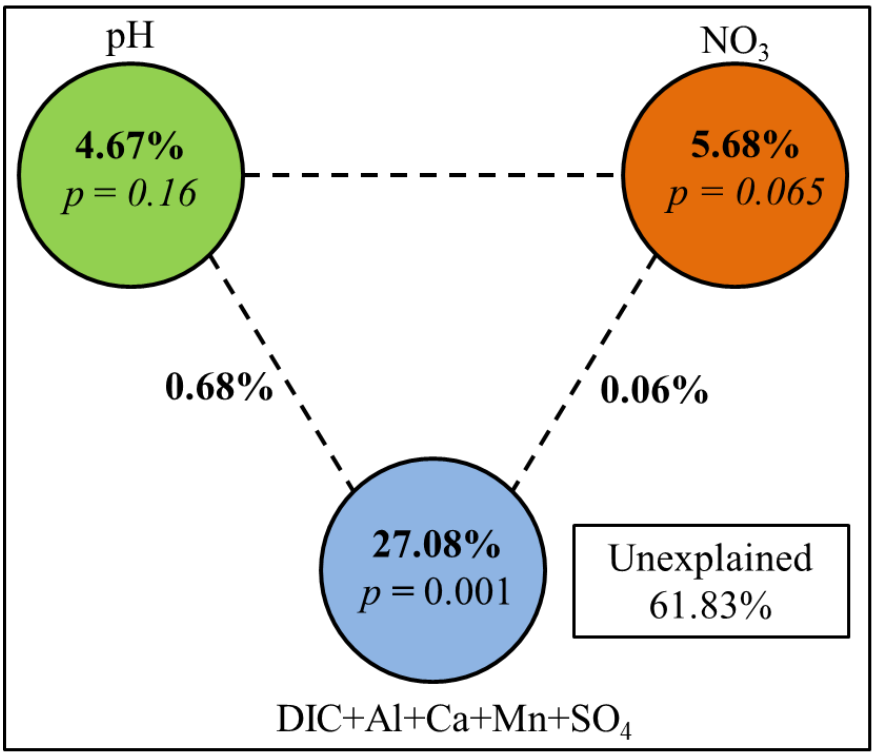
pH
NO3
4.67%
p = 0.16
5.68%
p = 0.065
0.68%
0.06%
27.08%
p = 0.001
Unexplained
61.83%
DIC+Al+Ca+Mn+SO4

Figure S10.

Taxonomy	OR_A	OR_{CN}	OR_{ALK}
OTU_1; Unclassified; Deltaproteobacteria	8.77475	0.00221	0.00278
OTU_15; Unclassified; Betaproteobacteria	7.27598	0.62106	0.47507
OTU_18; Sediminibacterium; Sphingobacteriia	2.05931	0.29595	0.55657
OTU_2; Dechloromonas; Betaproteobacteria	12.6548	0.21159	0.27511
OTU_23; Reyranella; Alphaproteobacteria	1.8343	0.60384	0.23416
OTU_25; Variovorax; Betaproteobacteria	2.38292	0.94617	0.50728
OTU_26; Unclassified; Betaproteobacteria	1.17119	0.34101	0.48899
OTU_33; Gp24; Acidobacteria_Gp24	1.44629	0	0.0008
OTU_36; Unclassified; Gammaproteobacteria	1.39222	0.00221	0.13079
OTU_4115; Brevundimonas; Alphaproteobacteria	2.20641	0.59588	0.22223
OTU_52; Paludibacter; Bacteroidia	1.02886	0.00177	0.0008
OTU_10; Unclassified; Gammaproteobacteria	0.00159	5.35144	0.00044
OTU_20; Pseudomonas; Gammaproteobacteria	0.0326	2.64491	0.15284
OTU_24; Acinetobacter; Gammaproteobacteria	0.00159	1.80329	0.01458
OTU_3; Streptococcus; Bacilli	0.00159	8.49686	0.00265
OTU_41; Unclassified; Betaproteobacteria	0.01113	1.58543	0.00177
OTU_588; Unclassified; Betaproteobacteria	0.24171	1.93409	0.38474
OTU_6; Unclassified; Unclassified	0.00398	4.02282	0.00309
OTU_11; Unclassified; Deltaproteobacteria	0	0.01153	3.01123
OTU_12; Nitrospira; Nitrospira	0.00954	0.15584	6.00656
OTU_13; Thiobacillus; Betaproteobacteria	0.00318	0.03498	8.9767
OTU_14; Unclassified; Deltaproteobacteria	0.00318	0.00278	4.60806
OTU_16; Unclassified; Unclassified	0.0008	0.01988	3.03022
OTU_17; Aridibacter; Acidobacteria_Gp4	0.0008	0	1.59109
OTU_19; Hydrogenophaga; Betaproteobacteria	0.81737	0.11768	5.11604
OTU_1901; Unclassified; Betaproteobacteria	0.00954	0.02783	2.26074
OTU_21; Unclassified; Clostridia	0	0.00199	1.94447
OTU_28; Unclassified; Clostridia	0	0.0008	1.57651
OTU_29; Unclassified; Betaproteobacteria	0.0008	0.00994	2.28945
OTU_4; Unclassified; Unclassified	0	0.0004	5.16772
OTU_42; Truepera; Deinococci	0.0008	0.0004	1.16394
OTU_43; Unclassified; Unclassified	0	0.01431	1.13788
OTU_46; Bradyrhizobium; Alphaproteobacteria	0.73785	0.42617	1.09194
OTU_7; Unclassified; Gammaproteobacteria	0.0008	0.0004	4.15529
OTU_9; Unclassified; Unclassified	0	0.00199	4.51309
OTU_8; Unclassified; Betaproteobacteria	0.06043	4.03735	3.28457
OTU_5; Brevundimonas; Alphaproteobacteria	3.85386	1.01155	1.58504

Figure S11.

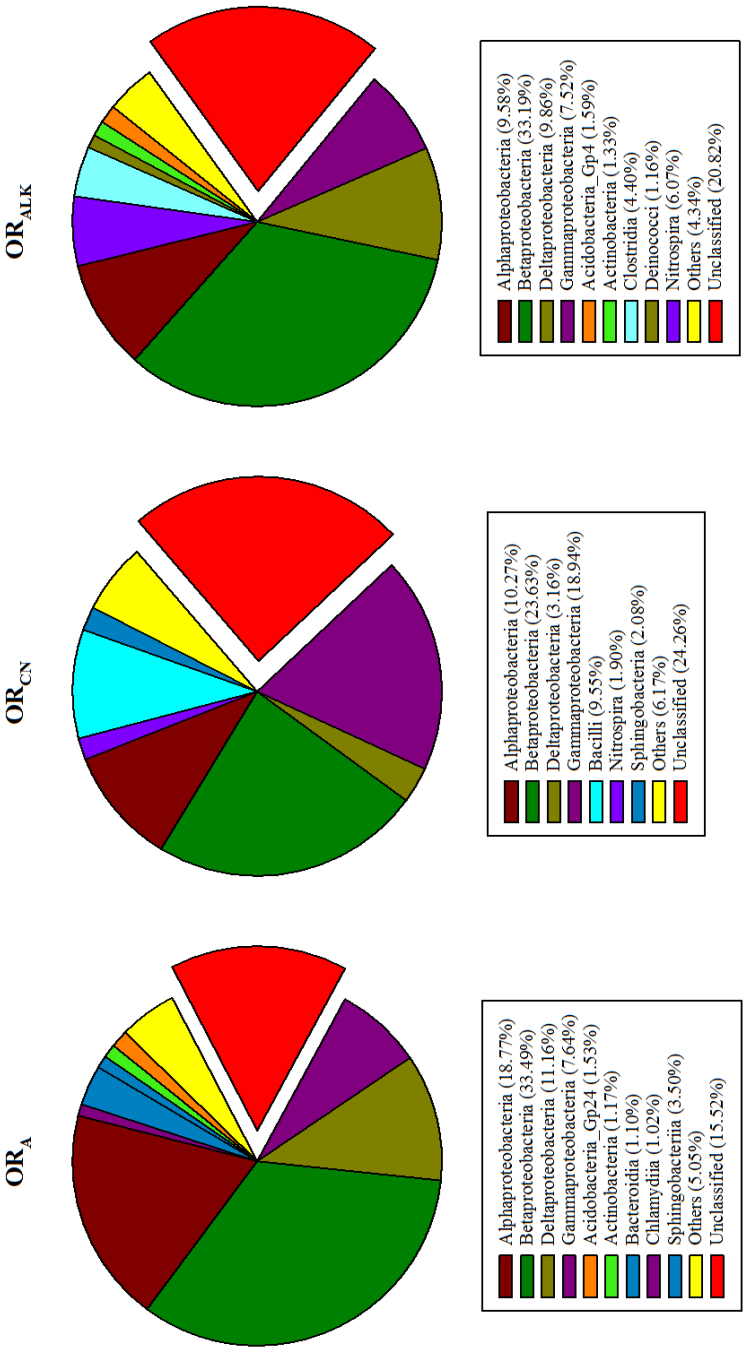
OR_ALK
Alphaproteobacteria (9.58%)
Betaproteobacteria (33.19%)
Deltaproteobacteria (9.86%)
Gammaproteobacteria (7.52%)
Acidobacteria_Gp4 (1.59%)
Actinobacteria (1.33%)
Clostridia (4.40%)
Deinococci (1.16%)
Nitrospira (6.07%)
Others (4.34%)
Unclassified (20.82%)
OR_CN
Alphaproteobacteria (10.27%)
Betaproteobacteria (23.63%)
Deltaproteobacteria (3.16%)
Gammaproteobacteria (18.94%)
Bacilli (9.55%)
Nitrospira (1.90%)
Sphingobacteria (2.08%)
Others (6.17%)
Unclassified (24.26%)
OR_A
Alphaproteobacteria (18.77%)
Betaproteobacteria (33.49%)
Deltaproteobacteria (11.16%)
Gammaproteobacteria (7.64%)
Acidobacteria_Gp24 (1.53%)
Actinobacteria (1.17%)
Bacteroidia (1.10%)
Chlamydia (1.02%)
Sphingobacteriia (3.50%)
Others (5.05%)
Unclassified (15.52%)